LOW PRESSURE FUEL INJECTION OF A TWO-STROKE CYCLE SPARK IGNITION ENGINE

P.L. McNaught

September 1986

Submitted to the University of Cape Town
in fulfilment for the degree of
Master of Science in Engineering

ABSTRACT

The two-stroke spark ignition engine has considerable advantages over four-stroke engines. These include, high power to weight ratios, and simplicity, and consequent low cost of construction and maintenance. However, it also has substantial disadvantages which have prevented its wider application. These are, high specific fuel consumption and high hydrocarbon exhaust emissions.

Research into obviating these disadvantages has met with mixed or little success. Efforts involving tuned exhaust pipes produced improvements over a limited speed range only. Direct fuel injection would provide a mechanically simple solution to the disadvantages of a two-stroke. The use of injection of fuel directly into the cylinder, however, has produced conflicting reports. Therefore, an experimental investigation was carried out to resolve this conflict.

A theory was proposed suggesting that stratification of the fresh charge should be possible using direct fuel injection. This would reduce loss of fuel due to short circuiting and mixing of the fresh charge, and as a consequence, reduce the specific fuel consumption and hydrocarbon emissions.

This theory was tested in the following manner. A carburetted engine, suitable for modification, was chosen and tested in standard form to provide a basis for comparison. The engine was then modified using four alternative locations for the electromagnetically operated injector.

Results showed that the injected engine, in no way improved upon the performance of the carburetted engine. The brake specific fuel consumption of the carburetted engine at full power was 340g/kWh. The injected engine could only approach this figure by using lean mixtures with a corresponding 32% drop in power. This indicated stratification of the fresh charge was not occurring and that there was little or no reduction in short circuiting and mixing. Therefore a scavenging analysis was carried out on the engine using two possible methods.

The first method involved analysing the exhaust gases to produce a curve of charging efficiency against delivery ratio. The second was a qualitative technique which produced 'three dimensional' scavenging pictures. To provide a basis for comparison for the second technique, a model of an engine of known carburetted performance was constructed and this method applied to obtain scavenging pictures.

From the analysis, reasons for the relative performance of the carburetted engines could be provided in terms of short circuiting and mixing of the fresh charge. It was noticed from the scavenging pictures of the model engine, that airflow from two of the four transfer ports formed a strongly separate charge at the 'back' of the cylinder, opposite the exhaust port. It was proposed that injection of fuel into these transfer passages should form a stratified charge with little or no short circuiting. This is suggested as a path for future investigation.

In conclusion then, direct fuel injection appears to have little advantage in terms of specific fuel consumption or power. It appears stratified charging is only possible if the separate charges are prepared before entering the cylinder, as suggested by other researchers. This would be possible using indirect fuel injection as suggested above.

ACKNOWLEDGEMENTS

The author would like to thank Andrew Yates for his guidance and encouragement in supervising this thesis, and the Energy Research Institute for allowing liberal use of their facilities

I Peter McNaught, submit this thesis in fulfilment of the requirements for the degree of Master of Science in Engineering. I claim that this thesis is my original work and that it has not been submitted in this or in a similar form for a degree at any University.

TABLE OF CONTENTS

LIST OF FIGURES

Glossary

Delivery Ratio	$\frac{\text{mass of fresh charge supplied per cycle}}{\text{mass related to stroke volume of cylinder at ITP}}$
Charging Efficiency	$\frac{\text{mass of fresh charge trapped in cylinder}}{\text{mass related to stroke volume of cylinder at ITP}}$
Trapping Efficiency	$\frac{\text{mass of fresh charge trapped in cylinder}}{\text{mass of fresh charge supplied per cycle}}$
ITP	Inlet temperature and pressure
Scavenging	The gas exchange process in a two-stroke engine
Expansion Chamber	An exhaust pipe used on two-stroke engines to increase power and reduce fuel consumption
Schnurle Scavenged	An engine with a port layout producing a reverse loop airflow in a cylinder with a flat topped piston

Short Circuiting	Loss of fresh air/fuel mixture straight out of the exhaust port without being trapped and burned
Mixing	The mixing of fresh air/fuel mixture with exhaust gases

CHAPTER ONE

1. INTRODUCTION

The ever increasing cost of fuel has forced internal combustion engineers to look at every conceivable alternative in attempting to make engines more efficient. The conventional carburetted four-stroke engine has been fuel injected resulting in small increases in performance and efficiency. However, these increases come with a significant increase in complexity and cost. At the other end of the internal combustion engine spectrum lies the two-stroke engine which has the following advantages when compared to a four-stroke engine;

* high specific power output
* compactness and light weight
* simplicity of construction and maintenance

Consequently it has been used where high power to weight ratios are essential as for example in motorcycle racing, power boats and chainsaws. Its wider use has been prevented by its major disadvantages which are;

* high specific fuel consumption
* high hydrocarbon emissions.

Figure 1.1 shows how a small industrial two-stroke engine compares to other internal combustion engines in terms of specific fuel consumption and specific power output.
The reason for the high specific fuel consumption is clear when considering the operation of a two-stroke spark ignition engine. **Figure 1.2(a)** shows the start of the gas exchange process of a conventional crankcase scavenged

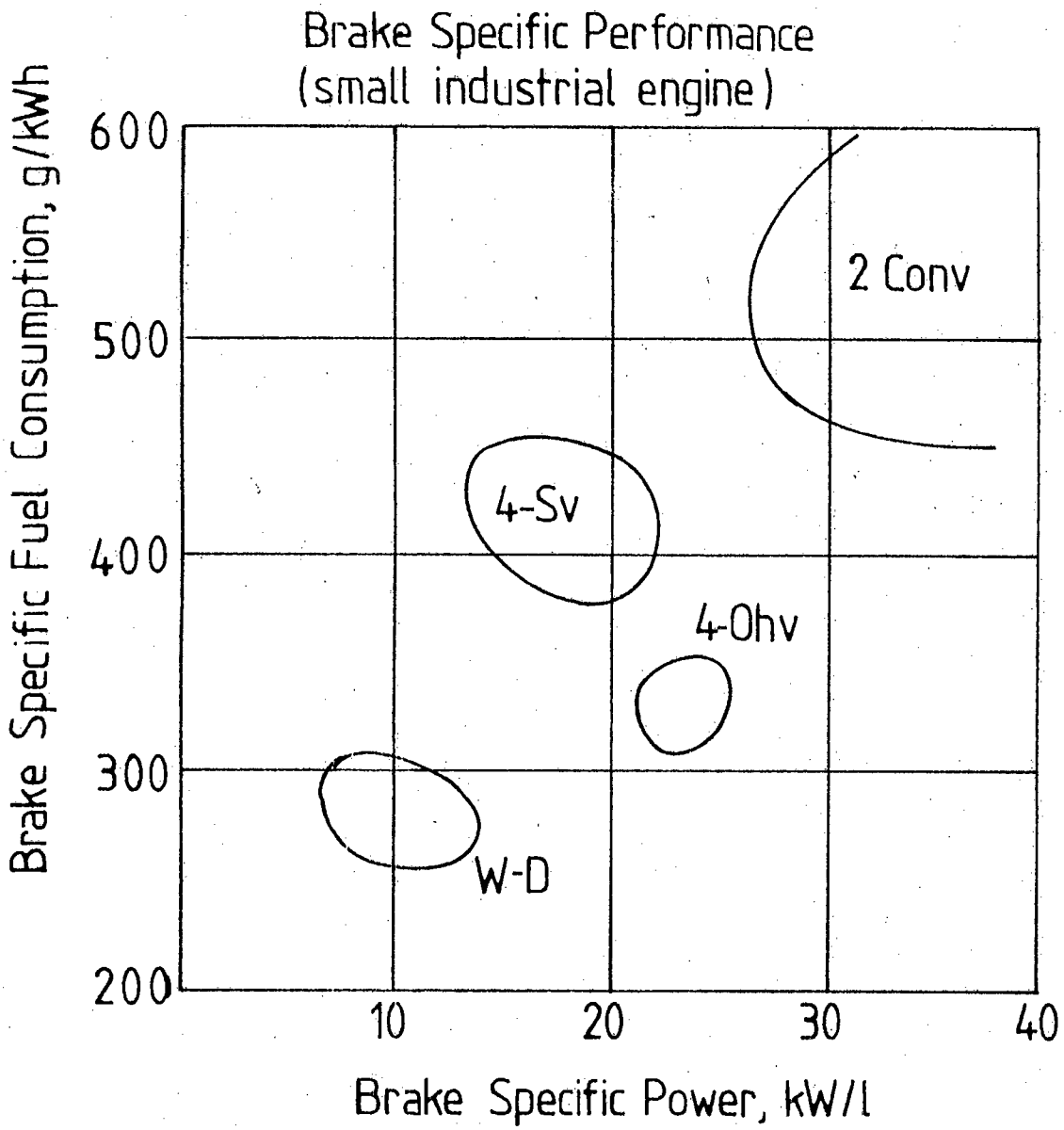

W-D = water-cooled Diesel
4 -Sv= four-stroke side valve
4-Ohv= four-stroke overhead valve
2-Conv= conventional two-stroke

Figure 1.1 Relative Two-Stroke Performance

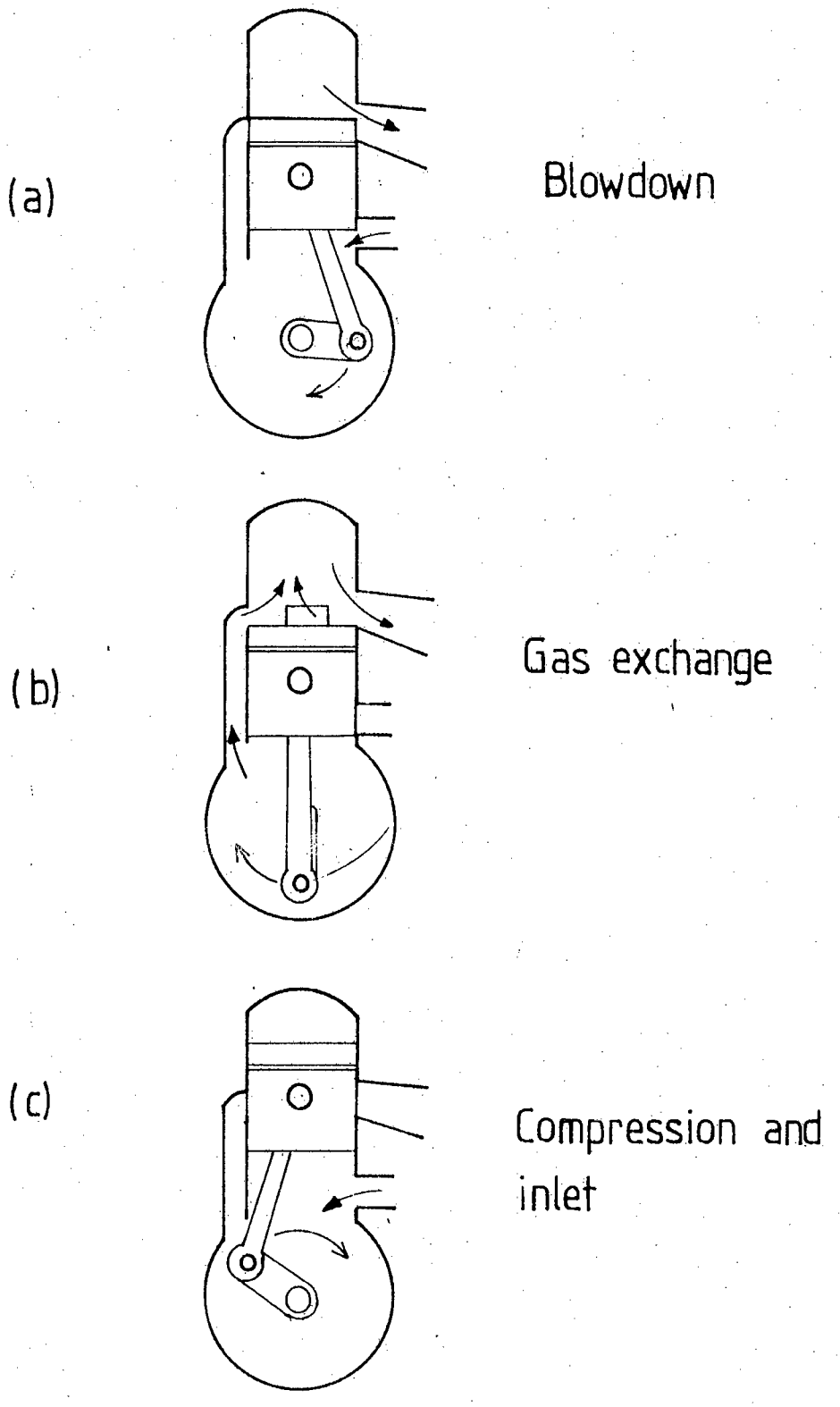

Figure 1.2 The Two-Stroke Cycle

engine. As the falling piston uncovers the exhaust port, blowdown commences, corresponding to a rapid drop in pressure in the cylinder as spent gases escape out of the exhaust. The descending piston causes fresh inlet gases trapped in the crankcase to be compressed so that when the transfer passages are uncovered, fresh charge begins to enter the cylinder, (**Figure 1.2b**). The exhaust and charging processes are, therefore, taking place simultaneously. As the piston rises, the increasing crankcase volume causes a negative pressure. As a result, fresh charge is induced through either a piston controlled port, rotary or reed valve, into the crankcase.

By the time the rising piston closes the exhaust port, the gas exchange or scavenging process is complete. Compression commences followed by ignition and combustion (**Figure 1.2c**). Expansion of the burning charge proceeds until the exhaust port is opened, completing the cycle.

The high specific fuel consumption is caused by the fact that the exhaust and charging processes take place simultaneously. A high percentage (as much as 40%) of the fresh fuel/air mixture supplied is lost by short circuiting and mixing.

Short circuiting occurs when fresh charge entering the cylinder from the transfer passages is lost through the exhaust without being trapped and burned.

Mixing refers to the fresh charge mixing with the exiting exhaust gases.

Loss of fuel through mixing and short circuiting occurs in all two-stroke engines to a greater or lesser extent depending on the port timing, transfer and exhaust port and passage layout, and engine operating condition.

Figure 1.3 shows the relationship between thermal efficiency, trapping efficiency and air/fuel ratio. The importance of trapping efficiency is immediately apparent. Using lean mixtures may increase thermal efficiency, but what is not apparent from the graph is the loss of power resulting from under-utilization of the trapped air.

A great deal of research has been done into reducing mixing and short circuiting with varying degrees of success. The most promising results have been provided by various methods of stratified charging. One reportedly effective method involves low pressure fuel injection. (These and other methods are discussed in the next chapter.)

If the charging process involves only fresh air and fuel is injected into the cylinder at an appropriate time and location, the short circuiting and mixing of the fuel could be minimised and therefore the specific fuel consumption and hydrocarbon emmissions would improve.

The literature reveals conflicting reports on the effectiveness of fuel injected stratified charging. This and the lack of research into the field provided motivation for a thesis on this topic. Although a fuel injected system would bring added complication to the simple elegance of the two-stroke, the advantages would be substantial.

From the above it follows that investigation into the subject must firstly resolve the problem of the conflicting reports and then either one of two paths must be persued depending on the outcome. Should investigation show that there is no advantage in fuel injection, then analysis of the scavenging process must indicate why this is the case. However, should the principle of fuel injection produce promising improvements in thermal efficiency, the logical

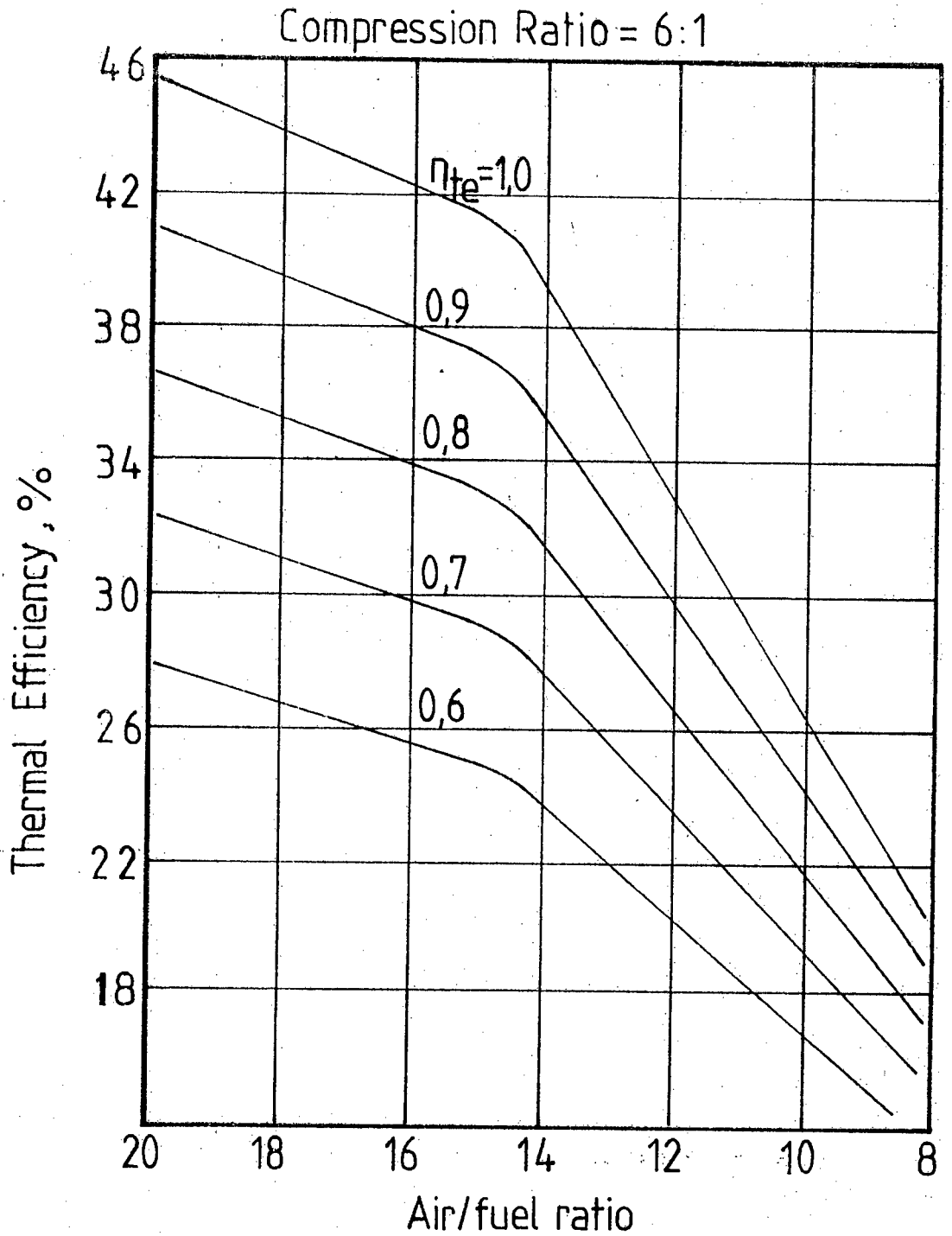

η_{te} = Trapping efficiency

Figure 1.3 Thermal and Trapping Efficiency versus Air/Fuel Ratio

course of action would be to develop a control system that would provide the required amount of fuel to the engine at any particular load and speed.

Major problems expected are listed below:

* modification of existing four-stroke fuel injectors to suit the flow requirements of a two-stroke engine.
* determining the optimun nozzle location, fuel supply pressure, and spray geometries.

The objectives of this thesis then, are to resolve by experimentation a conflict evident in the literature and to follow one of two paths of investigation depending upon the results of these experiments.

CHAPTER TWO

2. LITERATURE SURVEY.

2.1. The Two-Stroke Spectrum.

There are many variations to the design of two-stroke engines. **Figure 2.1** shows the extent of these variations. The principle on which they operate is the same in spite of the differences in mechanical design and arrangement.

As the maintenance of mechanical simplicity is thought to be of prime importance, the designs in **Figure 2.1 (c,d,e,f)** are mechanically too complicated and therefore too expensive to have found wide use as spark ignition engines, despite the slight increase in performance due to the mechanical design. Diesel engine manufacturers have, however, made good use of some of these designs, but compression ignition engines are beyond the scope of this survey.

The design that has found widest application amongst two-stroke spark ignition engines is the loop scavenged engine and in particular, the Schnurle scavenged, crankcase compression engine. This has proved to be the most simple method of supplying fresh charge to the cylinder. Other scavenging methods use supercharging devices such as the Roots blower, but these add expense and complication. The operation of a crankcase scavenged two-stroke has been outlined in Chapter One and will therefore not be detailed here.

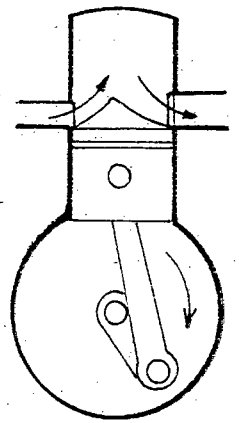

(a) Deflector piston

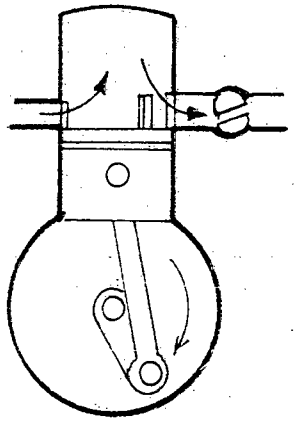

(a) Rotary exhaust valve

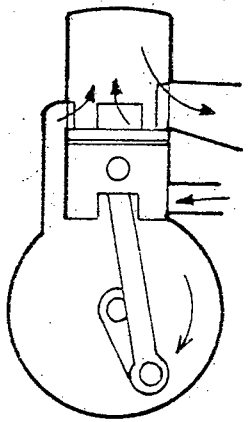

(b) Crankcase scavenged

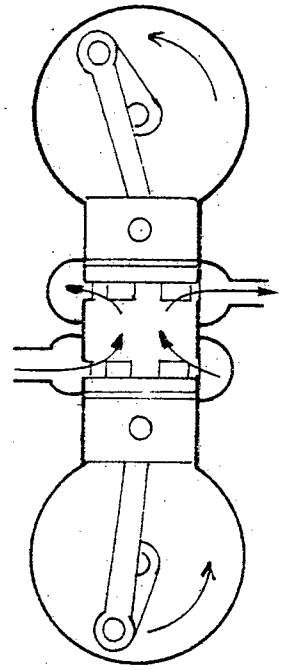

(c) Opposed piston

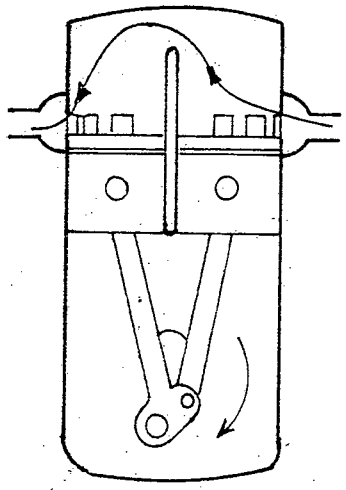

(d) U-cylinder

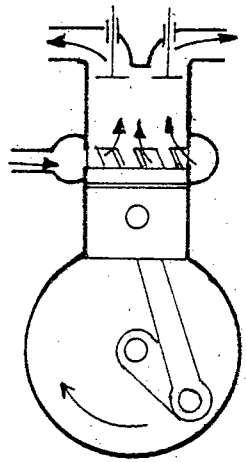

(e) Poppet exhaust valve

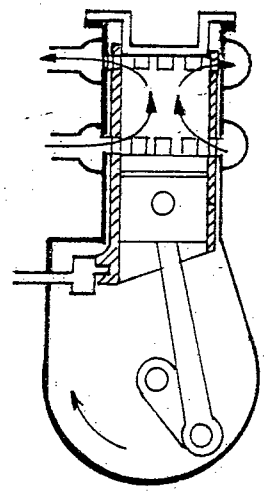

(f) Sleeve valve

Figure 2.1 The Two-Stroke Spectrum

2.2 High Pressure Fuel Injection

Various researchers [1,2,3] suggest fuel injection is the logical solution to the disadvantages inherent in the two-stroke engine. Earliest attempts to this end concentrated on the use of mechanical injection pumps [4] and showed considerable improvement in specific fuel consumption, (as low as 330g/kWh). However, most of these efforts showed up engine speed limitations. (Maximum mean effective pressure at 2500 rpm, and maximum speed of 4500 rpm for a 700cc two cylinder two-stroke). Furthermore, high pressure injection pumps are far more costly to produce than a carburettor, and therefore such a system would seldom find its way to the production line. A review of one such study is given below.

A study of high pressure fuel injection of a two-stroke engine [5] showed that brake specific fuel consumption (hereafter abbreviated to bsfc) could be reduced from a best value of 360g/kWh with a carburettor to 270g/kWh with cylinder head injection, - a reduction of 25% which is comparable to the performance of four-stroke engines of similar capacity.

The engine used in this study was a two cylinder 350cc Schnurle scavenged engine. Although the prime purpose of the paper was to reduce the exhaust emissions of a two-stroke, the study shows that fuel injection can be the solution to the disadvantages of the two-stroke engine. Exactly how this is done is the problem.

2.2.1 Injector Location.

If only fresh air is used to scavenge the two-stroke and fuel is injected in the closed part of the cycle, (exhaust closed to exhaust open), it can be expected that no fuel will be lost by short circuiting and mixing. Using the assumption that closed cycle injection is desirable, the alternative location of the injector in either the transfer passages of cylinder bore is immediately discounted as this would require open cycle injection, (exhaust open to exhaust closed), encouraging short circuiting. Furthermore severe timing limitation would be placed on the injector. Therefore the best location for high pressure fuel injection is logically, the cylinder head.

As it turns out, with the injector located in the cylinder head, injection during the open cycle is nevertheless, necessary, as time is required for the fuel to evaporate after injection. Whether this will promote losses due to short circuiting and mixing will depend on where the fuel spray is directed in relation to the scavenging pattern in the cylinder. The more remote the fuel is kept from the exhaust the better. Yamagishi, therefore directs the spray in a 20° cone, at a pressure of 42MPa, towards a point at the base of the cylinder, opposite the exhaust port.

2.2.2 Speed Restriction

The speed restriction imposed by the Bosch type injection pump shows up clearly on the plot of bsfc in relation to brake mean effective pressure (hereafter abbreviated to bmep) and engine speed. The bmep drops sharply above 5000rpm, with a corresponding sharp increase in bsfc. The

carburetted version of the same engine maintained good values of bmep above 6500rpm with almost constant values of bsfc. This highlights one of the major disadvantages of high pressure fuel injection, namely the inability of plunger type injector pumps to cope with high speeds, where, typically, the two-stroke shows most advantage.

2.2.3 Injector Timing.

Some interesting points arise out of examination of the effects of injection timing upon engine performance.

Figure 2.2 shows that in the interests of high bmep and low hydrocarbon emissions, it appears that timing position 3 is optimum at this speed, (40° ABDC). The high hydrocarbon emissions of timing points 1 and 2 are due to injection occurring in the open part of the cycle meaning that fuel can be lost through short circuiting and mixing. The high hydrocarbon emissionsof timing points 4 and 5 cannot be due to short circiuting as injection occurs in the closed part of the cycle This indicates incomplete combustion and is probably due to insufficient time being allowed for fuel evaporation. The point of interest here is that optimum timing calls for injection during the open cycle discounting the idea that closed cycle injection is advantageous.

2.2.4 Hydrocarbon Emissions.

A comparison between hydrocarbon emissions for the carburetted and injected engines as shown in **Figure 2.3** provides interesting information.

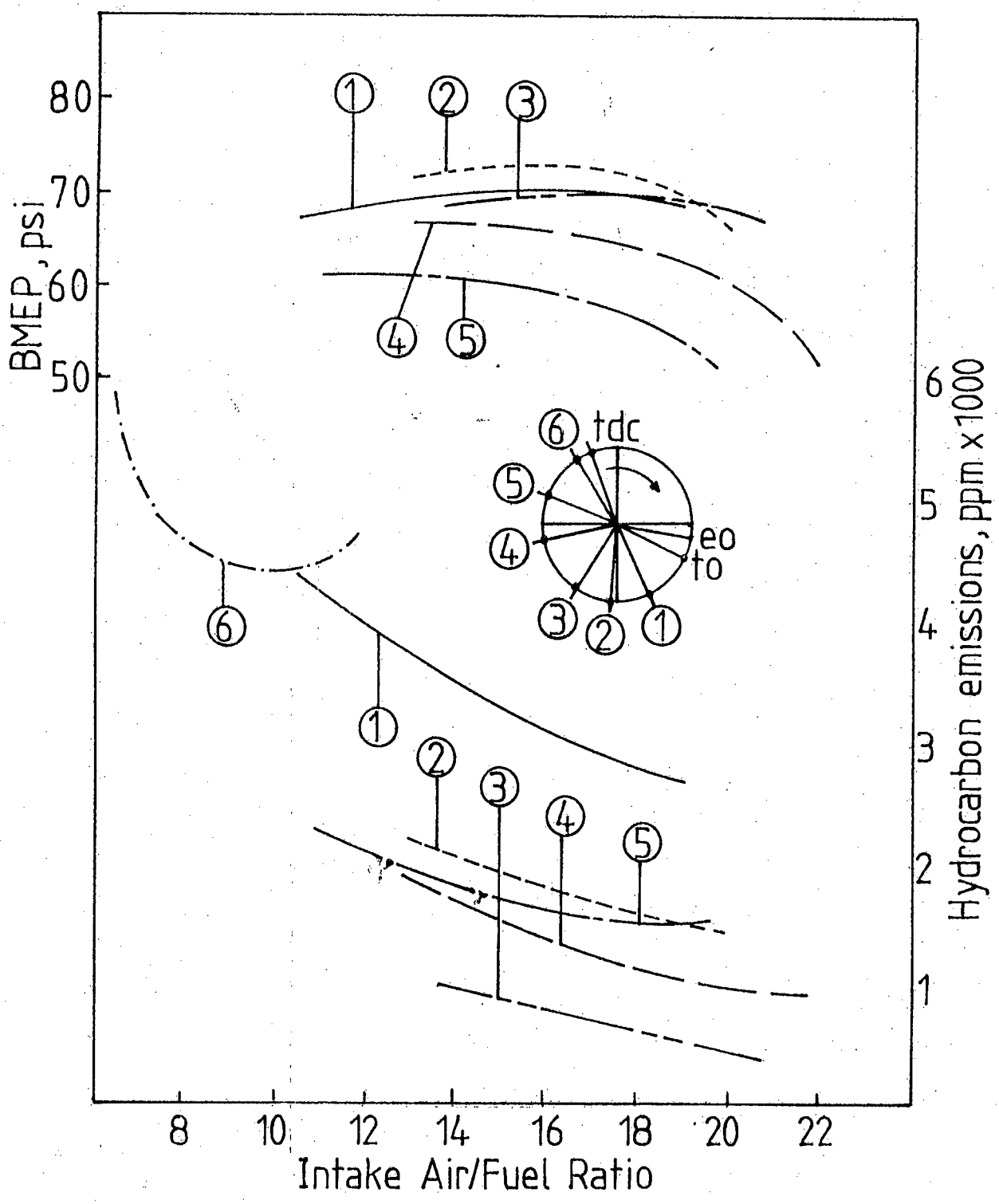

Figure 2.2 The Effect of Injection Timing

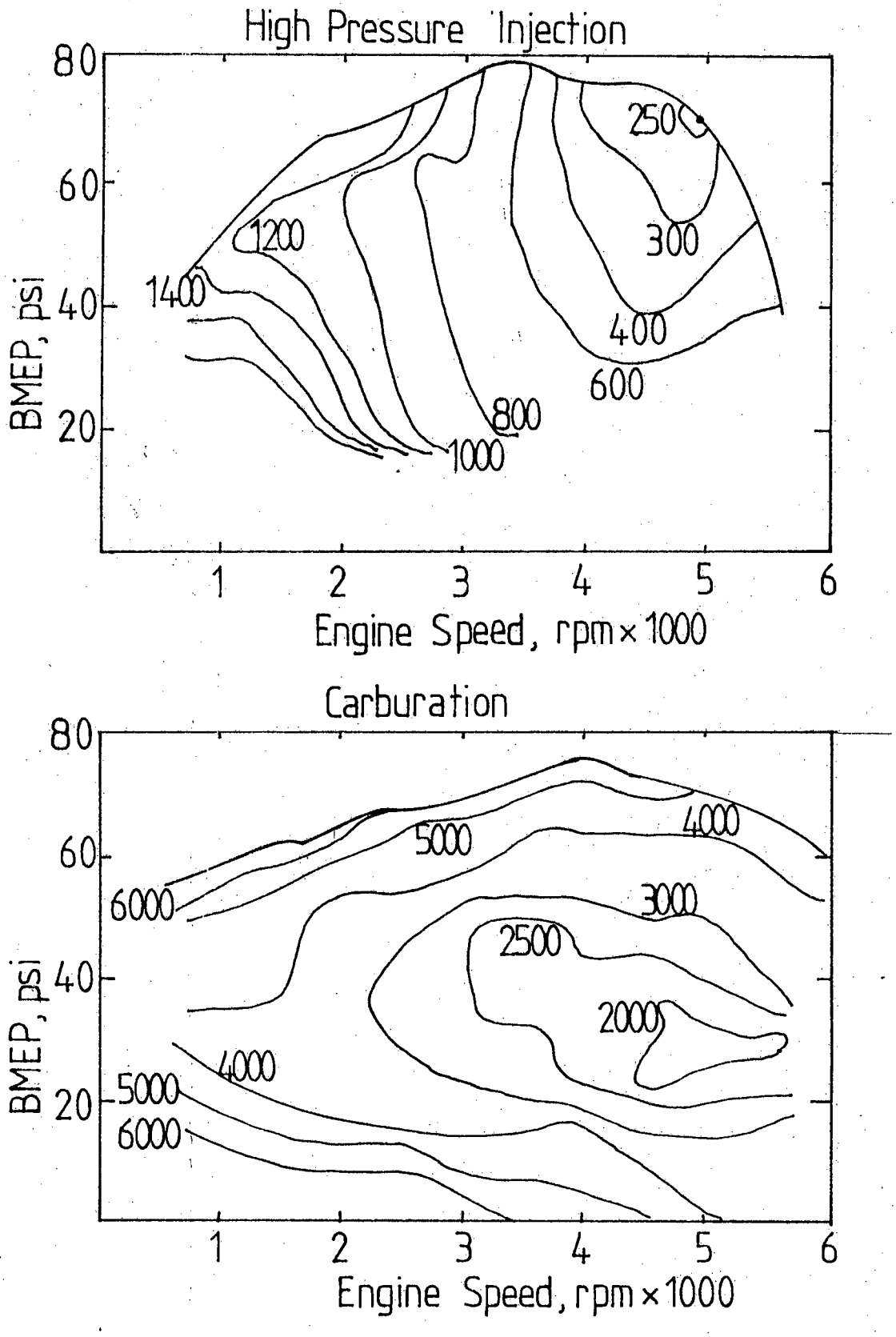

Figure 2.3 Hydrocarbon Emissions, ppm

The significance of the above becomes clear if the hydrocarbon emissions at a constant speed are considered. For the carburetted engine at 3000rpm, for example, the hydrocarbon emissions decreases from 6000ppm to 3000ppm as the load drops by 75%. This is explained by a graph of trapping efficiency versus delivery ratio,(**Figure 2.4**).

As the load drops so the delivery ratio decreases with a corresponding increase in trapping efficiency, i.e. decreasing percentage of hydrocarbons in the exhaust gases. As the load drops further, the sudden increase in emissions is due to irregular of incomplete part load combustion.

For the injected engine, however, at 3000rpm, for example, as the load drops, the percentage of hydrocarbon emissions remains at a relatively constant low value (700ppm) indicating that losses through short circuiting and mixing have been reduced over the full range of loads. The high emissions at low speed is once again due to irregular combustion.

2.2.5 Fuel Control.

The fuel metering was achieved by detecting engine speed by force of a flyweight and the load by throttle position. The following reasons were given for not using the inlet manifold pressure as an indication of load as is common practice on four-stroke engines.

* The absolute value of the intake manifold pressure of a two-stroke is small.
* The negative pressure in the manifold does not represent the delivery ratio.

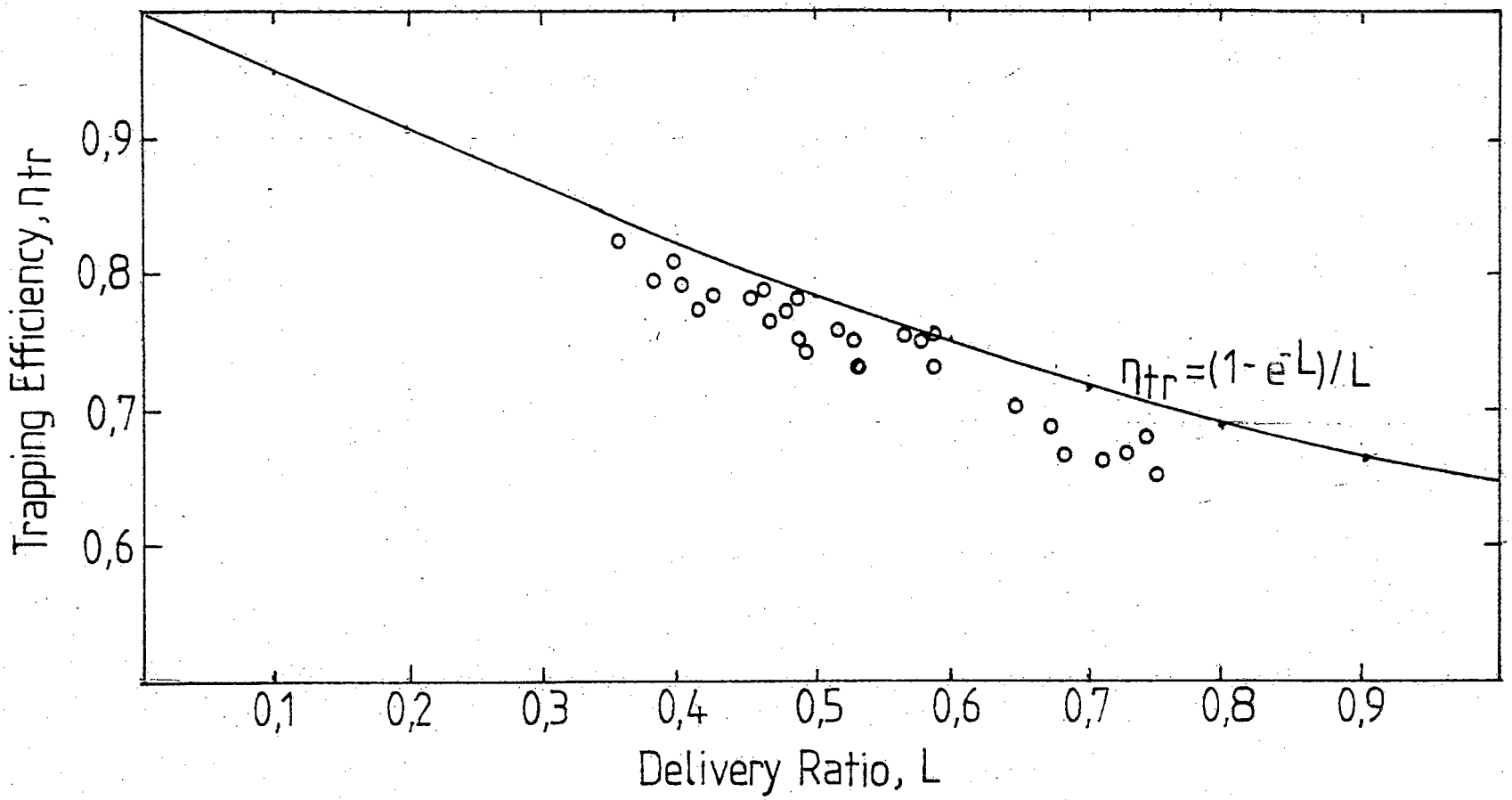

Figure 2.4 Trapping Efficiency vs Delivery Ratio

* Even if the delivery ratio were detected, there is a considerable difference between it and the charging efficiency.
* In order to obtain the fuel quantity to be injected corresponding to the charging efficiency, it is necessary to detect the engine speed.
* Change in manifold pressure lags change in engine operating condition. In terms of response therefore, it is inferior to a system based on throttle angle.

The values of the displacement of the controller for the fuel quantity as determined by throttle position and the force of the flyweight, are represented by the curved surface of a cubic cam, and its movement was transmitted to a control rod by a follower equipped with a roller and link. The cubic cam therefore acts as a mechanical memory system.

Even though the above system appears to work for the engine involved, it is certainly not correct, in general, to assume throttle position has a linear relationship with engine load. The engine used in this thesis had a very non-linear relationship between throttle position and load.

The above control system implies high cost of manufacture and maintenance, and coupled with the high speed limitations of the fuel pump, would discount high pressure fuel injection as being a reasonable means of reducing the bsfc of a two-stroke engine.

2.3 Low Pressure Fuel Injection.

Vieillident, in his design of a low pressure electronic fuel injection system [6], reports good reductions in bsfc and hydrocarbon emissions.

Typically a reduction of 35% in bsfc (to a best value of 295g/kWh) and by a factor of 3 in hydrocarbon emissions with no power loss is reported, making performance comparable to similar capacity four-stroke engines.

These results were obtained with a crankcase scavenged, piston ported, 115cc two-stroke engine of the Schnurle scavenged type. The electro magnetically operated injector was located directly opposite the exhaust port at an optimum to 20° crank angle after exhaust port opening. Fuel was supplied at a pressure of 2 bar (29psi) from a diaphragm pump.

2.3.1 Nozzle Modification.

The amount of fuel injected was controlled by a rectangular voltage pulse of varying duration which controlled the opening time of the injector through a high voltage (300-400V) capacitor discharge circuit. The injection time for maximum discharge was 2,5 milliseconds. Commercially available fuel injectors operating off a 12 volt supply typically require 0,8-1,0 milliseconds to open. This implies the capacitor discharge firing must open and close the nozzle extremely rapidly to allow the full range of fuel requirements to be spaced into 2,5 milliseconds.

The modifications made to the injector are outlined only very briefly. In hindsight, this aspect appears crucial to the successful use of fuel injection and should certainly have merited more attention. Judging from what information is given, it appears the stop ring of the injector pintle was removed allowing variable lift depending on the time of excitation. This would give a ballistic motion to the pintle as it opened against the return spring. No information was given regarding the modified flow curves.

2.3.2 Control System

The length of the injection pulse at any particular load and speed was stored in one of two memory systems.

The first was an opto-electronic system which scans an optical memory depending on the throttle position and engine speed. The memory comprises of a photographic disc of varying photometric density. The disc is rotated by a servomotor controlled by the engine speed and scanned radially by an infra-red photocoupler linked to the degree of throttle opening. The varying permeability of the disc to infra-red light at each speed and throttle position determines the length of the control pulse.

This obviously proved to be an expensive and cumbersome system. The alternative system used a microprocessor with a 1024 word memory capacity. Engine speed and throttle position were once again used as address parameters. Out of the 10 address bits, 6 were assigned to speed giving 100rpm calculation steps and 4 assigned to throttle opening giving calculation steps of 1/16th throttle opening. At the time of publishing, (1978), this system was still under development.

Unfortunately, no indication is given in the results as to which of the above systems produced the quoted results. Either way both should prove costly to produce.

Other advantages reported by Vieillecent are;

* better cyclic regularity, especially at low revs
* better pick-up during acceleration

* the air/fuel ratio is kept within tighter limits than with a carburettor.

2.4 Low Pressure, Manually Controlled Fuel Injection

In order to clarify the situation arising out of other small engine manufacturers' unpublished results disagreeing with those of Vieillident, Blair (et al) [7] conducted a study into fuel injection of a two-stroke cycle spark ignition engine.

2.4.1 Results

The results in this study show that very little improvement in bsfc was possible without a considerable loss of power. This indicates a reduction in short circuiting of fuel but only with lean air/fuel ratios.

By replacing the carburettor with an injector at the inlet, the performance of an engine with a 'perfect' carburettor can be approached. Considering then, the improvements in bsfc of direct injection (as per Vieilledent), over that of inlet injection, (perfect carburettor), are so small as to be offset by its high cost. A 30% improvement in bsfc was possible, 20% of which was accounted for by use of leaner mixtures, with 5% power loss, and the other 10% by direct fuel injection but with a further 10% loss of power.

2.4.2 Experimental Procedure

The engine used was a Yamaha YB 100cc. It is a single cylinder, disc valve controlled induction, two-stroke. The injector used was a Bosch unit as used in the L-Jetronic system for four-stroke automobile engines. The injector was

modified to reduce fuel flow rate and was supplied with fuel at a pressure of 280kPa (40psi), by a small electrical pump. As for Vieilledent, no indication was given as to the nature of the modification.

The injector electronic control was manual with two control circuits being tested. One was a conventional 12 volt square wave generator triggered by an inductive pick-up on the crankshaft. This was cheap to produce but showed up speed limitations due to injector lag as a result of the low voltage applied to the injector.

The second system used a capacitor discharge circuit (similar to that used by Vieillident) enabling injector opening times to be dramatically reduced in comparison.

Blair used four injector locations:

1. Inlet injection
2. Transfer port injection
3. Direct injection
4. Direct injection with a swirl chamber.

Inlet injection provided the best overall results in terms of bsfc and power. This indicates the advantages of open cycle direct injection are minimal.

It is felt however that Blair has not thoroughly investigated the matter. As pointed out by Vieilledent, fuel spray pattern and supply pressure are crucial and no mention is made of these parameters in Blair's study. Furthermore, the length of the timed pulses used is not mentioned and therefore, a complete analysis is not possible. The reason for this being, the shorter the timed pulse, the less chance there is for fuel to escape to the exhaust port.

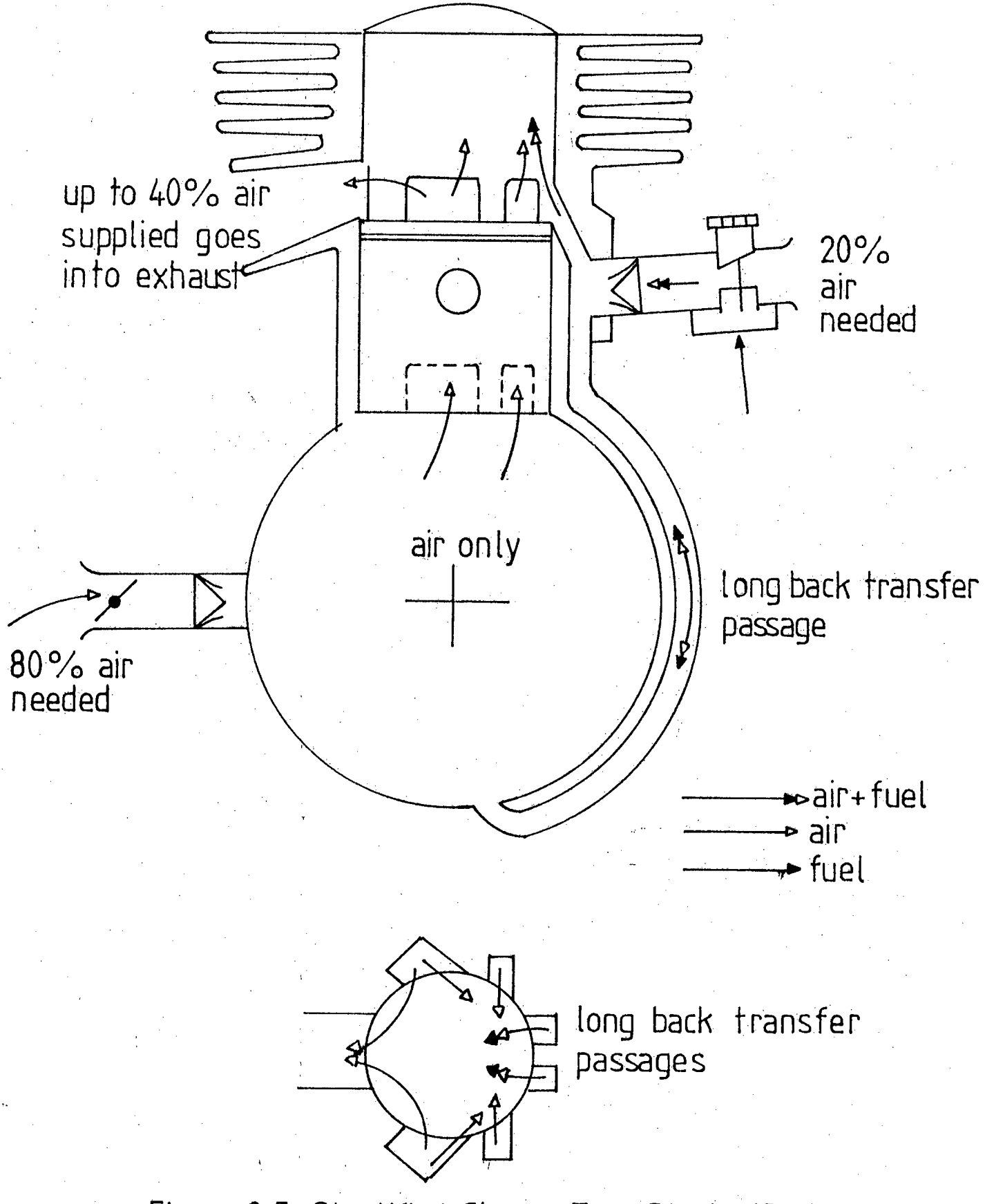

Figure 2.5 Stratified Charge Two-Stroke (Blair)

In both the previous studies, no mention is made of the transfer port layout. Vieilledent emphasizes that the success of direct injection relies on the 'aerodynamic wall' set up between fresh gases and exhaust gases during scavenging. The existence of this wall is very strongly dependent on the transfer port layout.

Since the overall results of the study were not promising, no indication was given on what parameters would be used for fuel control in a production engine. Another view on this subject would have been interesting.

2.5 Alternative Methods of Stratified Charging.

2.5.1 Stratified Charge Engine No.1

In a paper on the reduction of fuel consumption for a two-stroke engine, [8], Blair, et al, present a design of a two-stroke engine that reduces bsfc to well within four-stroke engine levels, (260-340g/kWh).

The basis of the design involves the stratification or separation of a rich air/fuel mixture from the exhaust gases by fresh air or a lean air/fuel mixture. **Figure 2.5** illustrates the operation of the engine.

The unusual features of the power unit are:

* two entries for air to the crankcase, one of them inducing a rich air/fuel mixture and the other containing air only, but both are throttled and the throttles are linked mechanically.

* a long back transfer port connecting the bottom of the crankcase with the cylinder wall opposite the exhaust port.
* the air only induction to the crankcase is shown here as being via a reed valve and induces some 70-80% of the required air at any speed and load.
* the air/fuel induction through a carburettor is shown as being via a reed valve into the long back transfer port and induces some 20-30% of the required air at any speed or load.
* further conventional transfer ports connect the top of the crankcase with the cylinder and pass air only as the rich mixture is gas dynamically retained in the long rear transfer passage.

The combined effect is that little or none of the fuel reaches the crankcase and when the scavenge process commences with the opening of the transfer ports, a stratified charging process begins with air only in the proximity of the exhaust port. Hence most of the fresh charge lost from the cylinder will be of air only composition at best, or a very lean air/fuel ratio mixture in the worst case.

The performance characteristics of the 400cc tested engine are quite remarkable. For example, 32,8kW/litre was produced at a modest speed of 5500rpm. The bsfc ranged over most operating ranges between 260 and 340g/kWh. This was achieved without the aid of an expansion chamber exhaust pipe found on most two-strokes. Also worth noting are the high overall air/fuel ratios (16:1-20:1), indicating that the stratified charging process works and that much of what is lost out of the fresh charge during scavenging is air only.

The only problem associated with the above engine is a sharp drop in power (18%) over the speed range 4000rpm to 5500rpm. This occurred at an air/fuel ratio of 21:1 and was attributed to pressure wave resonance in the long back transfer passage. However, if the air/fuel ratio is decreased to 17:1 this phenomenon disappears with little change in bsfc.

A follow up study [9] using exhaust pipe tuning reported further improvements in performance and bsfc.

The achievement of such a simple solution to the problem of high bsfc of two-stroke cycle engines is remarkable. Blair concedes that much work is still required to fully understand the operation of the engine. Unfortunately, substantial financial backing would be required to build even a prototype engine. Furthermore much trial and error experimentation involving varying scavenging patterns would be necessary to optimise the engine. This would involve further expense that is beyond the financial budget of a masters thesis.

2.5.2 Stratified Charge Engine No.2 - MULS.

A new method for stratified charging a two-stroke engine has recently been developed [10] called Multi-Layer Stratified Scavenging (MULS). The new method separates the air/fuel mixture into a rich and a lean mixture between the inlet manifold and transfer ports. The lean mixture is used to clear the engine of exhaust products while the rich mixture is kept remote from the exhaust port thereby reducing loss of fuel by mixing and short circuiting.

Two types of MULS engines were developed.

Type A. MULS Engine.

Figure 2.6(a) schematically describes the type A engine. Two separate transfer passages lead up to the three transfer ports. The passage nearest the exhaust carries the lean air/fuel mixture and splits into two transfer ports. The passage nearest the inlet carries the rich mixture.

The authors observed the presence of a film of fuel on the walls of the crankcase, attributing its presence to centrifugal force induced by the rotating crankshaft. By placing the entrance to the transfer passage at an appropriate place, this film of fuel was 'tapped off' into the transfer passage leaving a lean fuel/air mixture to be pumped into the other transfer passage. The transfer port furthest from the exhaust therefore has a rich mixture and the two ports nearest the exhaust a lean mixture. Most of what is lost through short circuiting and mixing should therefore be a lean mixture.

The reported results for a 175cc type engine, indicate a best bsfc of 300g/kWh and between full and half load the bsfc is lower than 370g/kWh. An interesting point is that the bsfc appears to be strongly dependent on the load, whereas the speed appears to have a small effect. However, as the speed increases, the bsfc does decrease slightly indicating the separation of the rich and lean mixtures is dependent on the increasing centrifugal force acting on the fuel film in the crankcase at increasing speed.

The type B MULS engine appears to produce better results than type A with an even less complicated transfer passage design.

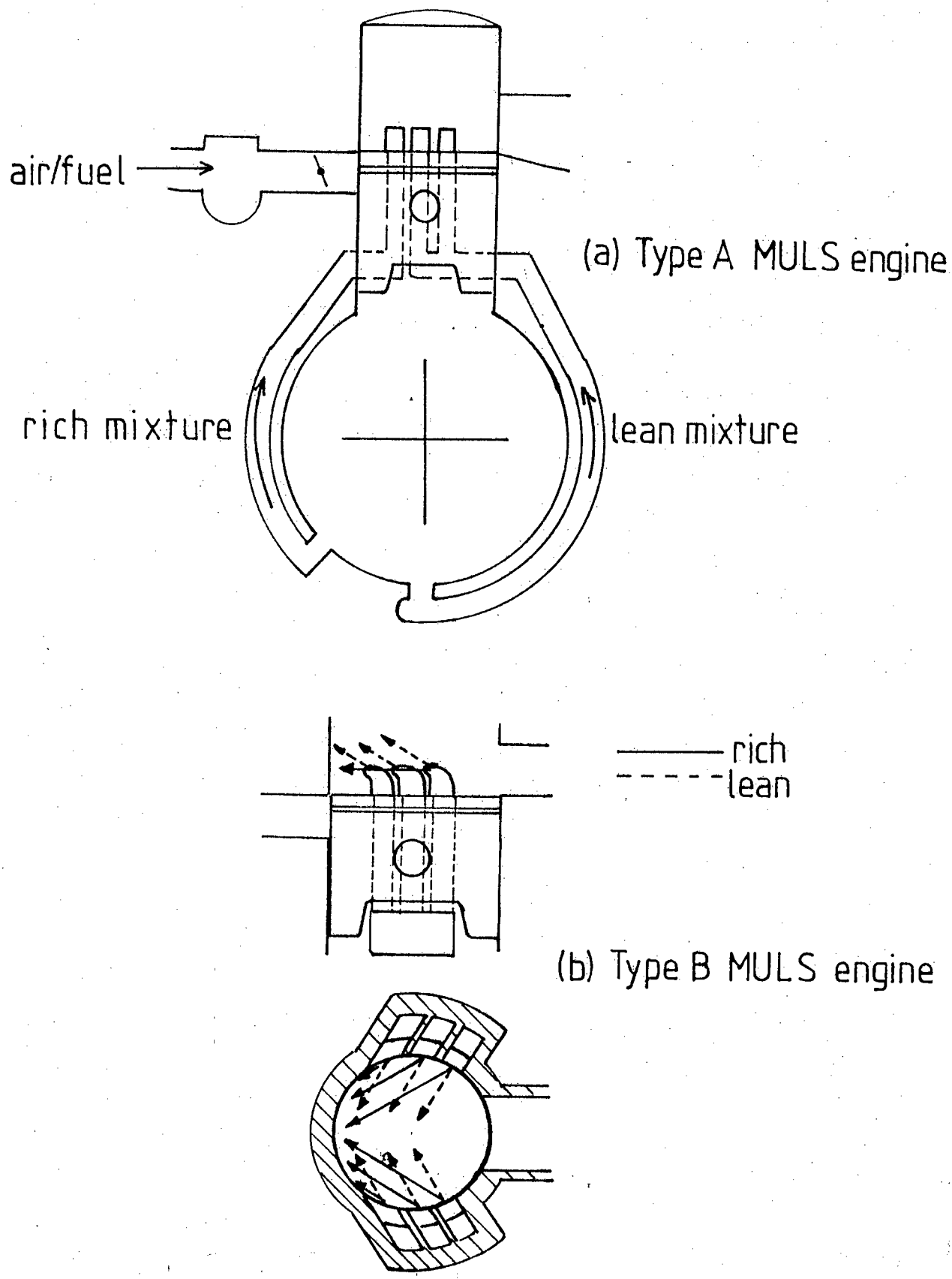

Figure2.6 MULS Type A and B

The operation of the type B engine relies on the fact that liquid fuel tends to adhere to the walls of the transfer passages and actually enters the cylinder as a liquid film from the top wall of the transfer passage.

Having observed this phenomenon, Oneshi, et al, set about producing a transfer passage and port design that would direct this liquid film towards the rear of the cylinder, leaving the hopefully lean air in the remainder of the passage to scavenge the cylinder of exhaust products. **Figure 2,6(b)** shows details of the transfer passage design. The performance of a 372cc type B engine produced a best bsfc of 241g/kWh and worst value of 414g/kWh.

For both the above designs a great deal of trial and error experimentation was necessary to achieve correct scavenging patterns. The results indicate success at preventing short circuiting of fuel. Type B appears to be superior to type A in both simplicity of construction and performance. For type A, one would certainly expect a resonance phenomenon in the long transfer passage to upset performance, as was reported by Blair. Type B would obviate this drawback.

The type B engine shows great promise, but would necessitate large financial support to manufacture the various cylinders necessary to test a running engine.

CHAPTER THREE

3. Theoretical Evaluation.

The previous chapters analysis of others work, shows that the success of stratified charging a two-stroke engine lies in the ability to retain the fuel as remote from the exhaust as possible, while purging the exhaust gases with a very lean air/fuel mixture.

Since a manually controlled fuel injection system provides the least expensive and perhaps easiest method of modifying an existing engine, it was decided that this path should be pursued.

In order to retain the injected fuel on the opposite side of the cylinder to the exhaust, four injector locations and spray patterns were proposed, **(Figure 3.1)**

Figure 3.1(a) shows a split divergent spray emanating from opposite the exhaust port. It was proposed that the spray would become entrained in the incoming air from the side transfer ports and be retained at the 'back' of the cylinder by this air. The injector was located at transfer port height, between the two rear boost ports.

Figure 3.1(b) shows a spray pattern directed up towards the cylinder head which is nearly as remote from the exhaust port as the back wall of the cylinder. This is essentially the same location as in **figure 3.1(a)**, but with a different spray pattern.

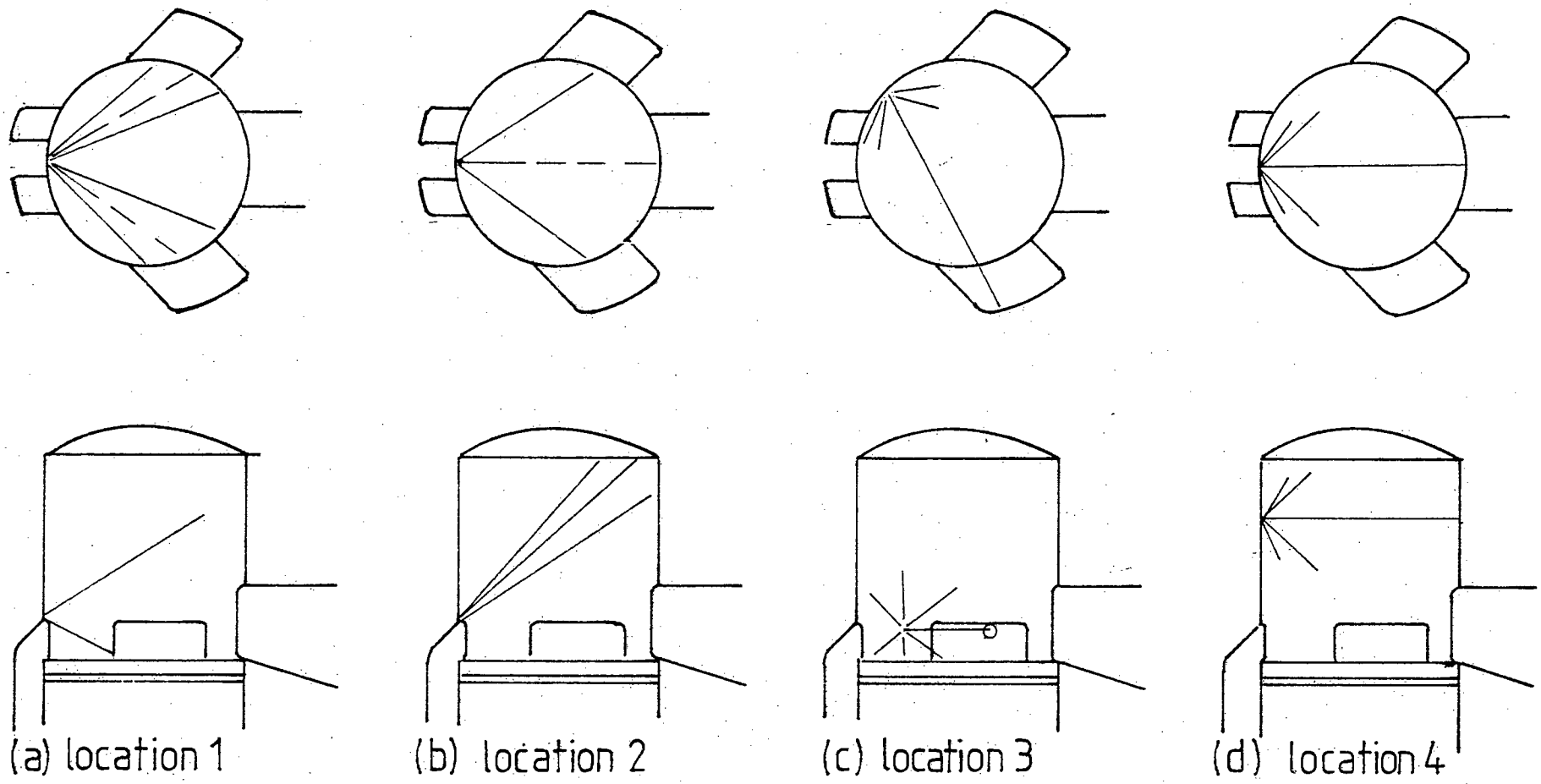

Figure 3.1 Proposed Injector Locations and Spray Patterns

Figure 3.1(c) shows injection from the side transfer port across the cylinder in a thin jet that should hit the opposite wall and disperse the fuel. The point of contact was chosen to lie between the main side transfer port and the rear boost port, where it was expected that turbulence between the incoming jets of air may assist in the evaporation of the fuel and furthermore help retain the fuel at the back of the cylinder.

Figure 3.1(d) illustrates injection from a point above the exhaust to a point directly opposite on the back wall of the cylinder. The dispersion of the fuel here, should occur in a strongly rising column of air up the back wall. Once again a thin jet was required to stand least chance of fuel becoming entrained in the exiting exhaust gases as the jet passed across the cylinder. Unfortunately higher than normal injection pressures would be necessary at this location as the nozzle was located such that it would be exposed to high pressures encountered in the closed cycle that might cause the injector to open when least required.

Injection into the rear boost port was not considered as the airflow to the port was cut off by the piston skirt as bottom dead centre was approached. This would occur when the aerodynamic wall is expected to be at its strongest, thereby leaving fuel in the boost port, only to be lost in the initial purging of exhaust gases in the following cycle.

In all cases a modified electro-magnetically operated injector will be used. The amount of fuel to be injected was controlled by the length of a timed rectangular 12 volt pulse. The length of this pulse was controlled manually. Furthermore, the timing of the pulse in relation to the crankshaft angle was varied by a manually controlled delay function.

To provide minimum chance for short circuiting of fuel of would be necessary to delay the injection of the fuel as late as possible before the injector was covered by the piston.

The supply pressure to the injector was variable to observe the effect of injection pressure on the bsfc. It was hoped that there would exist an optimum pressure that would cause good atomization and combustion.

Experimentation will either substantiate or disprove the above proposed theories. Should the results show substantial reductions in bsfc, then it will be necessary to propose a theory that would relate the amount of fuel required to the amount of air delivered to the engine. If the results show no reduction in fuel consumption, then the most logical step would be to examine the scavenging patterns to attempt to explain why stratification of the fuel is not occurring. The scavenging patterns are strongly dependent on transfer passage layout. Since this is unalterable for a particular engine it would be necessary to perform this scavenging analysis on a design of proven performance to provide a basis for comparison.

CHAPTER FOUR

4. Experimental Apparatus and Procedure.

In order to provide a basis for comparison for a fuel injected engine, it was necessary to test a standard two-stroke engine over its full range of load and speed before modifications were made.

4.1 Tested Engine.

The engine chosen for the tests was a Yamaha YBF 125cc, two-stroke spark ignition engine. The major reason for the choice of this particular power unit was that the rotary inlet valve would allow much greater freedom of choice for location of the injector than would a piston ported inlet engine.

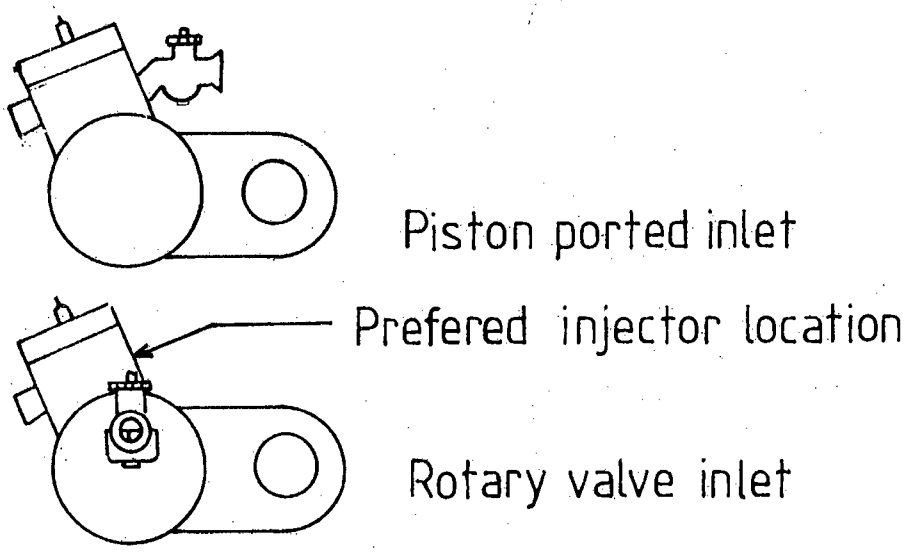

Figure 4.1 Carburettor Locations for Piston Ported and Rotary Valve Engines.

Figure 4.1 shows that the most favourable location of the injector as determined by previous researchers is located where the carburettor is situated on a piston ported engine. As was subsequently determined, it was necessary to run in both carburetted and injected modes alternately.

A further essential requirement was the use of an automatic lubrication device. separate to the fuel system that would inject oil into the crankcase. An engine using a pre-mixture of oil and petrol would therefore be unsuitable as once the fuel supply to the carburettor was cut off, the engine would be starved of oil. The Yamaha YBF 125 was equipped with an 'autolube'' device that injected oil into the incoming airstream between the carburettor and the crankcase. The quantity of oil injected was varied according to the throttle opening.

The ignition was of the magneto type with contact breaker, spark timing set at 15° btdc.

A list of the engine specifications is given in **Table 1.**

Initial tests on the engine showed power to be some 10%-20% less than expected with the torque dropping off rapidly during tests at full throttle. With airflow measuring devices removed, this proved to be repeatable. The exhaust pipe supplied with the engine was scrapped and an expansion chamber was designed and fitted.

Much investigation has gone into this aspect of two-stroke engines and has been finely detailed by Blair [11]. The principle on which an expansion chamber operates is briefly outlined below. For interested readers details are given in Appendix B.

ENGINE SPECIFICATIONS

Model	Yamaha YBF 125
Displacement	123cc
Bore x Stroke	56mm x 50mm
Trapped compression ratio	6,1:1
Connecting rod length	120mm
Inlet port opens	106° btdc
Inlet port closes	37° atdc
Exhaust port opens	98° atdc
Main transfer port opens	120° atdc
Boost transfer port opens	124° atdc
Number of exhaust ports	1
Number of transfer ports	4
Effective exhaust port area	$547mm^2$
Effective transfer port area	$723mm^2$
Gear ratios: 1st	9,8:1
2nd	5,8:1
Spark timing	15° btdc
Carburettor	24mm Mikuni

Table 1

Referring to **Figure 4.2** the expansion chamber consists of a header pipe, diffuser cone, a straight section and a reflecting cone with an outlet attached. Blowdown commences as the exhaust port opens, sending a positive pressure wave along the header pipe to the cylinder. This helps scavenge the engine of exhaust products. The positive pulse travelling towards the outlet, is reflected as positive pulse by the converging cone and travels back towards the exhaust port. This reflected positive pulse hopefully returns some of the fresh gases lost through short circuiting and mixing back into the cylinder as the piston closes the exhaust port.

The expansion chamber can only work well at design condition which will be over a limited speed range. The pipe fitted to the engine was designed, according to Blair, to operate at 6000rpm.

4.2 Dynamometer.

The engine drove a Heenan and Froude 'Dynamatic' dynamometer via a universal coupling attached to the gearbox output shaft.

The maximum power absorption of the dynamometer was 225kW at 10,000rpm. The maximum output from the engine was 7kW. To obtain a reasonable range of torque readings, it was necessary to run the engine in first or second gear. This, however, produced a very small speed range of up to one tenth of the full scale analogue read-out. It was therefore necessary to detect the engine speed separately.

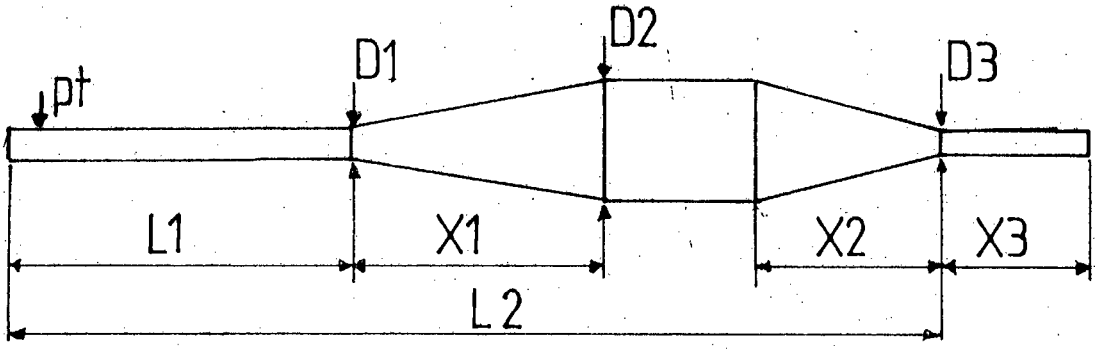

Dimensions (mm)

L1 = 420	D1 = 35
L2 = 1040	D2 = 70
X1 = 330	D3 = 20
X2 = 220	
X3 = 220	

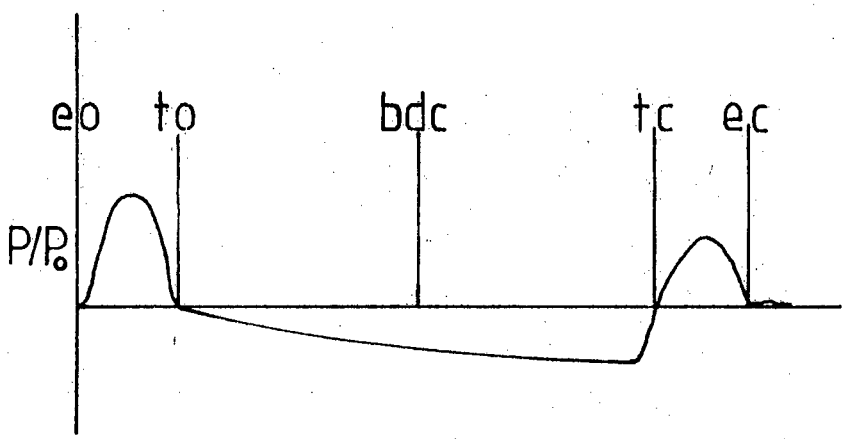

Desirable pressure-time history at point pt.

Figure 4.2 Expansion Chamber Design.

This was done with an optical pick-up that sensed the frequency of rotation of an aluminium disc attached to the engine magneto. The disc had sixty slots cut on its periphery. The pick-up's infra-red beam was interrupted by these slots and the resultant 12 volt square wave signal sent to a universal counter/timer. The reading gave crankshaft speed in revolutions per minute. This was checked with a Jaquets indicator and on an oscilloscope.

4.3 Fuel Consumption.

Fuel consumption was measured by noting the time taken for the engine to consume 161ml of fuel.

4.4 Airflow Measurement.

Airflow into the engine was measured by the tank and orifice method. The tank measured 0,4m x 0,4m x 0,6m and was connected via a 60mm diameter flexible hose to the air inlet of the engine. A point to note here is that the inlet to the engine is not the mouth of the carburettor, but an engine casing that surrounds the carburettor. If the tank had been connected directly to the carburettor, it would have been necessary to use a connecting hose having an area some forty times that of the carburettor throat. This is pointed out by Blair[12] as being necessary to avoid altering the normal pressure pulsation characteristics that are so important to the operation of a two-stroke engine. The engine casing surrounding the carburettor acts as a damping device for any pressure pulsations that may arise in the hose connecting the tank to the engine.

The orifice plate had a diameter of 32mm and was made according to BS 1042 (13).

The maximum pressure drop across the orifice plate was 180Pa and was measured with an inclined manometer calibrated to be read directly in Pascals.

4.5 Injector Calibration.

4.5.1 Injector Firing Circuit.

The injector used was a commercially available, electromagnetically operated unit made by Bosch. A previous study in this field used two types of injector firing circuit. The first was a low voltage 12 volt circuit that used variable pulse lengths to control fuel quantity with a constant fuel supply pressure. This system is used on many fuel injected four-stroke engines. The second system used a capacitor discharge circuit that employed a capacitor charged to approximately 400 volts and then discharged across the injector coils to open the injector. The opening times could then, theoretically, be drastically reduced. Vieilledent managed to obtain maximum discharge in a pulse width of 2,5ms using this technique. However, by varying the modified injector orifice size and the supply pressure, it would be possible, using the 12 volt system, to obtain the required fuel flow rates within a sufficiently short pulse length. It was therefore decided to use a 12 volt system. The minimum pulse length to which the injector would respond with the 12 volt system, was 0,7ms.

4.5.2 Pulse Shaping and Delay Function.

The trigger signal for the pulse shaping circuit was provided by an optical pick-up that sensed the passing of a single slot in the aluminium disc attached to the magneto. This slot was timed at top dead centre. The optical pick-up provided a neat 12 volt rectangular pulse. The use of the optical pick-up was thought to be superior to an inductive pick-up which would provide a noisy signal of varying amplitude.

When the trigger signal was connected into the pulse shaping circuit it was discovered that the amplitude dropped from 12 volts to 2 volts. This was thought to be due to mismatched impedances and as result failed to trigger the circuit. An inverting amplifier was used to correct this fault.

The pulse shaping circuit consisted of three 555 timers as shown in **Figure 4.3.** The first timer, IC1, was connected in Schmitt trigger mode. This converts any input signal into rectangular output signals. These signals are fed into IC2. This timer performs a delay function, controlled by the potentiometer P2 and had a maximum value of 18ms. The third timer, IC3, was used to control the pulse width. This has a maximum value of 6ms. For those interested, a detailed account of the operation of this circuit is given in Appendix C.

4.5.3 Fuel Pressure Control.

A variable fuel pressure supply was used to observe the effect that this parameter had on engine performance.

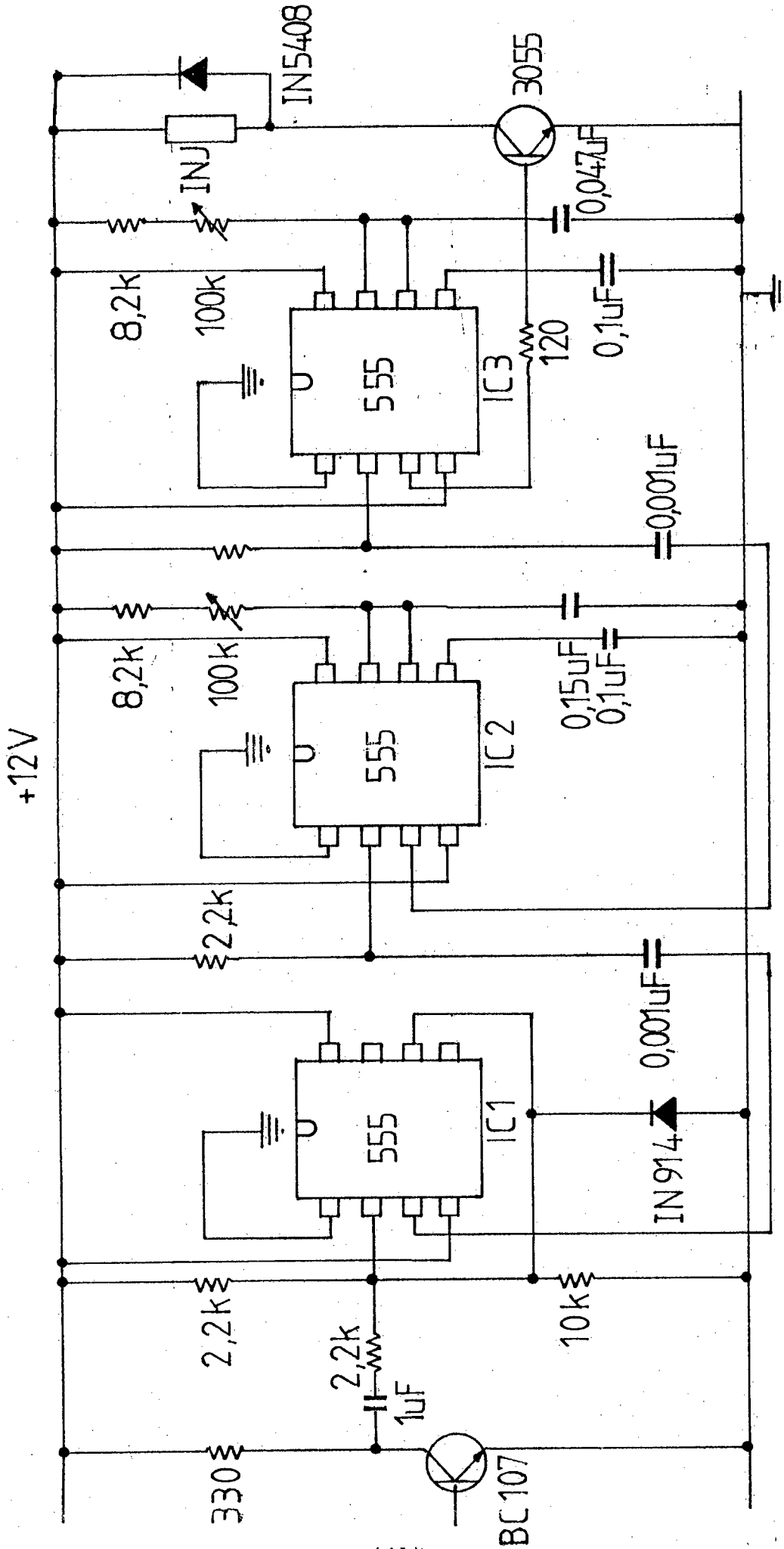

Figure4.3 Injector Control Circuit

Figure 4.4 shows the fuel supply system used. A small gear pump was capable of supplying fuel at a maximum pressure of 6 bar. The pressure was controlled by a regulator and bypass valve in parallel. The two taps are shown in the run position when the overflow from the regulator is passed through the measuring bottles back into the fuel tank. In the measuring mode, both taps must be operated simultaneously, shutting off fuel supply from the tank and allowing fuel from the measuring bottles to flow into the pump inlet reservoir.

4.5.4 Injector Modifications.

The injectors used in this project were calibrated using the above fuel pressure control, injector firing and pulse shaping circuits, together with a function generator in the square wave mode. This simulated the optical pick-up output of a running engine.

Using a standard injector, the flow rate proved to be some five times too high. It was necessary therefore to find some means of reducing this flow rate. **Figure 4.5** shows the pintle of the injector shaved off and an orifice plate placed in front of the nozzle. A housing was placed over the orifice plate to hold it in place. This was done by cutting a thread on to the injector and bolting a pipe nut over the housing.

By varying the orifice size and supply pressure, suitable flow rates could be achieved.

The spray pattern would have to be altered. This was done by placing an obstruction of the appropriate shape in the path of the jet. This obstruction formed part of the housing and its various forms are shown in **Figure 4.5.**

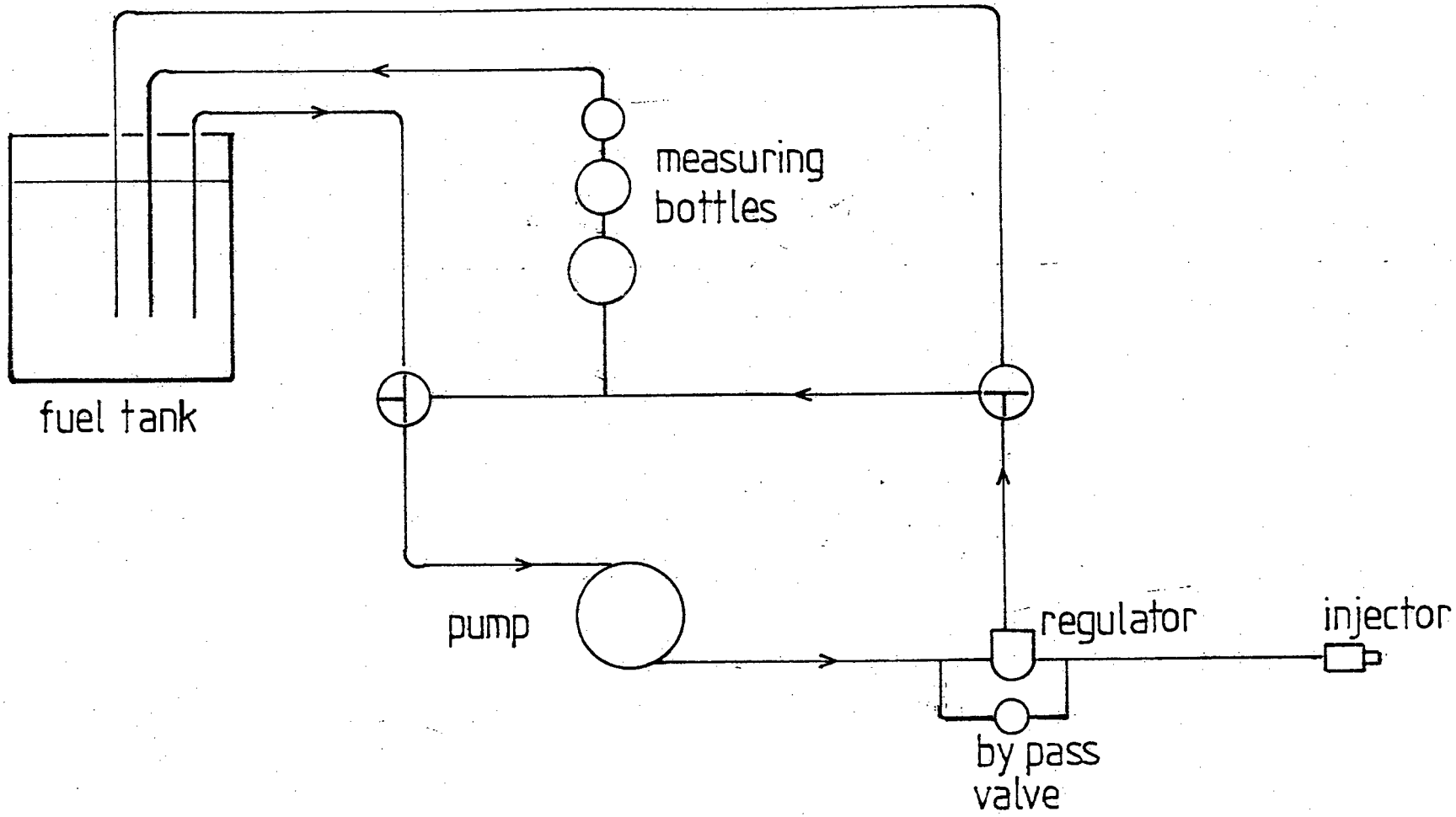

Figure 4.4 Fuel Pressure Control

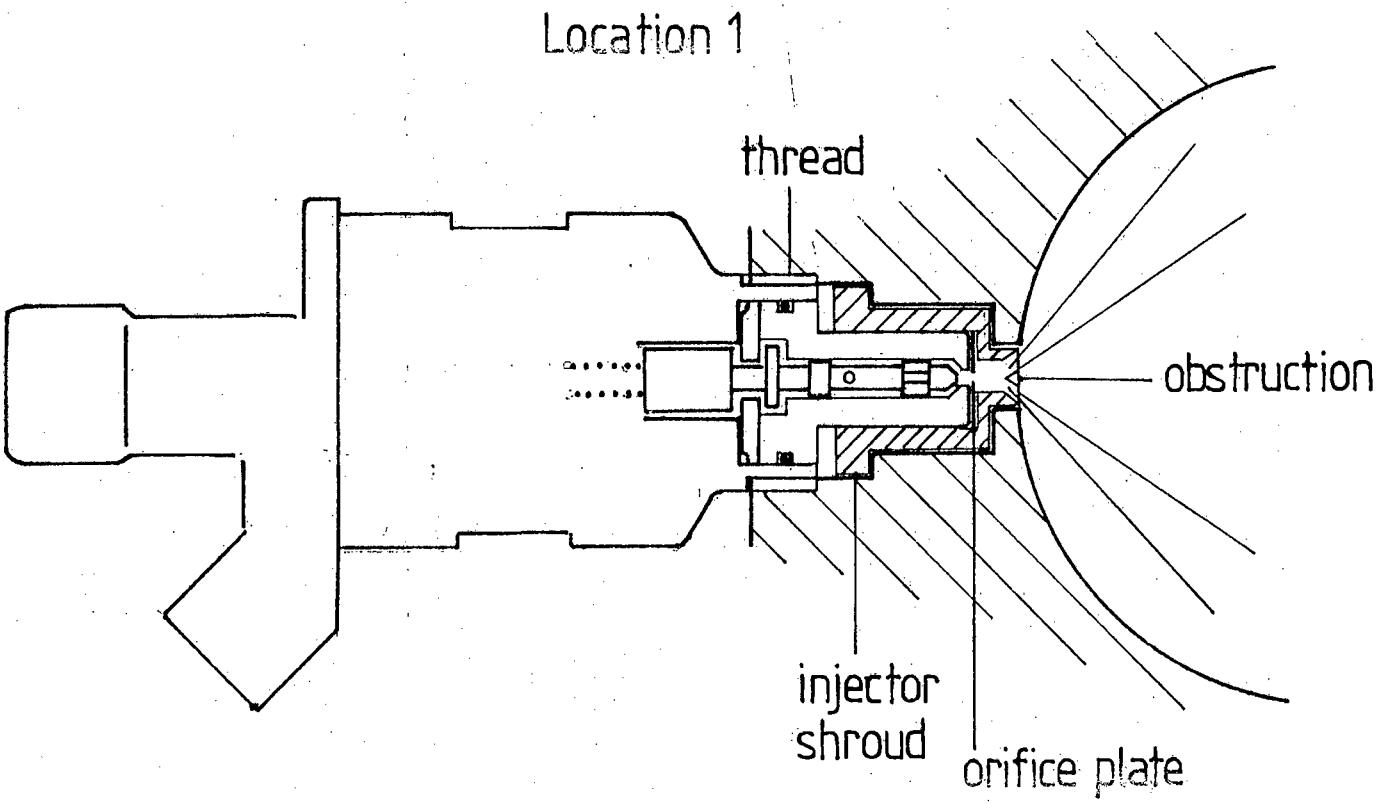

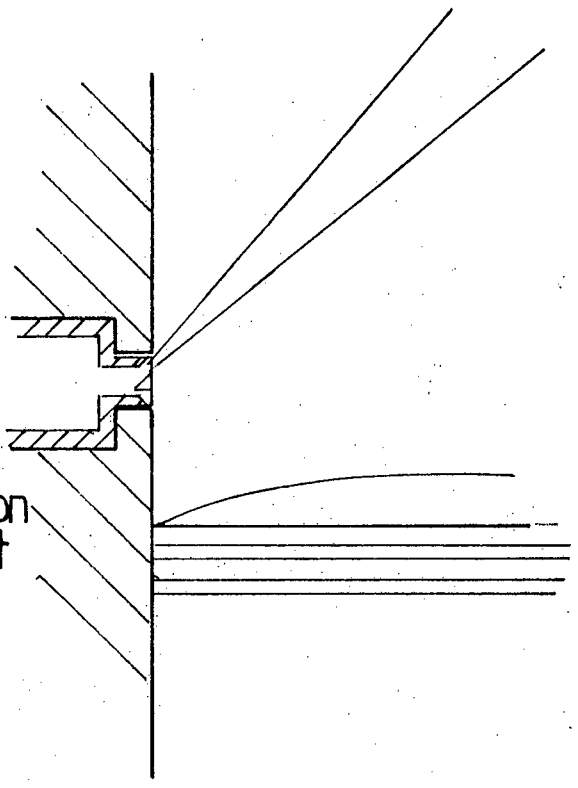

For locations 3 and 4 no obstruction was placed in front of the fuel jet

Figure 4.5 Injector Modifications

4.5.5 Ancillary Equipment.

A thermocouple was attached to one of the cylinder head nuts. The output was fed into a digital read-out, calibrated to be read in degrees centigrade.

A large centrifugal blower was used to cool the engine and a similar fan used to extract the exhaust gases from the test cell. A cell vent maintained the temperature at atmospheric levels.

Having detailed the apparatus required to test the standard and modified engines, it is now necessary to outline the test procedure.

4.6 Test Procedure.

4.6.1 Standard Engine.

The standard engine was run at its full range of loads and speeds. The torque, speed, fuel time, air flow and cylinder head temperature were noted in each case. The dynamometer control appeared to hold a constant speed while varying the torque, rather better than vice versa.

In the standard form, the engine had several running points for which it was difficult to collect data. This was due to misfiring which caused the torque and speed to fluctuate by some 5% and 10% respectively, about a mean.

4.6.2 Injected Engine.

To avoid problems associated with cold starting, it was necessary to run the engine in the carburetted mode from a separate fuel supply. This supply was then shut off. When the first indication was given that the float chamber was running dry, the fuel injection system was switched on having been set to run at the particular engine condition chosen, (i.e. carburettor fuel flow was noted and the injection pressure and pulse width set from calibration curves to match this flow rate).

Once in the injection mode, the engine proved to be sufficiently 'flexible' to be moved from one load and speed condition to the next. It was necessary to vary the injection delay (injection timing), appropriately while changing speed.

If stratification of charge was occurring in switching to the injection mode, it would have been immediately apparent in that it could be expected that the power output would remain the same, and the pulse width could be reduced. This was never the case. To the contrary, the pulse width and the fuel supply pressure generally had to be increased to prevent the power dropping off too sharply.

At a particular load and speed, the injection timing was varied to find the timing angle for best bsfc and power. With the timing set, the air/fuel ratio was altered by varying the pulse width.The torque, speed, air flow and fuel flow were noted in each case.

It was discovered that fuel supply pressure had very little effect other than to vary the flow rate through the injector. Spray patterns were not affected by the supply pressure in the range in which it was used, (150kPa - 300kPa) for locations 1,2 and 3. Location 4 necessarily required a high pressure (approximately 450kPa) as it was located above the exhaust port.

4.7 Scavenging Analysis.

It was apparent from these tests that stratification of the charge was not occurring. Indeed, results in terms of power and bsfc were inferior to those obtained for the carburetted engine. In an attempt to determine why this was the case, two scavenging analysis techniques were used.

Figure 4.6 shows the scope of methods of investigation into the scavenging process of two-stroke engines.

The first technique chosen was a quantitative method involving exhaust gas analysis. Orsat analysis equipment was used to determine the relationship between charging and trapping efficiency versus the delivery ratio as suggested by Baudequin and Rochelle,[14]. The determination of the charging and trapping efficiencies from the exhaust gas analysis is detailed in Appendix F

The second technique chosen was a qualitative study of the flow patterns in the engine cylinder, using the ammonia method developed by Phatak [15].

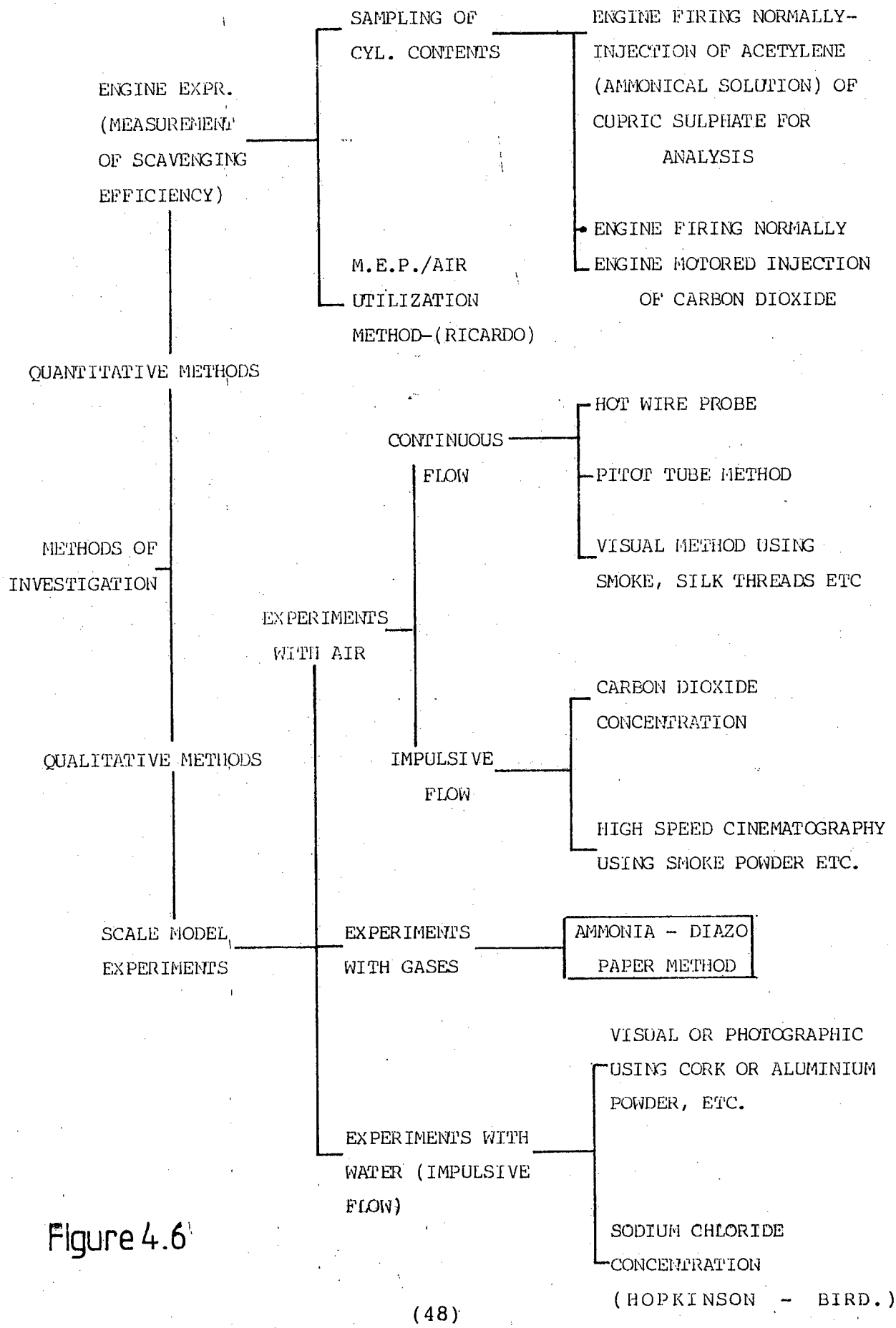
METHODS OF INVESTIGATION
QUANTITATIVE METHODS
ENGINE EXPR. (MEASUREMENT OF SCAVENGING EFFICIENCY)
SAMPLING OF CYL. CONTENTS
ENGINE FIRING NORMALLY- INJECTION OF ACETYLENE (AMMONICAL SOLUTION) OF CUPRIC SULPHATE FOR ANALYSIS
ENGINE FIRING NORMALLY
ENGINE MOTORED INJECTION OF CARBON DIOXIDE
M.E.P./AIR UTILIZATION METHOD-(RICARDO)
QUALITATIVE METHODS
EXPERIMENTS WITH AIR
CONTINUOUS FLOW
HOT WIRE PROBE
PITOT TUBE METHOD
VISUAL METHOD USING SMOKE, SILK THREADS ETC
IMPULSIVE FLOW
CARBON DIOXIDE CONCENTRATION
HIGH SPEED CINEMATOGRAPHY USING SMOKE POWDER ETC.
SCALE MODEL EXPERIMENTS
EXPERIMENTS WITH GASES
AMMONIA - DIAZO PAPER METHOD
EXPERIMENTS WITH WATER (IMPULSIVE FLOW)
VISUAL OR PHOTOGRAPHIC USING CORK OR ALUMINIUM POWDER, ETC.
SODIUM CHLORIDE CONCENTRATION (HOPKINSON - BIRD.)

Figure 4.6

4.7.1 Orsat Analysis.

In order to determine the charging and trapping efficiencies of the engine, it was necessary to know the percentage concentrations of CO, CO_2 and O_2 in the exhaust. This was achieved using the Orsat apparatus. It is the most simple in concept and the easiest to operate of the various gas analysis techniques available. Of the other widely used methods, non-dispersive infra-red absorption is used to measure CO, CO_2 and nitric oxide concentrations. Flame ionization detection is used to measure hydrocarbon concentrations and is therefore not applicable in this case. Gas chromatography is used to identify the hydrocarbon components and is therefore also not necessary. Chemluminescence measures the extremely small quantities of nitric oxide if required.

Figure 4.7 shows the layout of the Orsat apparatus.

Three reagent bottles with taps and a measuring burette filled with water, are connected as shown, to a levelling cup. Gas is drawn into the burette by opening the three-way valve and lowering the cup. Once the sample of gas is in the burette, a reading is taken with the level of water in the cup and burette being the same. This ensures the gas is at atmospheric pressure.

The tap to the first reagent bottle is opened and the sample gas forced into the bottle by raising the levelling cup. (The remote side of the reagent bottles breathe into an aspirator or bag). This is repeated in succession with the other two reagent bottles and a note taken of the change in volume of the gas in the burette. The order of absorption is CO_2, O_2 and CO.

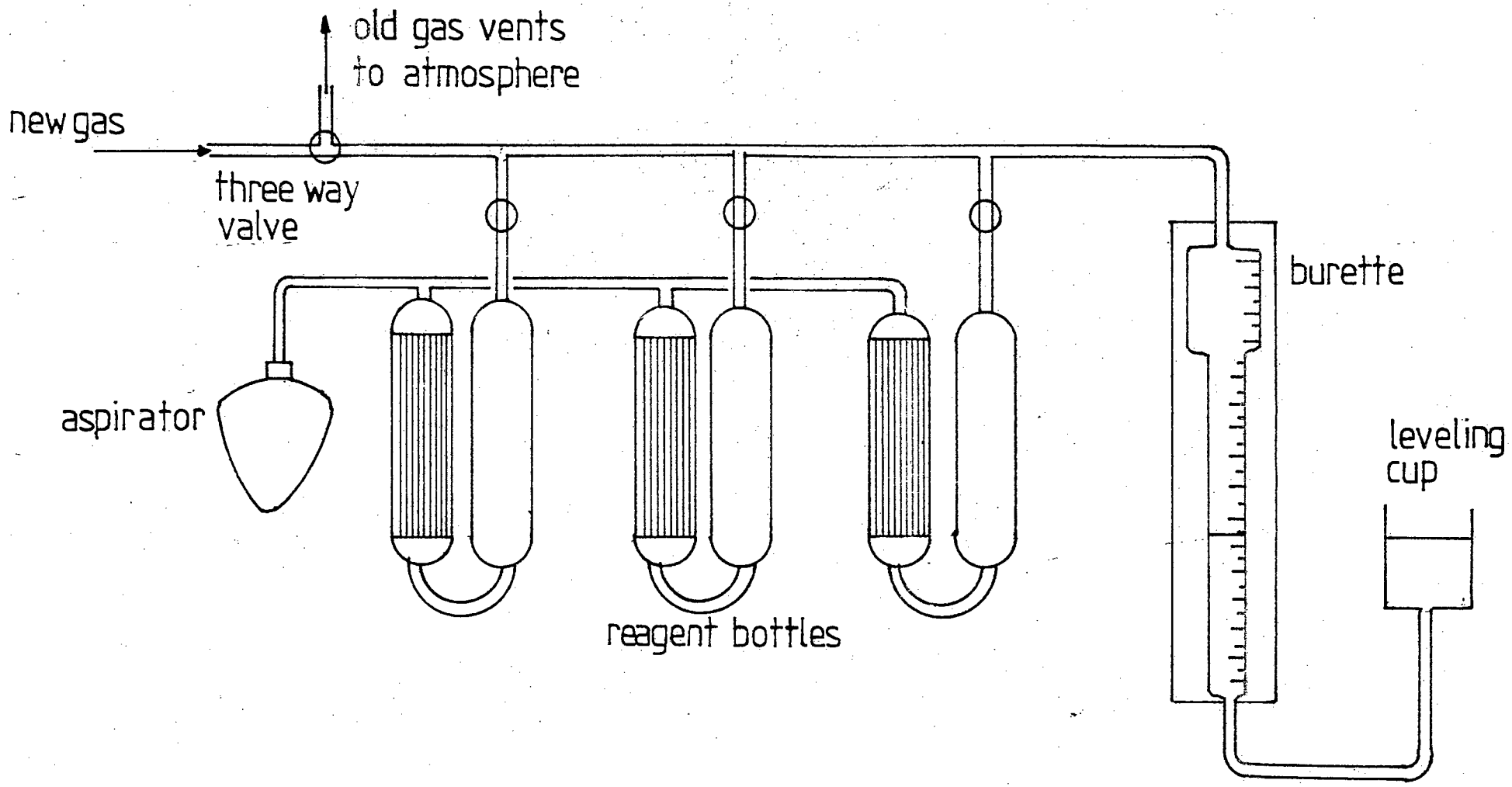

Figure 4.7 Orsat Apparatus

The first reagent bottle contains a solution of potassium hydroxide to absorb CO_2, the second, a solution of potassium hydroxide and pyrogallic acid to absorb O_2, and the third, cuprous chloride, to absorb CO.

The reagent bottles contain many thin tubes of glass. The tubes cause the reagent to adhere to them as the gas is forced into the bottle, resulting in a very large surface area of reagent being made available for the absorption of the respective gas.

Disadvantages of the method are that it is important that the reagents are fresh when used and that the cuprous chloride must be changed after every ten absorptions or so, if the carbon monoxide concentration is above 1 percent. Since cuprous chloride requires 2 days to a week to prepare, it is essential to make sufficient quantities for frequent tests with high carbon monoxide concentrations, as was the case in this study. However, knowing the air/fuel ratio and the concentrations of two of the three reagents, it is possible to calculate the concentration of the third reagent. (Appendix D). This proved necessary in the case of carbon monoxide as its absorption proved unreliable for the above reasons, namely, frequent absorption of high concentrations.

4.7.2 Ammonia Method of Scavenging Analysis.

This method has only recently been developed by Phatak, but promising results indicate the useful nature of this technique.

A paper (Diazo paper) coated with an emulsion sensitive to ammonia gas is pasted on the piston crown and cylinder walls. Ammonia is then flowed through the transfer ports at a controlled pressure for a specific time duration. Wherever the gas comes into contact with the sensitized paper, a chemical reaction takes place changing the colour of the paper from faint yellow to dark blue, depending on the emulsion used, and the concentration of ammonia. Low ammonia concentration produces a light shade whereas high concentration produces a dark shade. Similarly for gas of a fixed concentration, areas exposed to high velocities will produce darker shades than those exposed to lower velocities. These phenomena are the basis of the technique.

A very useful variation to this technique was used in this study. Rather than injecting ammonia gas through the engine or model, as an entity, air was flowed through and ammonia gas was injected into the various transfer passages to observe the effect that each passage has on the overall pattern.

For scavenging tests on the engine the following procedure was used. A car tyre was inflated using ammonia gas, thereby regulating the pressure from 7 bar to approximately 2 bar. The tyre, acting as a reservoir, was then connected to a Bosch fuel injector. This was located at various positions enabling injection into the crankcase, main transfer port and boost transfer port. A perspex plate was bolted over the cylinder replacing the cylinder head. The rotary valve was removed to allow air to be passed through the engine with the piston at bottom dead centre. Air was flowed through the engine and ammonia injected into the transfer ports and crankcase to observe the effect.

A pressure tapping was drilled into the crankcase allowing measurement of the crankcase pressure relative to atmospheric pressure. The maximum crankcase pressure ratio in a running engine depends on the crankcase compression ratio, and in the tested engine, this was expected to be 1;2:1 at transfer port opening. This falls off rapidly to 1,0:1 at bottom dead centre. The maximum pressure ratio attained using the ammonia method was 1,015:1 indicating that the method as used here is only useful near bottom dead centre.

Scavenging pictures were taken at bottom dead centre and with transfer ports half open. Ammonia was injected into the crankcase and the main transfer port at bdc and additionally into the boost transfer port with half open transfer ports. Ammonia was not injected into the boost port at bdc as this was closed off by the piston skirt in this position.

In order to compare the above analysis to an engine of proven performance, a model of such an engine cylinder was made and the ammonia method applied to this model.

Figure 4.8 shows details of the model constructed. The cylinder layout is taken from cylinder 1 tested by Sanborn and Blair[16]. This layout produced the best performance in terms of both charging efficiency, bmep, trapping efficiency and bsfc when compared to five other cylinders of different designs.

Ammonia was injected into the crankcase and alternately into each of the two transfer ports. Crankcase pressure ratios used were similar to those used for the tested engine. The resulting scavenging pictures are shown in Chapter Five.

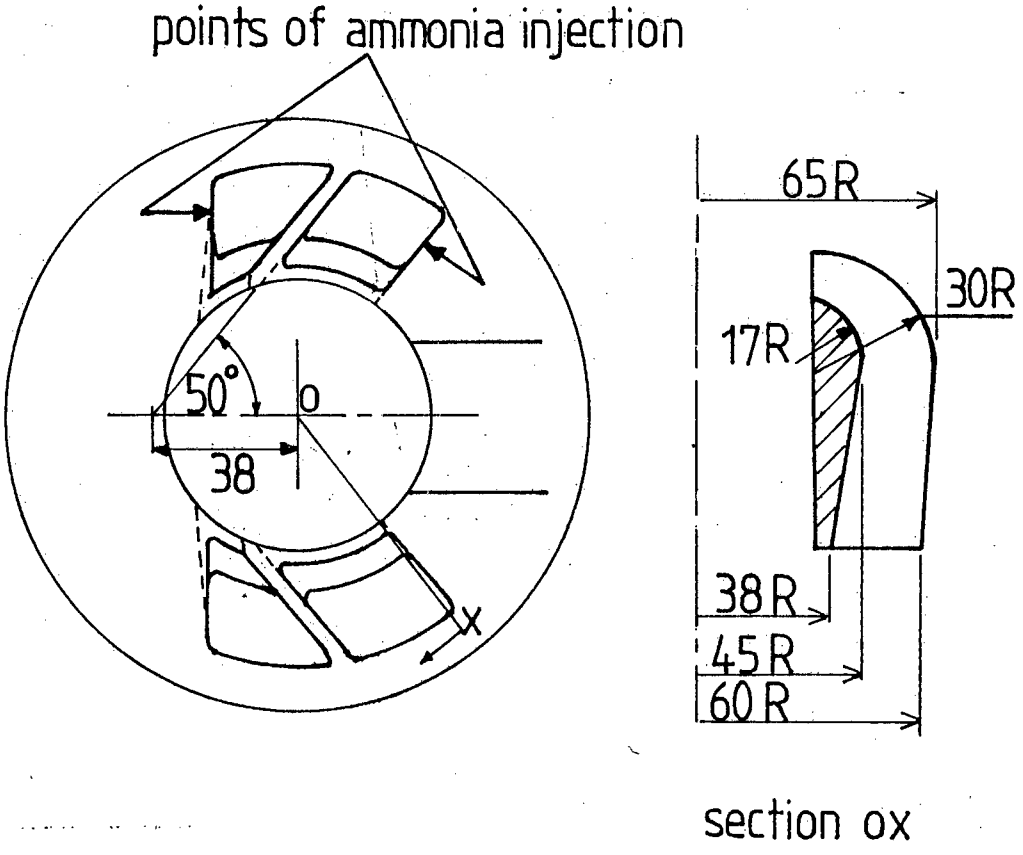

bore	70
stroke	64
exhaust port height	28
exhaust port width	39
transfer port height	12
total transfer port width	89

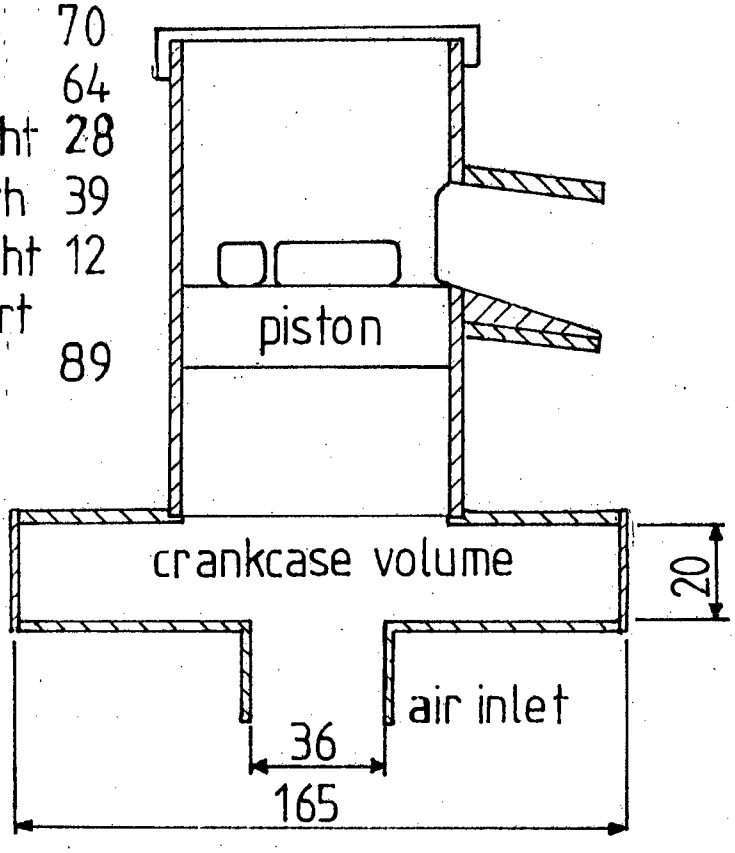

Figure 4.8 Model Cylinder

CHAPTER FIVE

5. Results.

5.1 Carburetted Engine Results.

The results for the standard carburetted engine are presented as an engine map of bsfc plotted against bmep and engine speed. This was done so as to be able to compare the performance, in terms of absolute values, to similar engines.

The full throttle values of bsfc, bmep and air/fuel ratio are plotted separately against engine speed to compare with the full throttle tests on the fuel injected engine.

Figure 5.1 shows the bsfc map for the carburetted engine. The least value of bsfc of 300g/kWh, is seen at 6000rpm. This increases gradually to a full throttle value of 360g/kWh, and minimum throttle opening value of 330g/kWh. At half throttle a 'plateau' of value between 400-350g/kWh extends from 3500rpm to 5300rpm.

The full throttle results show bsfc decreasing from 3500rpm to a minimum of 340g/kWh at 7200 rpm. Bmep shows a steady increase from 2500rpm to a maximum of 560kPa at 6800rpm. The air/fuel ratio varies greatly, but is on average, lean. The charging efficiency drops to a minimum at 4300rpm, then rises to a maximum of 0,45 at 6000rpm. The trapping efficiency varies until it reaches a maximum at 7200rpm.

5.2 Fuel Injected Engine Results.

The results for the fuel injected engine are presented as plots of bsfc and power against air/fuel ratio and injector timing for each location. (Appendix G)

5.2.1 Location 1.

For location 1, the best timing for both power and bsfc at 6000rpm coincided with opening of the exhaust port. At 3500rpm best timing was at 65° atdc.

For both speeds, best power occurred at an air/fuel ratio of 12:1, and best bsfc at 16,4:1 for 6500rpm, and 17,1:1 for 3500rpm.

5.2.2 Location 2.

Location 2 showed very similar results to those of location 1. Best timing for bsfc and power was 60° atdc at 3500rpm and 90° atdc for 6000rpm.

The values of bsfc were generally 15% better for location 2 when plotted against air/fuel ratio with similar trends for maximum power, and least bsfc occurring at 12:1 and 16-17:1, respectively.

5.2.3 Location 3.

The results for location 3 show a well defined point of best timing in terms of bsfc. For 6000rpm this point is 70° atdc and for 3500rpm, 110° atdc. The variation in power is not more than 8% over the range of timings at 35000rpm.

The bsfc and power trends when plotted against air/fuel ratio, show best power at air/fuel ratios of 12-12,3:1 and best bsfc at 15,4:1.

5.2.4 Location 4.

The best timing for bsfc and power at 3500rpm was 190° atdc. At 4600rpm this point moved to 125° atdc.

Once again the trends in the previous three locations were reflected on the power and bsfc curves plotted against air/fuel ratio. Best power occurred at 12,0:1 and best bsfc at 14,5:1. Not shown in the results is the high fuel supply pressure required (approximately 450kPa) to prevent combustion products blowing back into the fuel line.

In general, the cyclic regularity of the injected engine, for the first three locations, was very good. Speed variation about a mean was no more than 1% as opposed to some 4% for the carburetted engine. This is perhaps the only aspect of the injected engine that was superior the carburetted engine.

Injector flow rates on the running engine were generally lower than those for the calibrated injector using the same fuel supply pressure, pulse width and orifice size, (**Figure 5.11**).

5.3 Ammonia Method Results.

Figures 5.13 - 5.16, show the ammonia traces using Diazo paper pasted to the cylinder wall and piston crown.

Unfortunately, the original scavenging pictures had very subtle shades that proved difficult to emulate for reproduction purposes. For this reason, the reproduced pictures have been 'touched up' to show a clearer resemblance to the actual pictures.

Figure 5.13 shows the scavenging pictures for the tested engine. The disc represents the piston crown. This is positioned in relation to the cylinder wall, which should be imagined to be encircling the disc. The points of contact in the pictures are the true points of contact in a three dimensional visualization.

Figure 5.13(a) shows a dark area on the piston crown emanating from the right main transfer port, extending along the periphery to the back of the cylinder opposite the exhaust port. A lighter shaded area covers much of the sector from 9 o'clock to 1 o'clock.

The cylinder wall shows a dark area extending from transfer port height up towards the back of the cylinder.

Figure 5.13(b) shows a light and dark area extending from each main transfer, symmetrically towards the centre. A slight 'tongue' of darker shade is seen extending from the junction of the jets towards the exhaust port.

The cylinder wall shows a very gradual lightening of shade from right to left.

Figure 5.13(c) has a dark patch emanating from the rear right boost port. This stops where the two areas of lighter shade protruding from the main transfer ports meet.

The top right and left extremities of the cylinder wall trace have a darker shade than the rest of the wall.

Figure 5.14 shows the scavenging pictures for the model cylinder with the ports fully open.

Figure 5.14(a) has a light area covering most of the piston with a definite 'tongue', extending towards the exhaust port.

Shown on the cylinder wall is a strongly contrasting light and dark shaded area on the left.

Figure 5.15(a) has a dark area in strong contrast to the rest of the piston crown 'directed' from the secondary port towards the back of the cylinder.

The cylinder wall picture here, indicated a rising column of ammonia at the back of the cylinder.

The results for the model with the transfer ports half open reflect those of **Figure 5.14**, but the cylinder wall pictures indicate a strong swirl or loop towards a point above the exhaust port.

CHAPTER SIX

6 DISCUSSION

This chapter constitutes a discussion of the following points;

* A comparison of the performance of the fuel injected engine with that of the carburetted engine and possible reasons for the poor performance of the injected engine for each injector location.
* A comparison with the results obtained by Blair and Vieilledent This will include a comparison of the carburetted engine results with accepted performance figures for other carburetted engines and possible reasons for its good performance. A discussion on the scavenging analysis performed on the engine and on the model of an engine of proven performance, will also be included.
* Possible solutions to the problems preventing good performance of the injected engine.
* Possible solutions to problems associated with the fuel control of a fuel injected two-stroke engine.

6.1 Performance of the Fuel Injected Engine.

From a comparison of **Figure 5.2**, with **Figure 5.3 - 5.10**, it is clear that the fuel injected engine was, in most respects, inferior in performance to the carburetted engine. **Figure 5.5**, for example, shows a best bsfc value of 360g/kWh. However, this is accompanied by a 32% drop in power. This trend, though not quite as marked, is reflected in all locations for the injector, indicating that stratified charging is not occurring and that the low bsfc values are due only to the use of lean mixtures.

All locations show maximum power occurring at air/fuel ratios of between 12-13:1. Furthermore, maximum power is as much as 10% less than for the carburetted engine. Best bsfc occurs at air/fuel ratios varying between 14,5-17:1. If stratification of charge occurred, with no short circuiting and mixing with exhaust gases, then maximum power would correspond to a trapped air/fuel ratio of 12-13:1 (as expected from a carburetted engine. If the trapping efficiency of the engine at a particular load and speed was 0,5 for example, one would therefore expect maximum power at an overall air/fuel ratio of 24-26:1. This was quite obviously not the case with the injected engine. The carburetted engine, at 6000rpm, for example, produced maximum power at an overall air/fuel ratio of 19,2:1, showing stratification of charge was occurring to a limited extent. This was due to transfer passage design creating good scavenging patterns and will be discussed later in this chapter.

Discussing each location separately reveals some interesting points.

6.1.1 Injector Location 1.

Location 1 shows best timing of injection in terms of both power and bsfc to be generally, before the exhaust port opens. At 3500rpm, for example, this timing is 60° atdc. Bearing in mind an injector lag of 1ms, actual injection starts 20° later at 80° atdc. The pulse width is 1,5ms in this case, and covers a further 30° of crank angle. Since the injector housing is uncovered only some 125° atdc in this location, this means injection has occurred before the port has been uncovered. The suggestion here, is that the fuel is injected into the modified injector shroud where it mixes with the small amount of air stored there, before the housing is uncovered. Once the falling piston opens the housing to the cylinder, the mixture is sucked out by the rapidly decreasing pressure.

This proposal of events would appear to operate better in terms of preventing loss of fuel out of the exhaust than would injection timed to occur directly into the cylinder. In this case the fuel spray penetrates the 'aerodynamic wall' at the back of the cylinder as proposed by Vieilledent (17). The spray reaches the opposite side of the cylinder near the exhaust port and is lost with the exiting gases. Therefore little of no stratification of charge occurs. Power is some 10% less than that obtained for the carburetted engine with comparable fuel flow rates indicating inferior ability to trap fuel in the cylinder. The presence of two black patches on the piston crown after several hours running as indicated in **Figure 6.1**, supports the above suggestion, i.e. those patches would indicate that the fuel is hitting the cylinder wall.

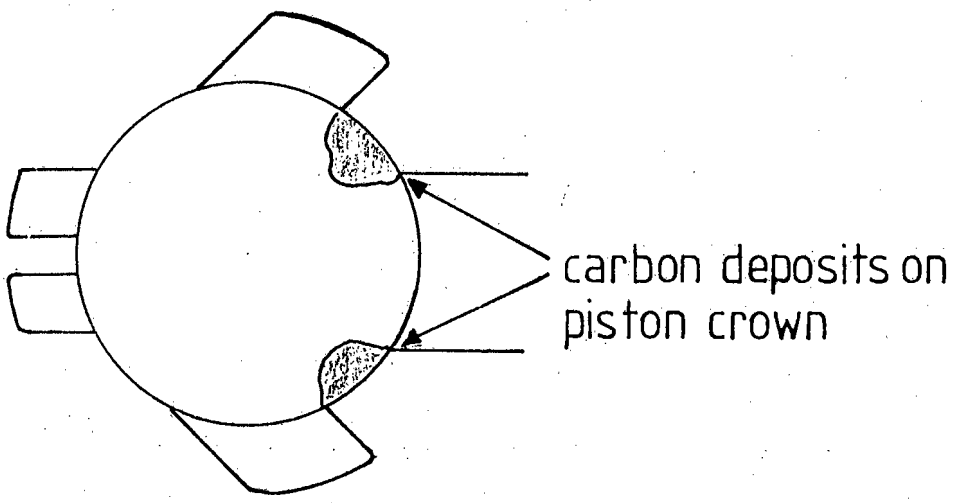

Figure 6.1 Piston Colouring for Location 1

6.1.2 Injector Location 2.

Location 2 shows very similar results to location 1 despite the difference in spray pattern and direction. Maximum power is only slightly less (8%) with a corresponding bsfc some 40% higher (470g/kWh) than for the carburetted engine. Minimum bsfc (340g/kWh) occurs with a corresponding 28% drop in power at an air/fuel ratio of 15:1. This reasonably good value of bsfc is due to the use of lean mixtures only.

One would expect that the later the injection process occurs, in the open cycle, the less chance there is for loss of fuel and hence the bsfc should drop. This is not substantiated in the results. **Figure 5.6** shows the effect of late timing. For example, a pulse width of 1ms timed at 180°, with an air/fuel ratio of 14,9:1 produced an appalling bsfc of 730g/kWh. Allowing for a 1ms injector lag, the entire injection process in this instance, takes 40°, ending 20° before the injector is again covered by the piston. This 20° added to the further 25° before the exhaust port closes is sufficient time for the fuel to be lost. Any later injection timing produced deteriorating results indicating a minimum time is required for fuel preparation. As this time overlaps with the open cycle, losses due to short circuiting and mixing can only be minimally reduced.

6.1.3 Location 3.

At this location two modes of injection were possible depending on the injection timing.

With the transfer port open it was possible to inject directly into the cylinder. The spray pattern in this case was a thin jet issuing from the modified injector. It was

hoped that the jet would travel across the cylinder and impinge on the opposite wall, forming a splash spray that would be caught in the 'aerodynamic wall' caused by the strong flow of scavenging air at the back of the cylinder.

The second mode of injection occurs when the piston covers the transfer port. The fuel jet then splashes onto the piston wall forming a rich air/fuel mixture in the transfer port.

The results show that the best bsfc figures occur with early injection, (20° before transfer port opening an 6000rpm). Allowing for injector lag, pulse width and the time for the jet to travel (at a velocity of 20m/s), across the cylinder, the fuel hits the opposite wall some 20° before the transfer ports close. However, the best bsfc figures occur at an air/fuel ratio of 15:1, implying little stratification of charge. At this operating point the bsfc is 15% higher and the power 14% lower than for the carburetted engine despite the air/fuel ratio being 16% richer (15,4:1).

As the engine speed decreases one would expect best power and bsfc to occur at a later injection timing (for constant pulse width), as the constant timed injection process takes less percentage of one revolution. This is reflected in the results. At 3500rpm, for example, best timing is 110° (40° later than for 6000rpm). With a 1ms injector lag, 1,5ms pulse width, and 2,8ms required for the jet, travelling at 20m/s, to cross the cylinder, a total injection time plus travel time, of 5,8ms is required. Thus a further 110° crank angle is needed until the injection process ends at 220° atdc. Unfortunately, there exists a further 45° until the exhaust port closes and this is sufficient for fuel loss to occur.

Timing on either side of the optimum angle produced deteriorating bsfc as the injection became timed nearer to transfer port closure.

Injection onto the piston skirt while the port was closed, understandably produced poor bsfc. The main transfer passage is used to purge the cylinder of exhaust gases. A rich mixture in this passage would stand a good chance of being lost out of the exhaust port. For the carburetted engine, on the other hand, the mixture in the main transfer passage is, generally, lean. Therefore, what is lost is a lean mixture, as opposed to a rich mixture for (non optimum) transfer injection.

Long pulse widths of, for example, 6ms at 4300rpm produced poor bsfc. This was the result of a combination of injection directly into the cylinder and injection onto the piston skirt, with the consequent bad results.

6.1.4 Location 4.

For this location, it proved a surprise that the engine ran at all. This was only possible, however, with injection pressures in the region of 450-550kPa. These high pressures were necessary to hold the injector needle closed under the high combustion pressures present as the injector was uncovered at 54° atdc, exposing it to approximately 10 bar of combustion pressure. At lower fuel supply pressures, the injector acted as a sampling valve with combustion products blowing into the fuel line.

The test results were very much a reflection of the three previous locations results with best power at an air/fuel ratio of 12:1, and best bsfc at an air/fuel ratio of 15:1, with a poor overall power output. This indicates no stratification of charge with the resultant loss of fuel.

Injection timing for best bsfc was 160° atdc for 4500rpm. The engine would not run with later timing than 180° atdc and a pulse width of 1,5ms for example. This shows That early injection during the open cycle is necessary to allow time for fuel evaporation. Unfortunately this means loss of fuel through mixing.

A further reason for the poor bsfc is the high injection pressure used. This would cause a large rebound splash on the opposite cylinder wall. This, perhaps, extends across the whole cylinder, preventing stratification and promoting loss of fuel.

In general then, at comparable power levels, the bsfc for the injected engine was 40-60% higher than for the carburetted engine. A decrease in bsfc could only be attained with a substantial (typically 25%) power drop.

6.2 Comparison with Reported Results.

A comparison of the test results with those reported by Blair[18], reveals general agreement. Bsfc cannot be reduced without the use of lean mixtures with a resultant power drop. Blair, however, managed to produce air/fuel ratios of 24:1, and hence the bsfc could be reduced to values of approximately 320g/kWh. As expected, this produced a power drop of 24% when compared to full power at air/fuel ratios of 12:1. With the injector located at the crankcase inlet, Blair's figures are similar to those for the carburetted engine tested in this study, (340g/kWh at 6500rpm). One can deduce from this that the carburetted engine had a finely tuned carburettor performing its function as well as an inlet injector. From Blair's study it can be concluded that the inlet injector location produces the best overall results, and that there is very

little improvement in economy at other injector locations without a considerable loss of power. Blair performed part throttle tests that supported these conclusions.

The use of a high voltage capacitor discharge injector firing circuit by Blair, showed that the timing angle for best bsfc was retarded from 30° atdc to 210° atdc at 5500rpm, for example. The value of the bsfc rose from 330 to 345g/kWh showing no advantage in the use of this form of firing circuit. Using a 12 volt firing circuit means account must be taken of the injector lag, and timing advanced accordingly, otherwise there is no apparent disadvantage in using this system. The use of the early timing of 30° atdc for the 12 volt system shows that injection is occurring before the injector is uncovered supporting the results obtained in this study, i.e. the injected spray must penetrate the 'aerodynamic wall' proposed by Vieilledent.

Unfortunately, Blair gave no indication of the pulse widths used or the modifications made to the standard Bosch fuel injector. These important facts could be helpful.

Comparing the test results to those reported by Vieilledent reveals some interesting points. **Figure 6.2** shows a comparison between the carburetted engine used in this study and Vieilledent's results for indirect and direct cylinder injection.

At low speeds it is evident that the carburetted engine produces similar performance to the indirect inlet injection system. At high speeds the small power difference is due to the slightly larger capacity of the Yamaha engine. The interesting point however, is that the carburetted engine approaches the bsfc values of the direct injection system. This effect will certainly be due to the expansion chamber

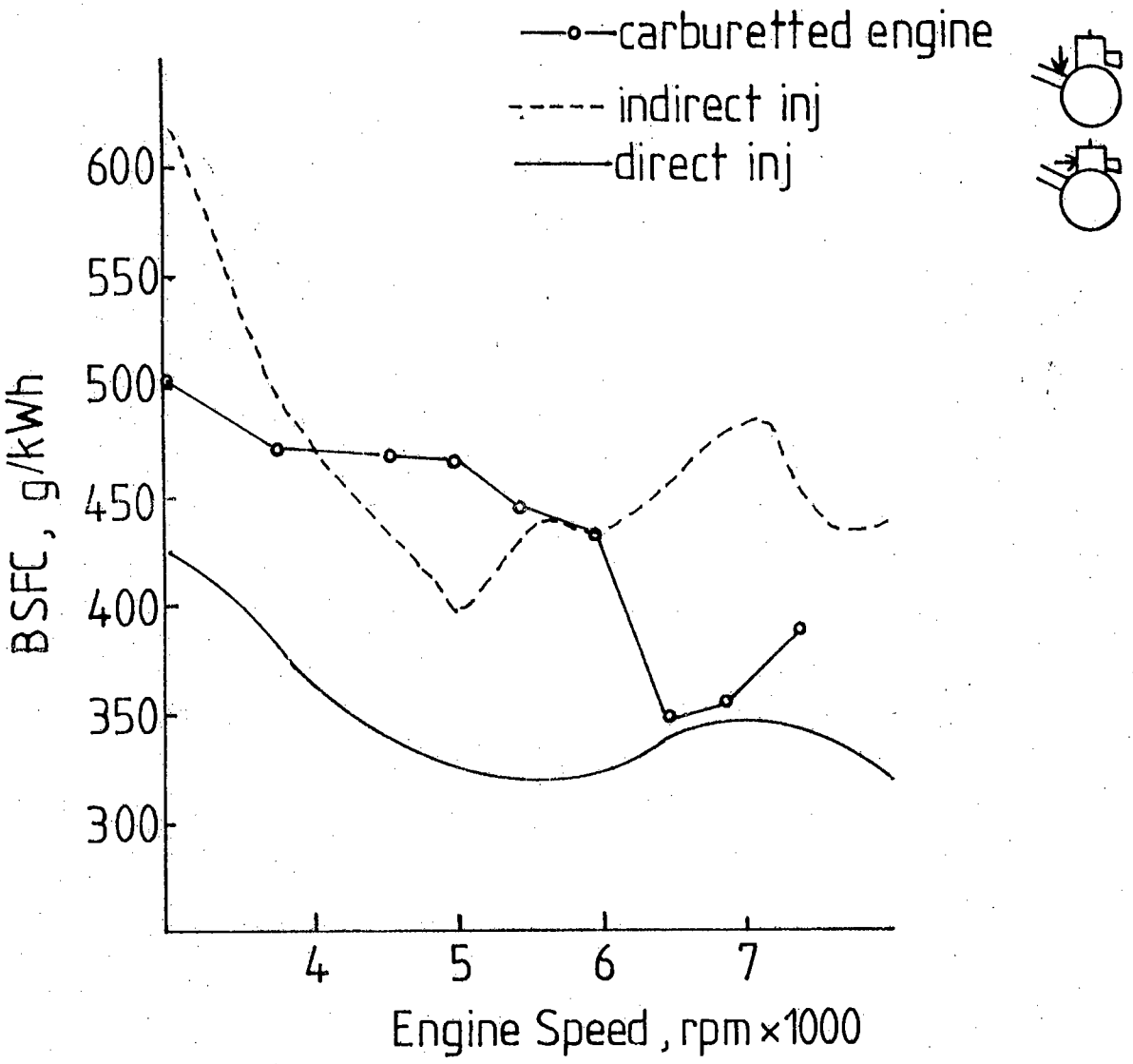

Figure 6.2 Carburetted Engine vs Vieilledent's Fuel Injected Engine.

used on the carburetted engine. If a well designed expansion chamber had been used by Vieilledent, the advantages of direct injection may have been less impressive. Nevertheless, at low speeds direct injection certainly appears to produce good values to bsfc.

If a clearer indication had been given of details such as injector modifications, spray patterns, transfer port design, and injector timing, the reasons for the good performance may be apparent. Vieilledent stresses that the success of the injected engine lies in the 'aerodynamic wall' set up, during scavenging, opposite the exhaust port. The spray should be entrained in this wall and not penetrate it as was obviously the case in this study.

6.3 Analysis of the Carburetted Engine Performance.

From the above it is apparent that the performance of the carburetted engine is as good if not better than the performance of the two engines reported having inlet injection as being indicative of perfect carburation.

Examination of the plot of bsfc against bmep and engine speed **(Figure 5.1)**, reveals the good performance that the carburetted engine delivers in terms of specific fuel consumption.

The effect of the tuned expansion chamber is clearly visible at 6000rpm. At this speed the bsfc varies from 300g/kWh to 340g/kWh over the entire load range. Below 6000rpm the bsfc increases to 600g/kWh at 2500rpm showing that the expansion chamber assists in preventing loss of fuel through mixing and short circuiting over a limited speed range only.

Figure 5.2 shows the wide open throttle results. Bearing in mind the definition of charging efficiency, it can be expected that charging efficiency should have a linear relationship with bmep.

In the speed range 4400rpm to 6800rpm an increase in charging efficiency corresponds to an increase in bmep as expected. As more fresh charge is trapped in the cylinder so one can expect the bmep to increase. This should be interpreted in conjunction with the varying air/fuel ratio. If, for example, the air/fuel ratio at 6000rpm had been stochiometric instead of 18:1, the bmep may have been higher. The reason for the increase in charging efficiency is evident from a plot of delivery ratio versus engine speed for the engine with and without an expansion chamber.

Figure 6.3 shows the delivery ratio for an engine without an expansion chamber dropping off from a highest value at low speed. The effect of the expansion chamber is to increase the delivery ratio and hence the charging efficiency at high speeds.

An interesting feature of **Figure 5.12** is the close relationship between the charging efficiency and the perfect mixing line, ($n_{ce} = 1-e^{-L}$). See Appendix E for derivation.

This shows that what occurs during scavenging approaches the concept of perfect mixing.

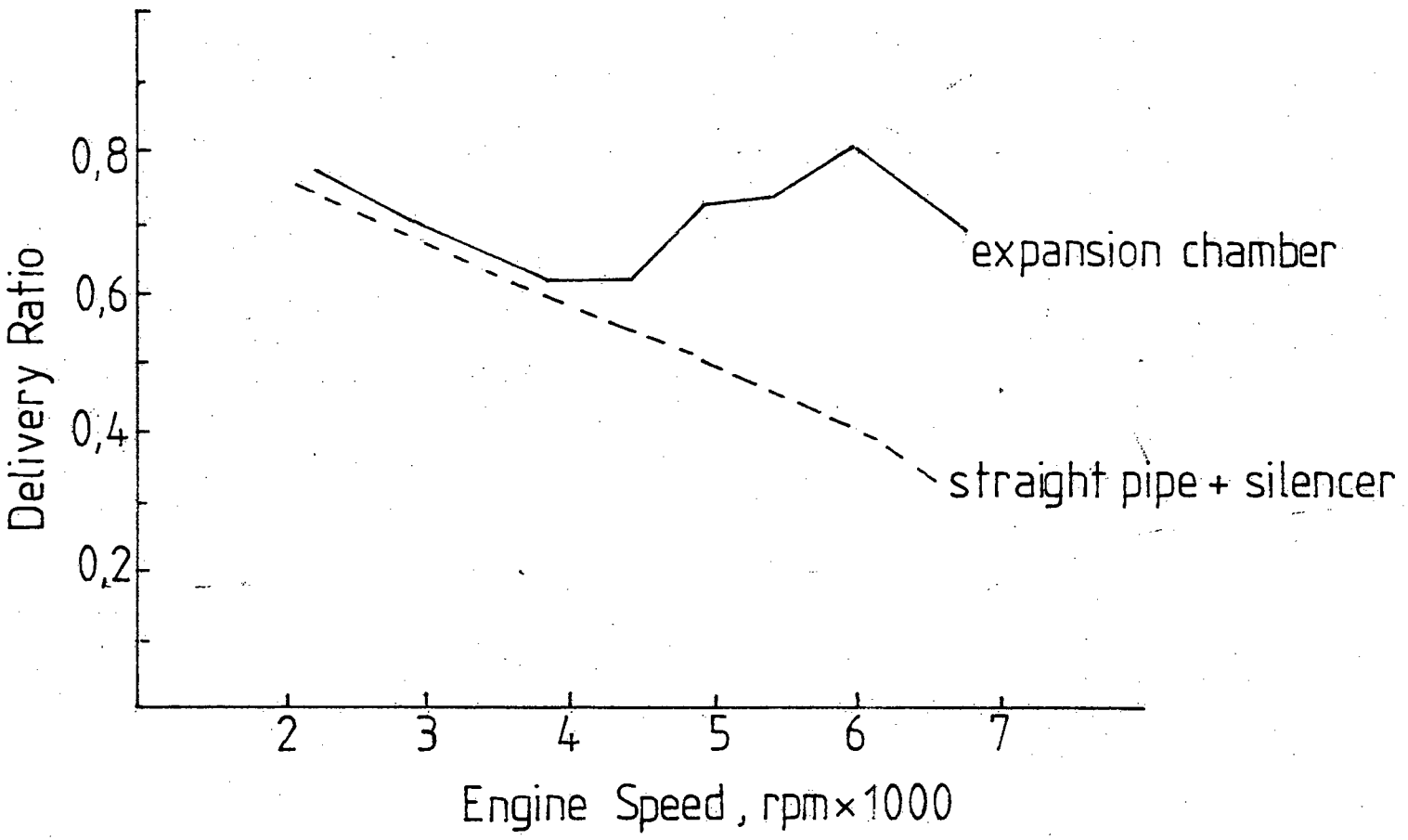

Figure 6.3 Delivery Ratio versus Engine Speed

6.3.1 The Ammonia Method of Scavenging Analysis.

The ammonia method of scavenging analysis, provides some clues as to the reasonably good performance figures obtained for the carburetted engine.

Figure 5.13(a), shows injection of ammonia gas into the right side main transfer port and the resulting air flow pattern obtained by pasting of Diazo paper onto the cylinder wall and piston crown.

A tendency for the ammonia to build up at the 'back' wall of the cylinder is evident on both the wall and piston crown as shown by the dark patches.

Figures 5.13(b,c) show ammonia injection into the main transfer port (b), and boost transfer port (c), with the ports half open. Both pictures show the jet from the main transfer ports to be convergent. The point of intersection of the two main transfer jets has moved forward towards the exhaust port promoting a small degree of short circuiting. As a result a small 'tongue' extending from the junction of the two jets towards the exhaust is evident. This is not seen with the piston at bdc. Furthermore, there is no tendency for the gas to build up at the back of the cylinder. The above would indicate that scavenging is best at bdc and deteriorates on either side of this position.

Gas from the right rear boost transfer port shows a strong tendency to be retained at the back of the cylinder. This port is closed off by the piston skirt at bdc when the scavenging process is expected to be strongest. The advantage of these ports seems to be lost if one takes **Figure 5.13(c)** to be indicative of the airflow.

From the above then, there appears to be little evidence of short circuiting in comparison with the other gas flow patterns in the cylinder. There is also a strong tendency for gas to build up at the back of the cylinder.

Figure 5.13 therefore indicates to a certain degree why the bsfc figures for the carburetted engine are better than average.

The advantage of the ammonia method is the ability to obtain three dimensional visualizations of the scavenging process which is not possible with any other analysis technique known to the author. The ammonia method may be applied to models of engine cylinders implying that expensive trial and error development on running engines is not required.

The limitations of the technique as used in this thesis are realized. As with any steady state study of an impulsive phenomenon, the results are only approximate and in this case qualitative. In this study, the pressure ratio between the crankcase and the atmosphere is very close to unity, which is only true at, or close to bdc[19], and therefore perhaps, only illustrates the actual scavenging process for an instant. It is fortunate that this instant corresponds to the moment when scavenging is most strongly developed.

Injection of ammonia into the crankcase caused the Diazo paper to turn a uniformly darker shade. Thus no scavenging patterns could be seen. This was due to the low concentration of ammonia. Nevertheless a good overall idea of the scavenging pattern could be obtained from the separate injection of ammonia into each transfer port.

The ammonia method could be developed to include impulsive studies on model cylinders. The following technique maybe **useful:**

A container with a volume equal to the crankcase volume could be charged to a pressure equal to the maximum crankcase pressure before the transfer ports open.. This container could be connected to the crankcase inlet via a rapid action valve. If ammonia could be timed to be injected into the air stream on opening of this valve, it may be possible to obtain accurate representations of the actual scavenging process. Work would be necessary to obtain a means of simulating the conditions at the exhaust port. If this could be achieved, it would provide a scavenging analysis technique perhaps superior to any used at present.

6.3.2 Ammonia Method Applied to Model Cylinder.

Figures 5.14 and 5.15, show the ammonia traces for the model cylinder.

Figure 5.14(a) shows the air flow from the left main transfer port to be strongly vertical towards the cylinder head. However, short circuiting is strongly evident from the path of the gas form the transfer port out through the exhaust port and by the formation of a 'tongue' of gas directed towards the exhaust port from where the main transfer jets meet.

Figure 5.14(b) shows air flow from the secondary transfer port to be retained at the back of the cylinder. No evidenc of short circuiting from this transfer port is apparent.

These trends were repeated with the ports half closed, **(Figure 5.15).**

The scavenging pictures may then, provide some reason for the performance of this model in firing configuration as obtained by Blair[20]. **Figure 6.4** shows the plot of bsfc against engine speed at 1/4, 1/2 and full throttle for this engine. It is interesting to compare these results with those obtained for the engine used in this study.

The best bsfc value for Blair's cylinder was 330g/kWh at 3000rpm and 1/4 throttle. However, at full throttle this value changes to 490g/kWh. Compared to a 1/4 throttle best value of 300g/kWh and a full throttle value of 340g/kWh at 6000rpm for the engine tested in this thesis. It can be concluded then, that there is a sound basis to the ammonia method of scavenging analysis. That is, if one takes the evidence for short circuiting to be greater for the model cylinder than for the tested engine, which certainly seems to be the case.

6.4 Alternative Method of Stratified Charging.

The major problem encountered in this study was the inability of the fuel spray to form a stratified charge, remote from the exhaust port. A possible solution to this problem lies in the model cylinder.

It would appear that direct injection into the cylinder does not form a stratified charge. However, in the above model, the air entering the cylinder via the two secondary ports forms a strongly separate charge at the back of the cylinder with no indication of short circuiting. If fuel was injected into these transfer ports it would seem likely that stratification of fresh charge would be easily attained.

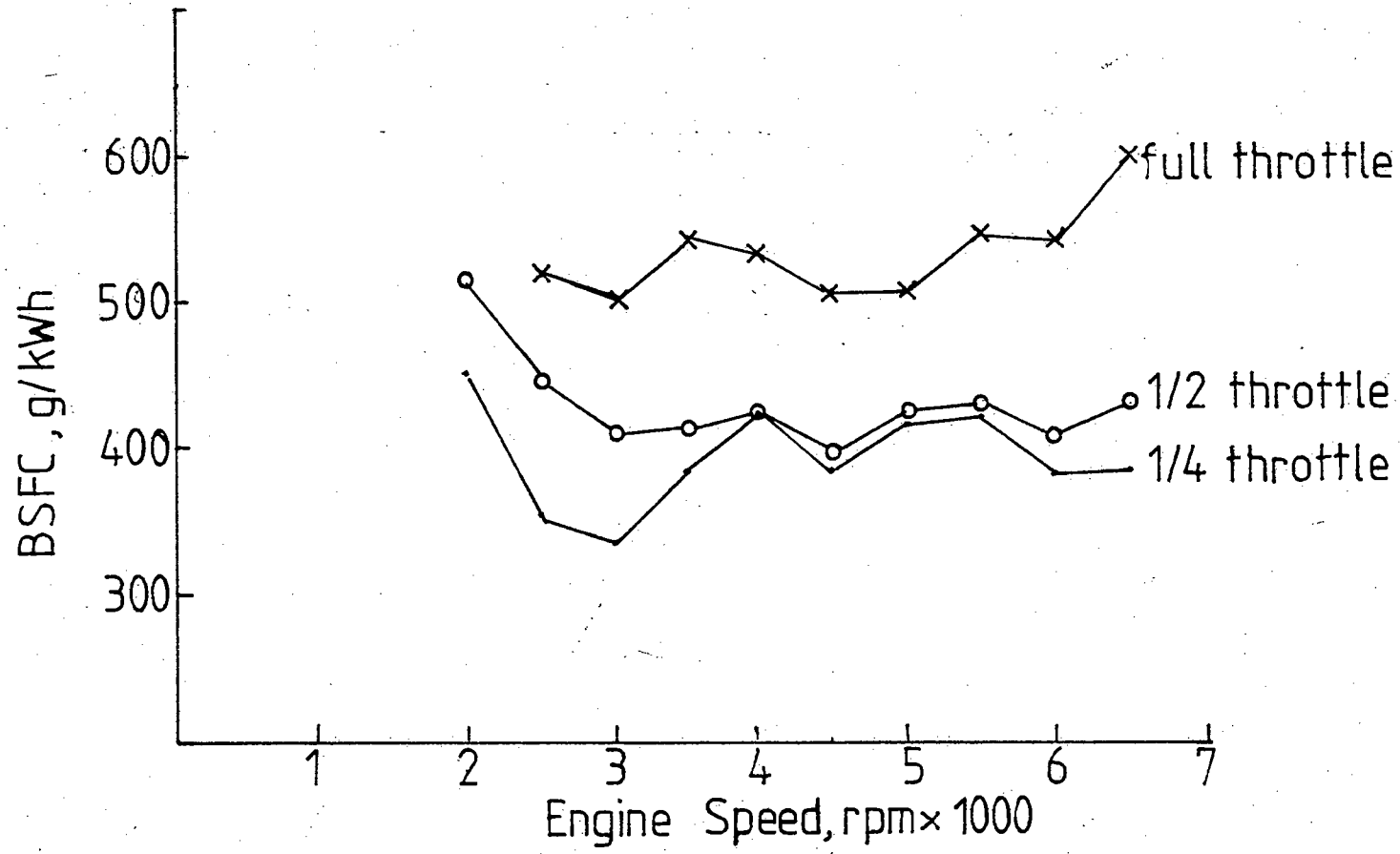

Figure 6.4 BSFC for Running Model Cylinder

Losses due to mixing may still exist but could certainly be minimized by judicious timing of injection.

Unfortunately, a working engine with the above port layout could not be found and therefore could not be tested.

A further problem anticipated would be the high variation in flow rates required if fixed nozzle geometry and short pulse widths were used. This would require the use of high pressures to produce maximum discharge within a short pulse width. If the nozzle outlet diameter was increased as might be suggested, the ability to cope with the smallest discharge would be lost bearing in mind injector lag. A solution to this might be the use of one injector located in each secondary transfer port, thus halving the 'flow load' on each injector.

6.5 Possible Solutions the Problem of Control.

The only reported control system[21], used a memory map of injected fuel quantity required for each engine load and speed. This is the system as used on fuel injected four-stroke engines.

With the aid of exhaust gas analysis, it is possible to produce a curve of charging efficiency versus delivery ratio, as done in this study. If the delivery ratio could be measured on a running engine, the charging efficiency, and hence the air/fuel ratio and required fuel quantity could be calculated. This would provide a simple and inexpensive means of control if for example, an analogue computer was used to simulate the relationship between charging efficiency and delivery ratio. Vieilledent and Yamagishi report that measuring the airflow and hence the delivery ratio of a two-stroke (for a production engine) is

difficult and both use throttle position as an indication of load. It is felt however, that a hot wire anemometer should cope with the pulsating flow in the inlet system of a two-stroke engine and give a more accurate indication of the airflow.

The above suggestions should perhaps be the subject of a future thesis.

CHAPTER 7

7. Conclusions.

The performance of the carburetted engine used in this study was excellent in terms of both brake specific fuel consumption and power. This was due to good scavenging patterns and an expansion chamber which limited short circuiting and mixing. A minimum value of bsfc of 300g/kWh was achieved at 6000rpm and a maximum bmep of 560kPa.

The theory proposed a strong 'aerodynamic wall' at the back of the cylinder, remote from the exhaust, through which little injected fuel was expected to penetrate. Stratification of charge could then be expected, as reported in one study, with further reduction in short circuiting and mixing losses. This however, did not occur, despite judicious variations in injector location,spray pattern, supply pressure and injection timing.

The results obtained from the fuel injected engine were disappointing in that, the performance of the carburetted engine always proved superior. Maximum bmep for location 2 for example, with the injected spray directed from the back of the cylinder towards the cylinder head, was 5,9kW,(some 8%) down on the carburetted engine at 6000rpm. This occurred at an air/fuel ratio of 12:1. Increasing the air/fuel ratio to 16:1 reduced the bsfc to a minimum of 360g/kWh, with a further 32% drop in power. This indicated no stratification of charge was occurring.

From the evidence provided by other types of stratified charged engines it appears that it is necessary to separate the lean and rich charge before it enters the cylinder.

The model cylinder used in this study, appears to be an ideal layout for this particular purpose. Scavenging analysis shows that the incoming air from the two secondary transfer ports is strongly separated from the rest of the charge. If fuel was injected into these transfer passages, there would be little difficulty in attaining stratification of charge.

Unfortunately, this hypothesis could not be tested for a running engine, and this should, perhaps, be the subject of a future thesis.

Judging from the above, the objectives of this thesis have, to a good extent, been fulfilled. The experiments showed the very limited advantages of direct fuel injection. An investigative path was followed which showed that fuel injection could be applied to form an alternative form of stratified charged two-stroke engine.

REFERENCES

1. **FISHER, C.H.,** "Carburation Volume II: Spark Ignition Engines - Fuel Injection Development", 4th Ed., Chapman and Hall, London, (1966) p.40

2. **DRAPER, K.G.,** "The Two-Stroke Engine", 3rd Ed., G.T. Foulis & Co, London (1966) p.109

3. **TAYLOR, C.F.** and **TAYLOR, E.S** , "The Internal Combustion Engine", 2nd Ed., Int. Testbook Co, Scranton, Pennsylvania (1962) p.274

4. **HEINRICH, H.** and **STOLL, H.,** "Petrol Injection in Germany", Proc Instn Mech Engrs (A.D.), No 6, London, (1957 - 58) pp. 185 - 189

5. **YAMAGISHI, G., SATO, T.,** and **IWASA, H.,** "A Study of Two-Stroke Cycle Fuel Injection Engines for Exhaust Gas Purification", SAE 720195, (1972).

6. **VIEILLEDENT, E.,** "Low Pressure Electronic Fuel Injection of System for Two-Stroke Engines", SAE 780767, (1978).

7. **BLAIR, G.P.** and **DOUGLAS, R.** "Fuel Injection of a Two-Stroke Cycle Spark Ignition Engine", SAE 820952, (1982).

8. **BLAIR, G.P., HILL, B.N., MILLER,A.J.,** and **NICKELL, S.P.,** "Reduction of Fuel Consumption of a Spark Ignition Two-Stroke Cycle Engine", SAE830093, (1983).

9. **BLAIR, G.P.,** and **HILL, B.W.,** "Further Tests on Reducing Fuel Consumption with a Carburetted Two-Stroke Cycle Engine." SAE 831303, (1983).

10. **ONISHI, S., JO, P.D.,** and **KATO, S.,** "Multi-Layer Stratified Scavenging (MULS) - A New Scavenging Method for Two-Stroke Engines", SAE 840420, (1984).

11. **BLAIR, G.P.,** and **JOHNSTON, M.B.,** "Simplified Design Criteria for Expansion Chambers for Two-Cycle Gasoline Engines", SAE 700123, (1970).

12. See Reference 11, p. 505

13. British Standard 1042, Part 1: 1964, "Methods for the Measurement of Fluid Flow", British Standards Institution, London 1964.

14. **BAUDEQUIN, F.,** and **ROCHELLE, P.,** "Some Scavenging Models for Two-Stroke Engines", Proc. Instn. Mech. Engns, Vol 194, (1980).

15. **PHATAK, R.,** "A New Method of Analyzing Two-Stroke Cycle Engine Gas Flow Patterns " SAE 790487 (1979).

16. **SANBORN, D.S., BLAIR, G.P., KENNY, R.G., KINGSBURY, A.H.,** "Experimental Assessment of Scavenging Efficiency of Two-Stroke Cycle Engines", SAE 800975, (1980)

17. As for Reference 6

18. As for Reference 7

19. **BLAIR, G.P.,** and **ASHE, M.C.,** "The Unsteady Gas Exchange Characteristics of a Two-Cycle Engine." SAE 760644, (1976).

20. As for Reference 16

21. As for Reference 6

22. **DAUGHERTY, R.L.,** and **FRANZINI, J.B.,** "Fluid Mechanics with Engineering Applications" 7th Ed., McGraw-Hill Kogakusha, Ltd, Tokyo, (1977), p396

23. **ORTOLANI, C.,** and **MARIANI, G.,** "Potentialities of Exhaust Emission Reduction of a Small Two-Stroke Cycle Spark Ignition Engine" in "The Design and Development of Small Internal Combustion Engines", Inst of Mech Eng, London, (1978), pp.217-219

APPENDIX A.

Example of Reduction of Data.

Carburetted Engine:

Speed (rpm)	Torque (Nm)	Pressure Drop (Pa)	Fuel Time (seconds)
6700	64	228	145

This is an example of data taken for the carburetted engine.

Brake Power (B.P.)

$$B.P. = T \times \omega$$
$$= T \times rpm \times 2\pi/60 \times 5,8$$

where 5,8 is the gear ratio between the crankshaft and gearbox output shaft.

$$B.P. = 64 \times 6700 \times 2\pi/60 \times 5,8$$
$$= 7,74kW$$

Brake Specific Fuel Consumption (Bsfc).

$$bsfc = Vol \times S.G. \times 3600/B.P. \times fuel\ time$$

where Vol = 161ml
specific gravity = 0.678
therefore bsfc = 357g/kWh

Brake Mean Effective Pressure (Bmep).

bmep = B.P. x 60/s.v. x rpm

where s.v. is the swept volume

therefore bmep = 7,74 x 60/1,23 x 10^{-4} x rpm

= 563,5kPa

Mass Air Flow (M_{air})

From the Bernouilli equation, if the pressure drop is small, as it has to be, if the orifice is not to throttle the air flow to the engine, the incompressible form of Bernouilli's equation can be applied.

$v_{air} = \sqrt{2 \Delta P/\rho_{air}}$

From the continuity equation:

$M_{air} = \rho_{air} \times v_{air} \times A_o \times C_d$

results in $M_{air} = C_d A_o \sqrt{2 \Delta P \ \rho_{air}}$

where C_d = coeff. of discharge for the orifice

= 0,61 see ref (22)

A_o = Orifice area = $\pi(0,032^2)/4$

ρ_{air} = density of the air = P/RT

Therefore M_{air} = 0,61 $\pi(0,032^2)/2,4$ x 228/4

= 0,0115 kg/s

Air/Fuel Ratio(A/F).

$$A/F = M_{air}/M_{fuel}$$

$$= M_{air} \times \text{fuel time/Vol.S.G.}$$

$$= 15,3:1$$

Delivery ratio (L)

$$L = M_{air}.60/rpm.1,23 \times 10^{-4}.\rho_{air}$$

$$= 0,697$$

For the injected engine, the extra required in addition to the above, was delay time, pulse width and fuel pressure. This provided information so that the mass flow rate of fuel through the injector could be plotted against pulse width, for the running engine. This is compared to the calibrated flow rates in **Figure 5.11.**

Appendix B.

Expansion Chamber Design.

The purpose of an expansion chamber is to increase engine power as well as reducing fuel consumption. It achieves this by using the pressure wave reflection characteristics of the blowdown pulse as illustrated in **Figure A1.**

The three pressure time histories show the output of a pressure transducer placed near the exhaust port. The purpose of the header pipe and diffuser is clearly to assist in clearing the cylinder of exhaust products. However, in doing so, fresh air/fuel mixture will be lost in the process. Hence, the reflector cone is designed to 'plug' some of this lost charge back into the cylinder, with a positive reflected pulse, just as the port is closed be the piston. There is dispute over whether this pulse actually reverses the flow of exiting charge.

Referring to Blair, it is assumed that these pulses travel at the local speed of sound. Experiments have revealed the following criteria with respect to the design of expansion chambers.

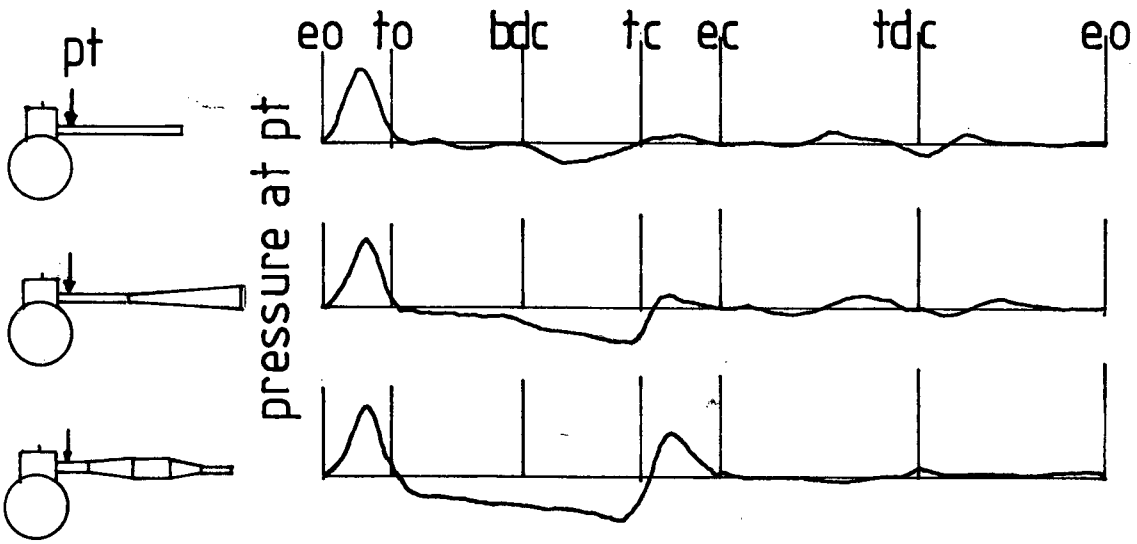

Figure A1 Pressure time histories for three exhaust systems.

$1,3 < A_{hp}/A_{ep} < 1,75$

$2,65 < A_{hp}/A_{tp} < 4,7$

$3,4 < A_{cs}/A_{hp} < 4,5$

$L_2 = 154.(320-2B)\sqrt{T}/N$

$0,4 > X_1/L_2 > 0,25$

$0,25 > X_2/L_2 > 0,125$

$L_1+X_1/2 = 134,3\sqrt{T(180-B)}/N$

A_{hp} = header pipe cross sectional area
A_{ep} = exhaust port area
A_{tp} = tail pipe sectional area
A_{cs} = centre section cross sectional area
B = crank angle between tdc and exhaust opening
T = gas temperature in °R (1200-1500°R)
L_1, L_2, X_1, X_2 = indicated lengths in cm
N =engine speed in rpm, (6000rpm).

These criteria were derived on an empirical basis and certainly seem to apply to the engine used in this study.

Appendix C.

The 555 Timer.

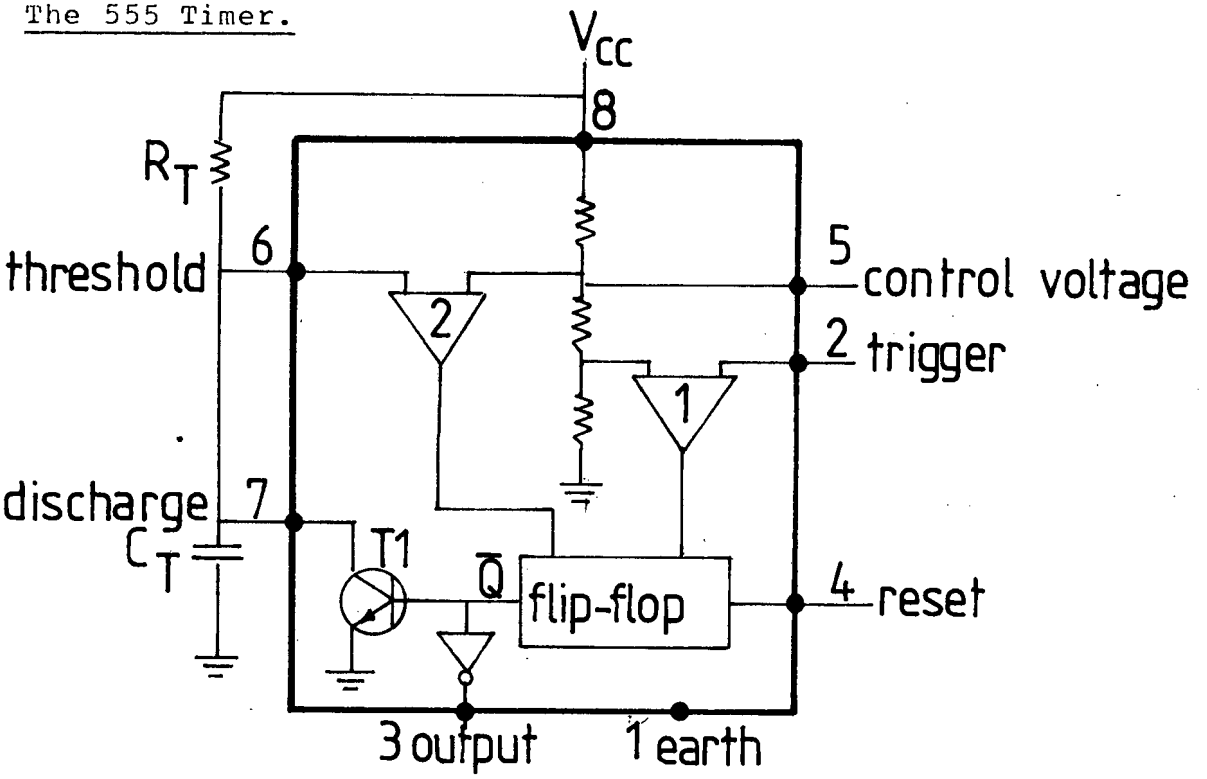

The basis of the circuit is a flip-flop with set and reset inputs controlled be comparators. The quiescent condition is with the $\bar{Q}$ flip-flop output high, so that the timing capacitor C_T is shorted by the transistor T_1. The output is then low due to the inverting output stage.

The trigger is normally held high by the internal circuit and operates on a falling voltage. When the trigger input falls to $V_{CC}/3$, comparator 1 changes state and sets the flip-flop. The $\bar{Q}$ output goes low, sending the output terminal high, as well as switching of T_1. Capacitor C_T, therefore begins charging through the external resistor R_T. Once the voltage across C_T reaches 2/3 V_{CC}, comparator 2 resets the flip-flop. This switches on T_1 and discharges C_T.

The timed period depends on the values of R_T and C_T and can be calculated from the charging equation for an RC circuit.

$$V = Vo\ [1 - \exp(-t/CR)]$$

In this case $Vo = V_{CC}$ and the value of V at the end of the timed pulse (time = t) is $2/3V_{CC}$.
Therefore $2/3 = 1 - \exp(-t/C_TR_T)$

or $t = 1{,}1\ C_T\ R_T$

Thus from **Figure 4,3** it can be seen that the maximum and minimum delays will be 18ms and 1,4ms respectively, and the maximum and minimum pulse widths will be 0,4 and 6ms.

The pulse edge rise and fall times should be less than 50ns for maximum noise immunity. For this reason the first 555 timer is connected in a Schmitt trigger mode.

Appendix D.

Calculation of CO Concentration in the Exhaust Gas.

Ortolani and Mariani[23], derive an equation relating the air/fuel ratio to the exhaust concentrations of CO, CO_2, and O_2. Because of the excess air in the exhaust gas due to mixing and short circuiting of fresh charge, this equation is substantially different from that used for four-stroke engines where excess air is not accounted for.

The derived equation is given below.

$$A/F = \frac{28,97}{(12,01 + 1,008y)} \cdot \frac{(100-[H_2O]_d/2)\ ((21 - [O_2]_e)/21 - [CO]_e)}{[CO]_e + [CO_2]_e}$$

$[H_2O]d$ is the concentration of water vapor after drying and is typically 2,3% at 20°C.

Therefore, knowing the air/fuel ratio the CO_2 and O_2 contrations it is possible to calculate the CO concentration whose measurement using Orsat apparatus proved unreliable.

Appendix E.

Theoretical Derivation of Perfect Mixing Line.

Perfect scavenging or pure displacement scavenging would occur if fresh charge of certain mass entered the cylinder and caused an equal mass of exhaust gases to leave via the exhaust port with no mixing or short circuiting, Therefore for displacement scavenging, the charging efficiency is equal to the delivery ratio up to a delivery ratio of 1,0 where it remains as 1,0 for larger delivery ratios.

Displacement scavenging is the upper limit of the scavenging process. In practice, the scavenging process is far less efficient. Mixing scavenging provides a more realistic model. The following assumptions are made:

* The process occurs at constant cylinder volume.
* The densities of inlet and exhaust gases are the same, hence volumes can be equal to mass.
* The addition of a mass of air dM_a to the cylinder causes an equal mass of exhaust gases dM_e to leave the cylinder.
* The process is one of perfect mixing. The air enters the cylinder contents, causing a mixture of gas and air to leave at the same time.
* The instantaneous charging efficiency is given by $Z = M_{al}/M$ where M_{al} is the mass of air retained in the cylinder. Hence Z is the proportion of air in the cylinder at any instant.

The mass of air entering the cylinder at any instant dM_a and the mass of air plus gas leaving is dM_e. Of this, the mass of air leaving the cylinder at any instant is ZdM_{al}.

Thus $dM_{al} = dM_a - ZdM_e$ (1)

and $Z = M_{al}/M$ (2)

Hence $MdZ = dM_{al}$ (3)

Substituting (3) into (1)

$$MdZ = dM_a - ZdM_e \quad (4)$$

Now the mass of air entering the cylinder, dM_a, equals the mass of gas plus air leaving the cylinder dM_e.
Substituting for dM_e in (4),

$$MdZ = dM_a - ZdM_a = dM_a(1-2)$$

or $dZ/(1-2) = dM_a/M$ (5)

In this differential equation, M is a constant, i.e. the cylinder mass remains constant. Z and M_a are variables. If we integrate between the following limits:

$Z = O$, $M_a = O$ (commencement of scavenging)

and $Z = \eta CE$, $M_a = M_a$ (end of scavenging where Z is now the charging efficiency, ηCE, and M_a is the total air supplied).

Now the delivery ratio is defined as:

$$L = M_a/M$$

So the second limit becomes:

$$Z = \eta CE,\ M_a = L.M$$

Integrating (5) between the limits

$$\int_0^{\eta_{CE}} dZ/1-2 \quad = \quad \int_0^{L.M} dM_a/M$$

$$-\ln (1-\eta CE) = L$$

Therefore $\eta CE = 1-e^{-L}$ (6)

This produces the perfect mixing line relating the charging efficiency to the delivery ratio.

More realistic models suggest that the scavenging process is one of pure mixing and pure displacement, with a term for short circuiting involved.

Appendix F.

Determination of the Charging Efficiency from the Exhaust Gas Analysis.

The basic stoichiometric chemical eqation for a hydrocarbon-air reaction is:

$$CH_y + aO_2 + 3{,}76aN_2 \longrightarrow CO_2 + y/2H_2O + 3{,}76aN_2$$

Performing an O_2 balance,the stoichiometric number of moles of O_2 is:

$$a = 1 + y/4 \qquad (1)$$

The basic chemical equation for combustion of hydrocarbon fuel with excess air is:

$$CH_y + aO_2 + 3{,}76aN_2 \longrightarrow bCO + (1-b)CO_2 + cH_2O +$$

$$(a+b/2-c/2-1)O_2 + 3{,}76aN_2$$

The percentage volumetric concentrations of CO, CO_2 and H_2O are defined as:

$$[CO] = 100b/n_t$$
$$[CO_2] = 100(1-b)/n_t$$
$$[H_2O] = 100c/n_t$$

where n_t is the total number of moles of exhaust gas.

From this

$$n_t = 100/([CO] + [CO_2])$$

Now, the trapping efficiency n_{tr} is defined in terms of air supply to, and air trapped in the cylinder as:

$$n_{TR} = \text{air trapped/air supplied}$$
$$= \text{(air supplied - excess air)/air supplied}$$
$$= 1 - \text{excess air/air supplied}$$

where excess air refers to the excess air in the exhaust gases.

It can be assumed that:

excess air/air supplied = excess oxygen/oxygen supplied

Reference to excess air and air supplied is to the number of moles in each case.

Using the following nomenclature:

Thus the number of moles of O_2 in the exhaust gas, O_{2e}, is:

$$O_{2e} = [O_2]/([CO] + [CO_2])$$

If
- O_{2f} = Number of moles of O_2 supplied
- O_{2st} = Stoichiometric number of moles of O_2
- O_{2e} = Number of moles of O_2 in the exhaust
- A/F_{st} = Stoichiometric air/fuel ratio
- A/F = Actual air/fuel ratio
- n_{TE} = Trapping efficiency
- n_{CE} = Charging efficiency
- L = Delivery ratio

It can further be assumed that

$$(A/F)/(A/F_{st}) = O_{2f}/O_{2st}$$

Therefore

$$O_{2f} = (O_{2st} \times A/F)/(A/F_{st})$$

$$= (1+y/4).(A/F)/(A/F_{st})$$

So

$$n_{TE} = 1 - \frac{[O_2]/([CO] + [CO_2])}{(1 + y/4).(A/F)/14.5}$$

and

$$n_{CE} = n_{TE} \times L$$

Appendix G

Results

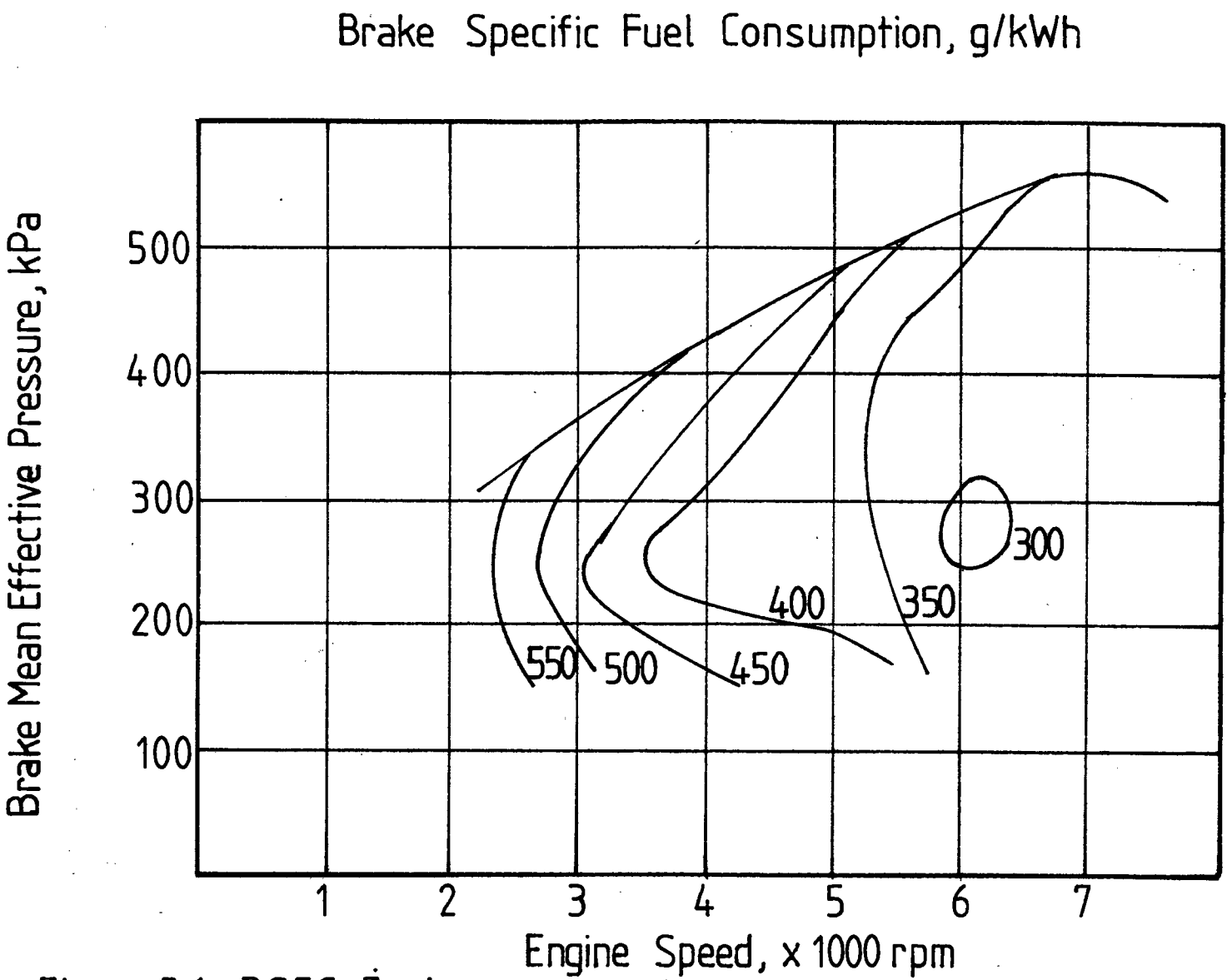

Figure 5.1 BSFC Engine map

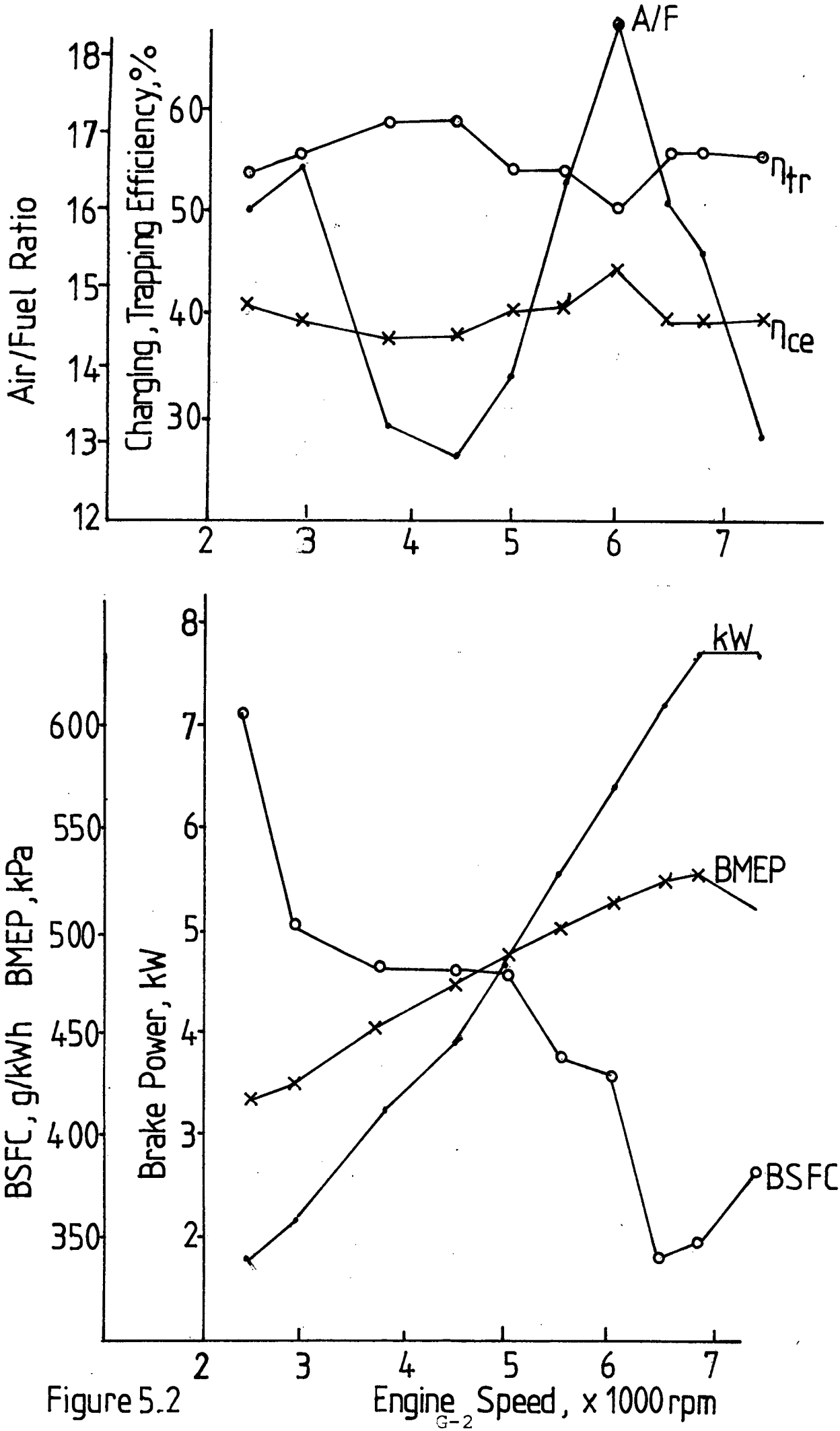
A/F
η_{tr}
η_{ce}
Air/Fuel Ratio
Charging, Trapping Efficiency, %
18
17
16
15
14
13
12
60
50
40
30
2
3
4
5
6
7
kW
BMEP
BSFC
BSFC, g/kWh BMEP, kPa
Brake Power, kW
600
550
500
450
400
350
8
7
6
5
4
3
2
Engine Speed, x 1000 rpm

Figure 5.2

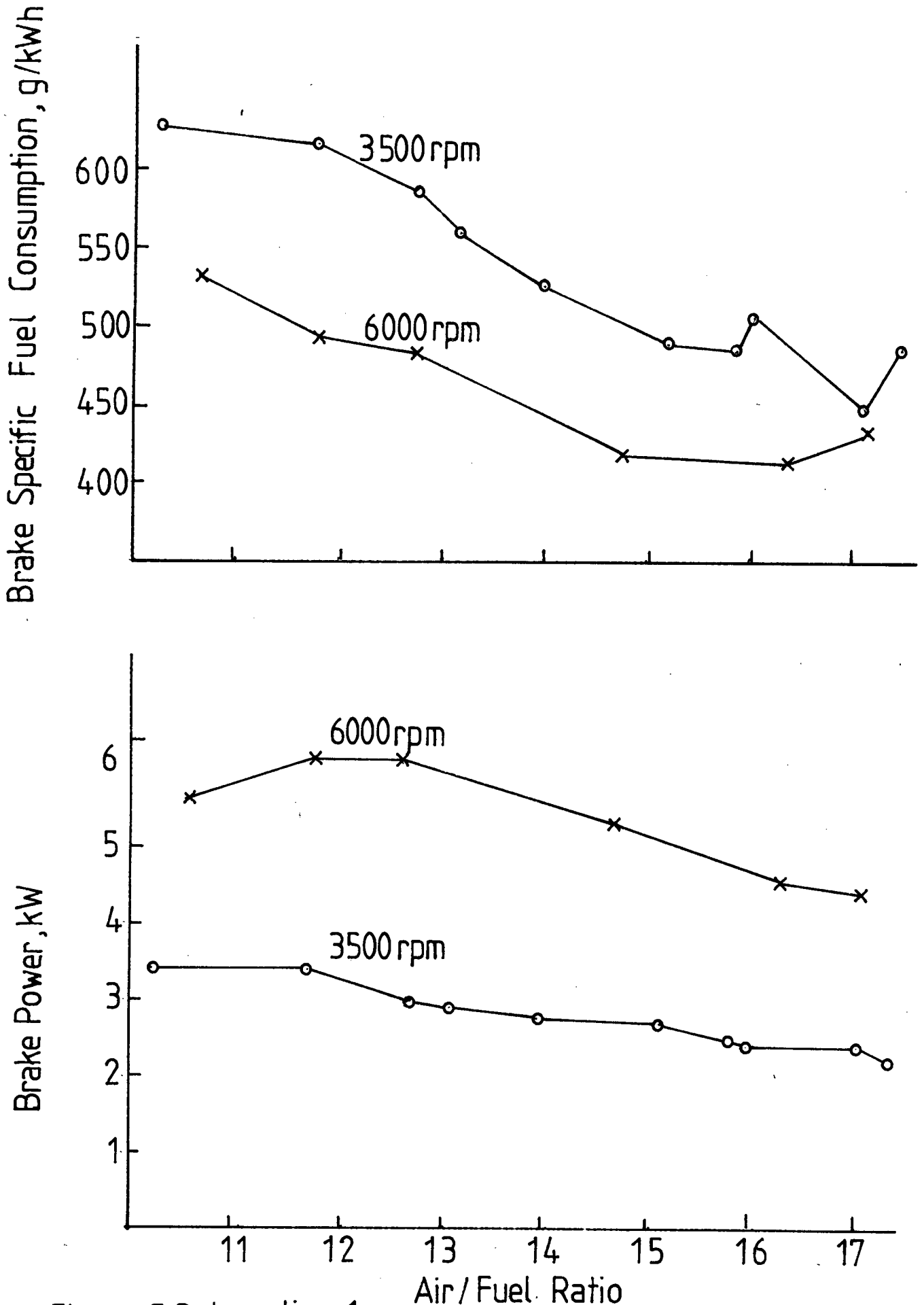

Figure 5.3 Location 1

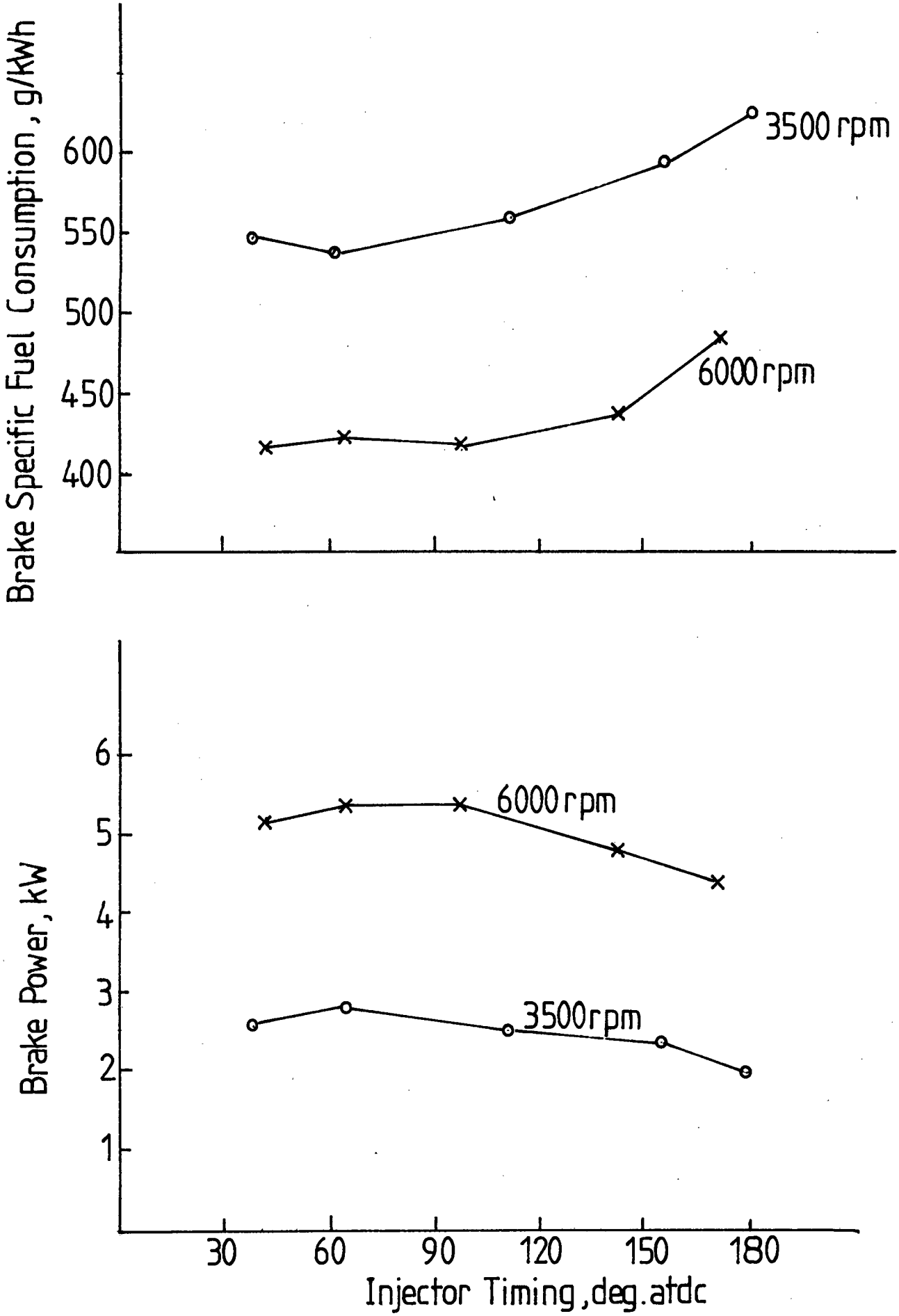
Brake Specific Fuel Consumption, g/kWh
600
550
500
450
400
3500 rpm
6000 rpm
Brake Power, kW
6
5
4
3
2
1
6000 rpm
3500 rpm
30
60
90
120
150
180
Injector Timing, deg. atdc

Figure 5.4

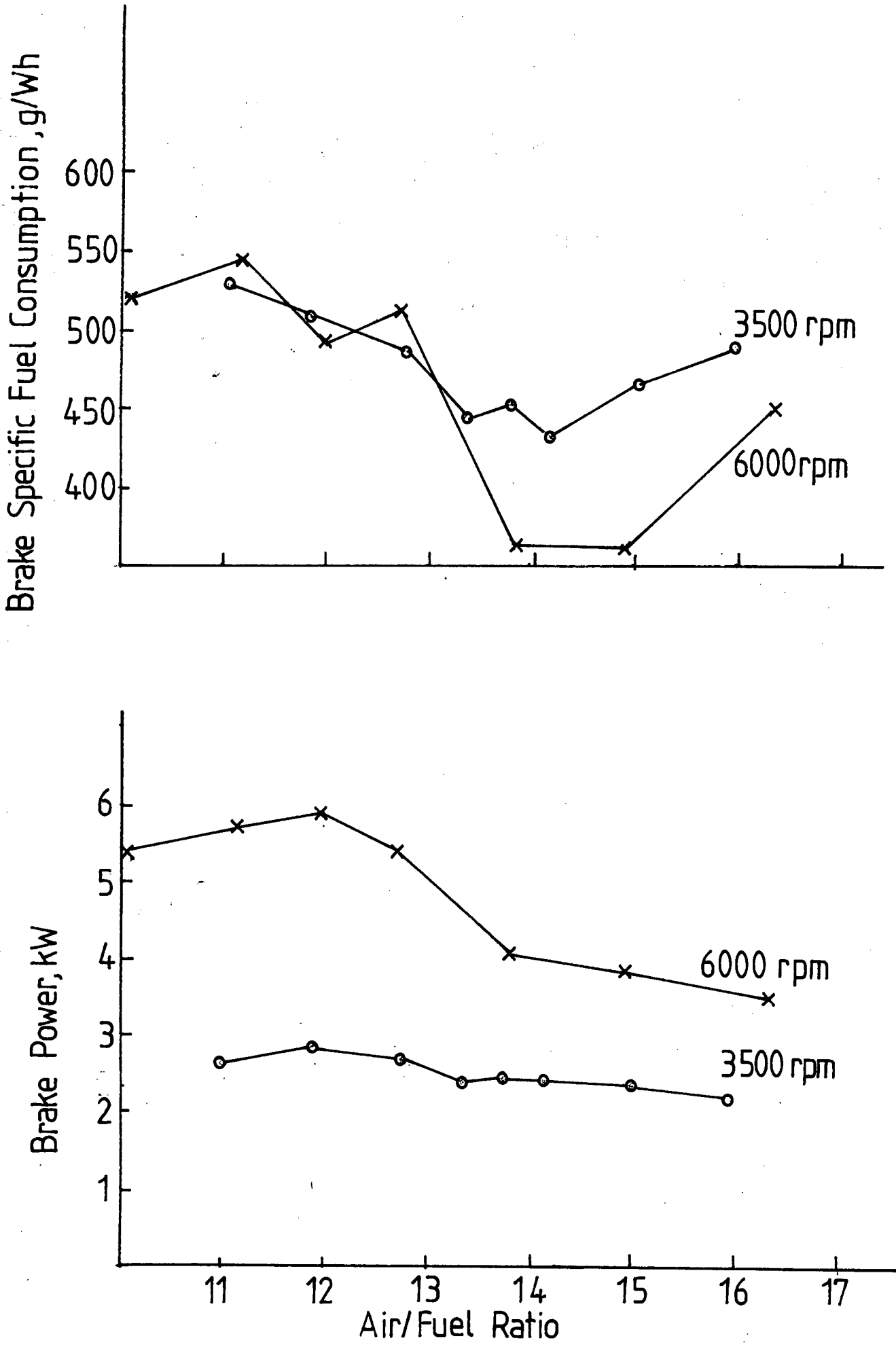

Figure 5.5 Location 2

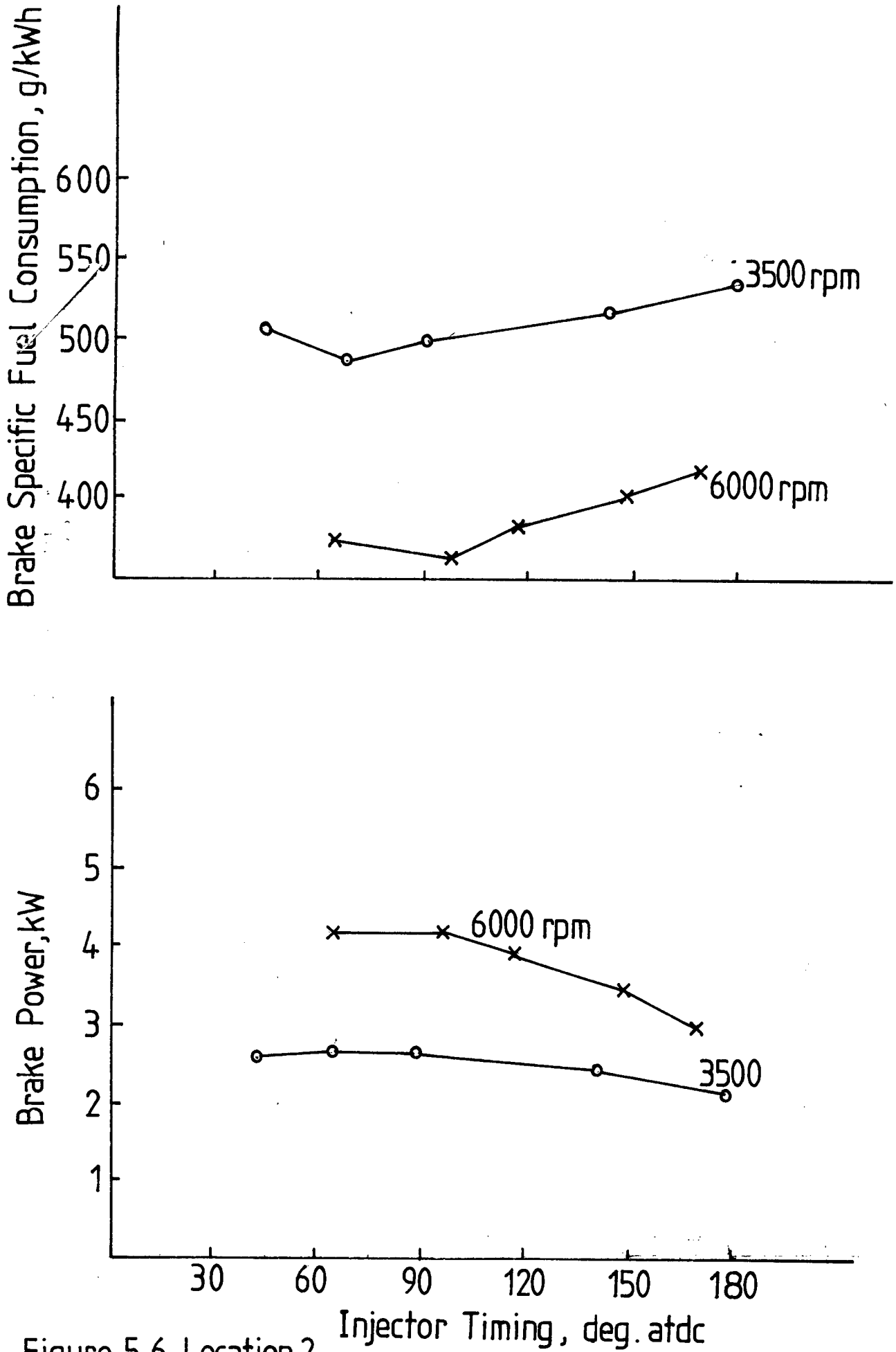

Figure 5.6 Location 2

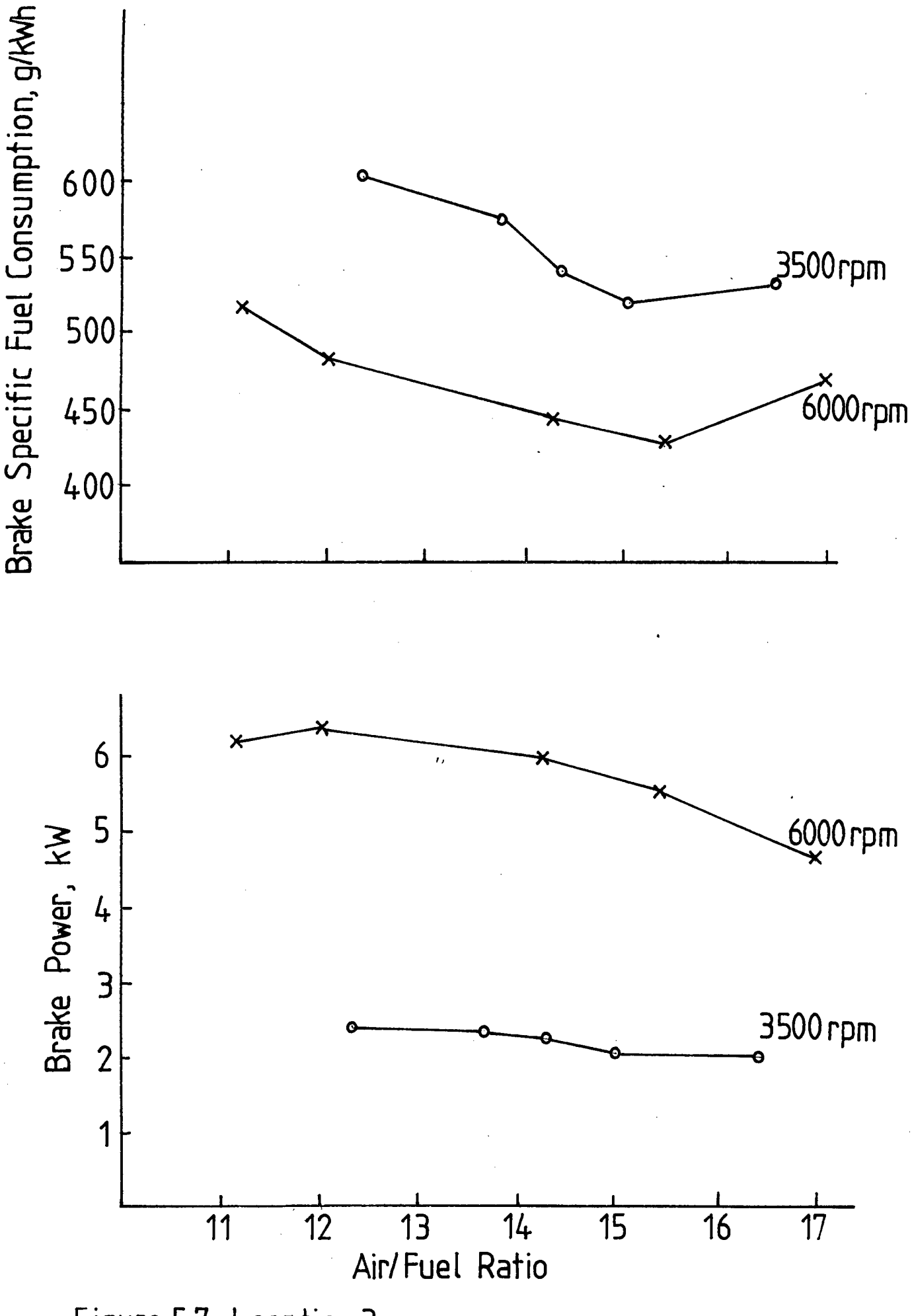

Figure 5.7 Location 3

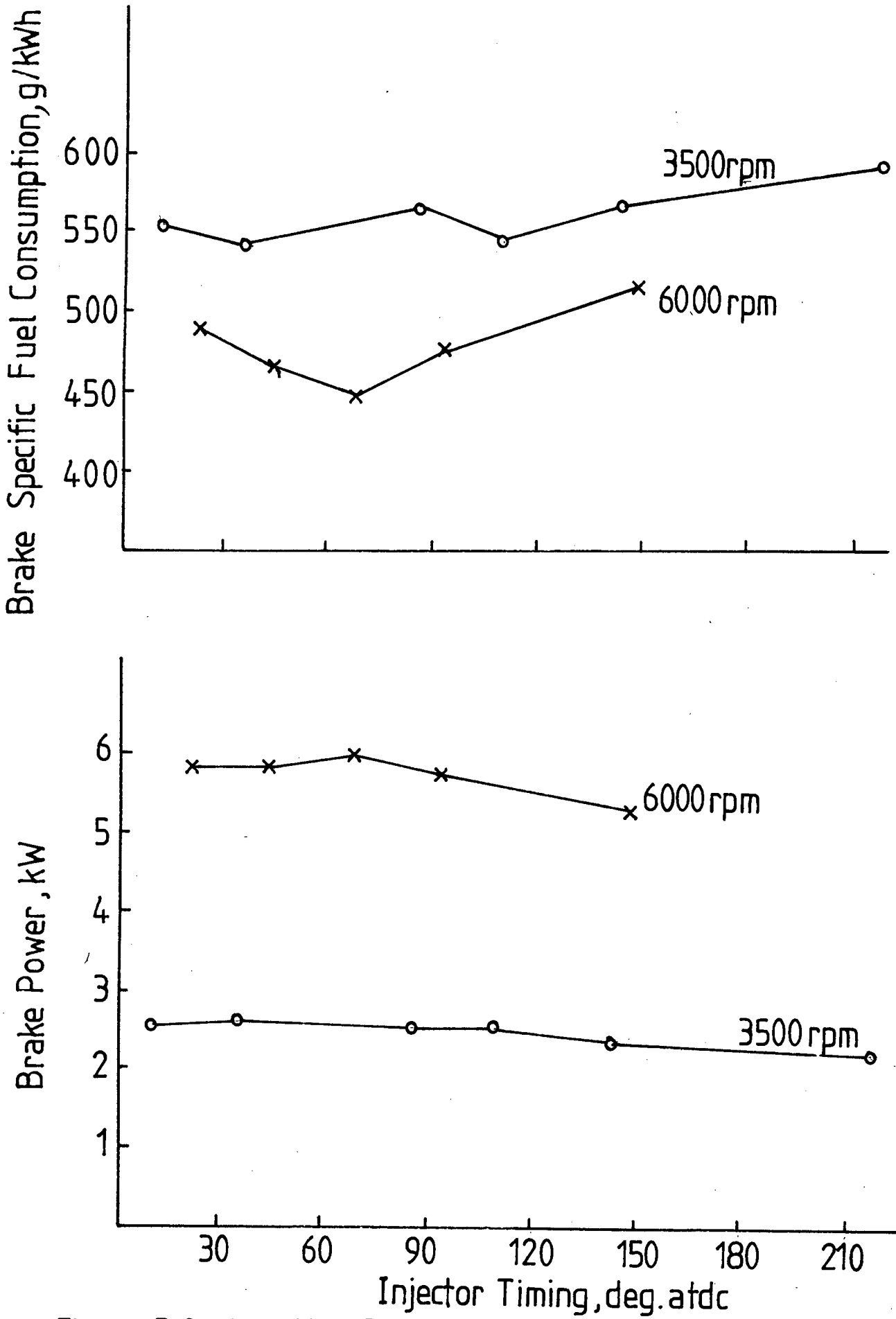

Figure 5.8 Location 3

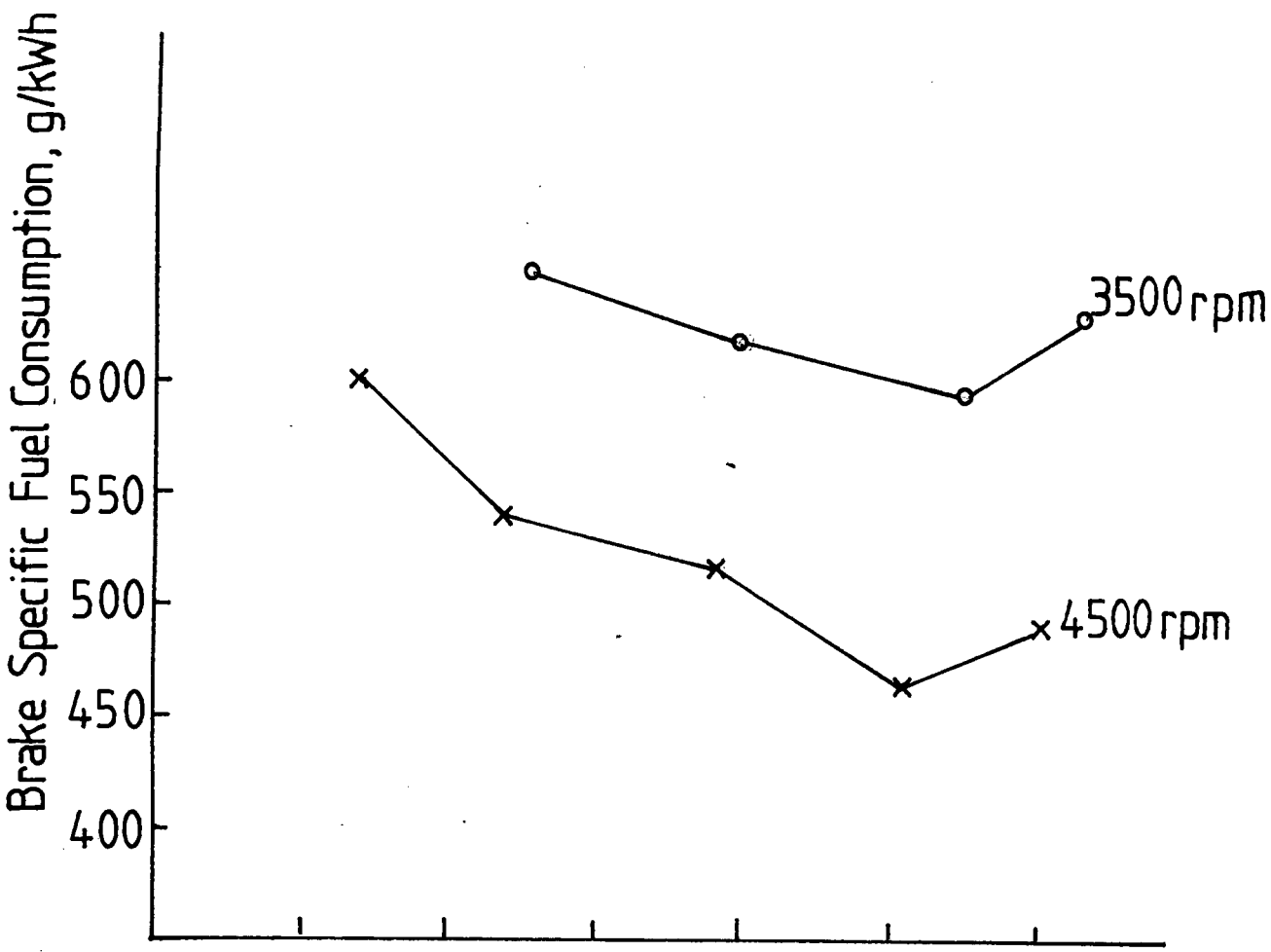

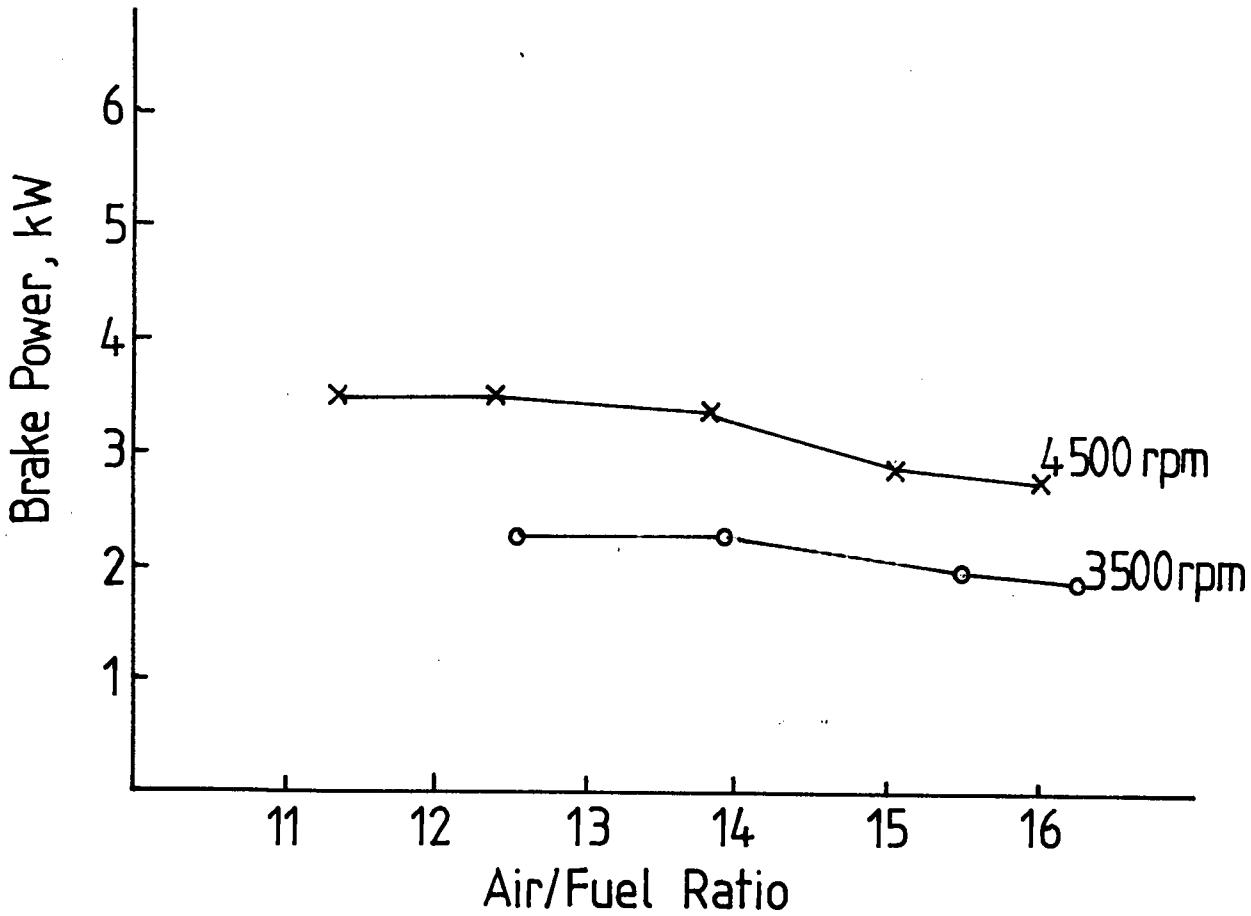

Figure 5.9 Location 4

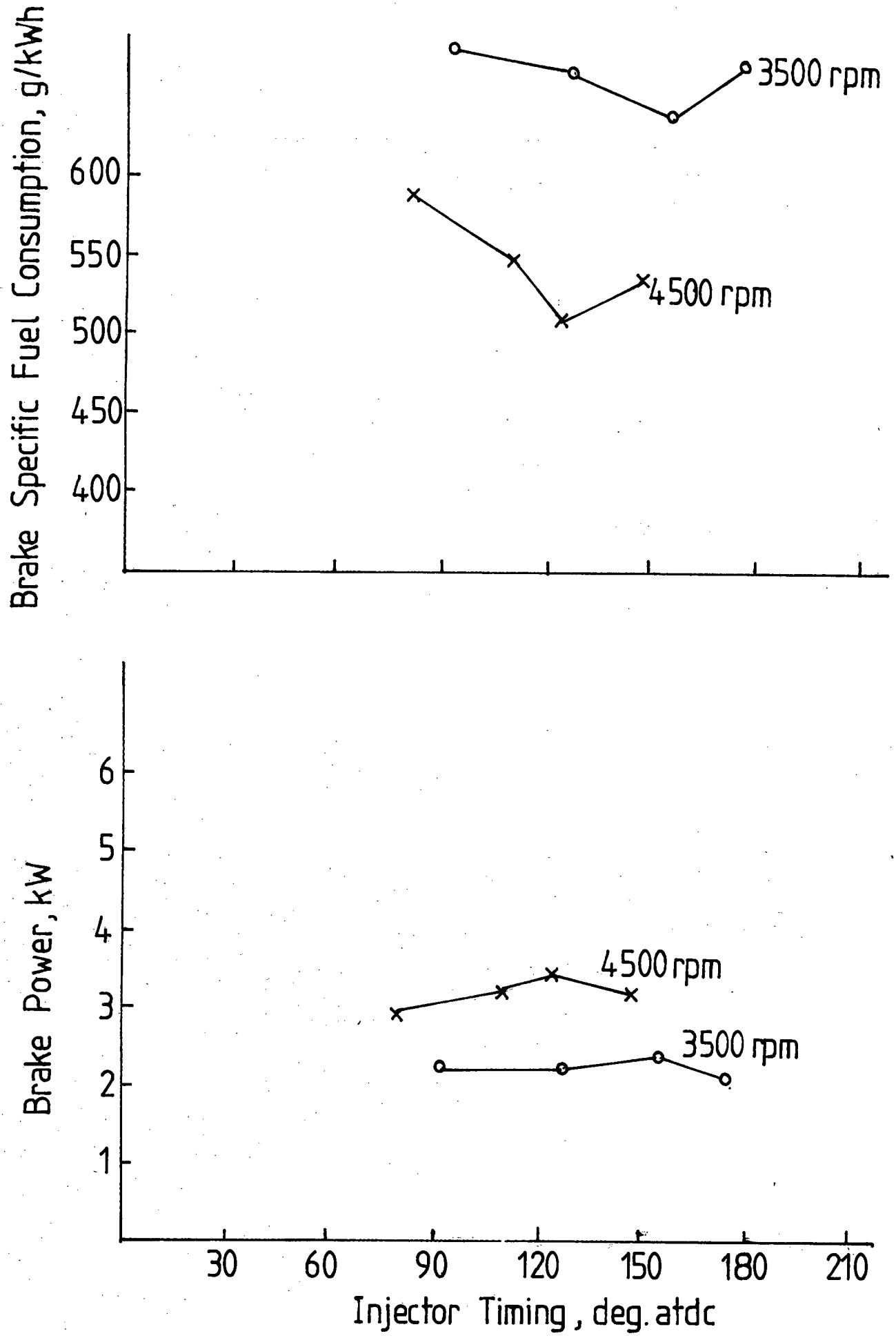

Figure 5.10 Location 4

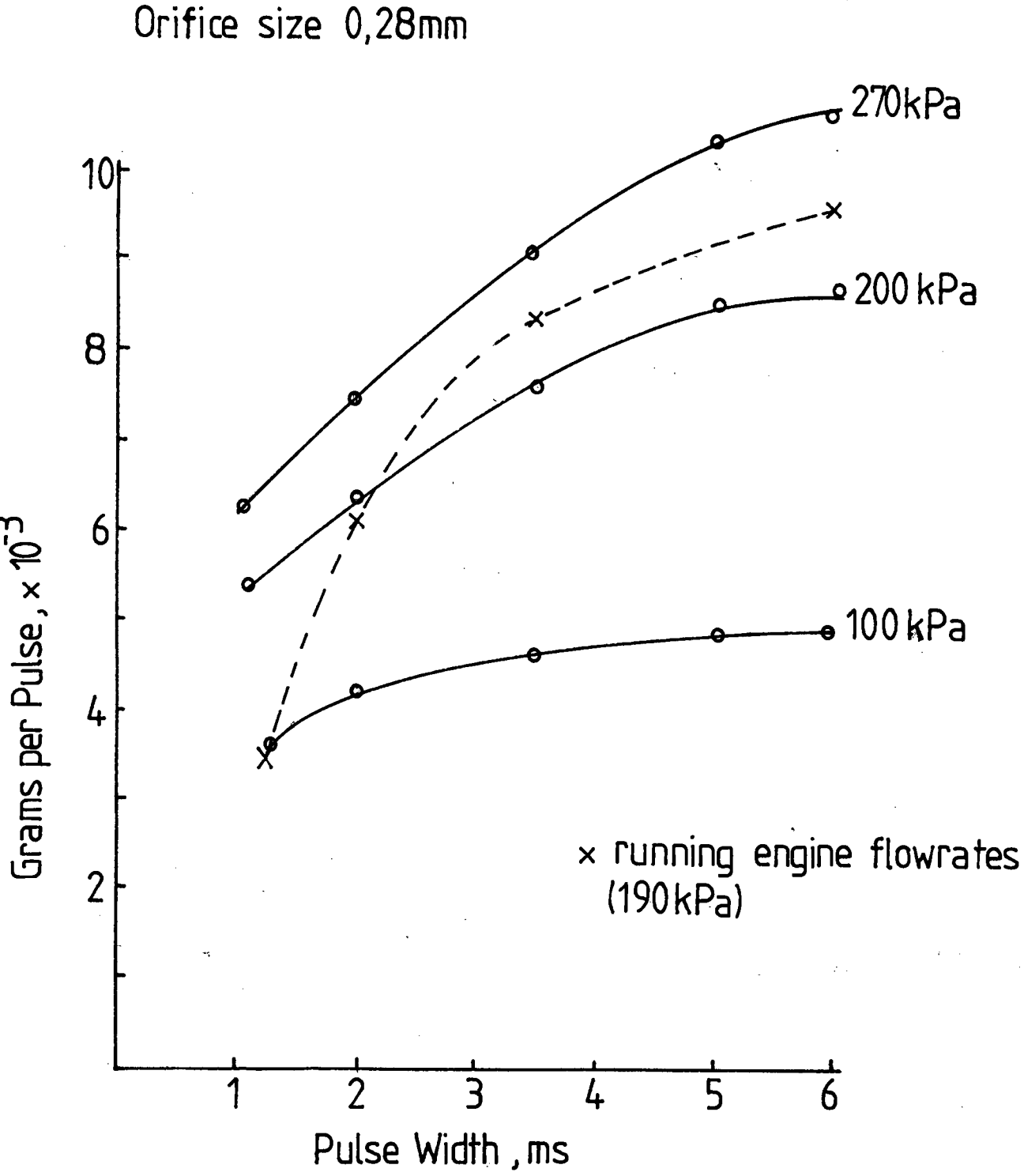

Figure 5.11 Injector Calibration

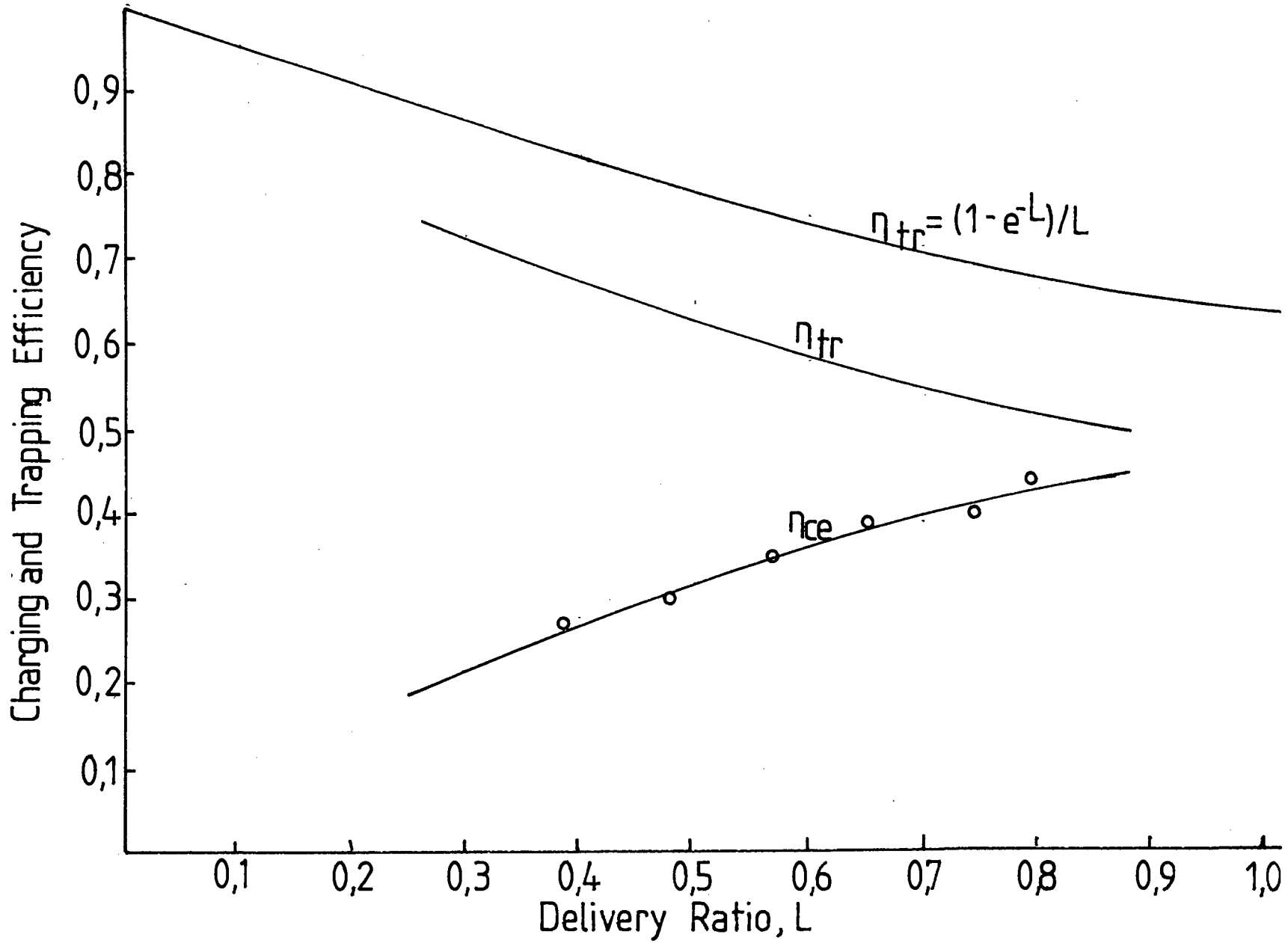
Charging and Trapping Efficiency
0,9
0,8
0,7
0,6
0,5
0,4
0,3
0,2
0,1
$\eta_{tr} = (1 - e^{-L})/L$
η_{tr}
η_{ce}
0,1
0,2
0,3
0,4
0,5
0,6
0,7
0,8
0,9
1,0
Delivery Ratio, L

Figure 5.12

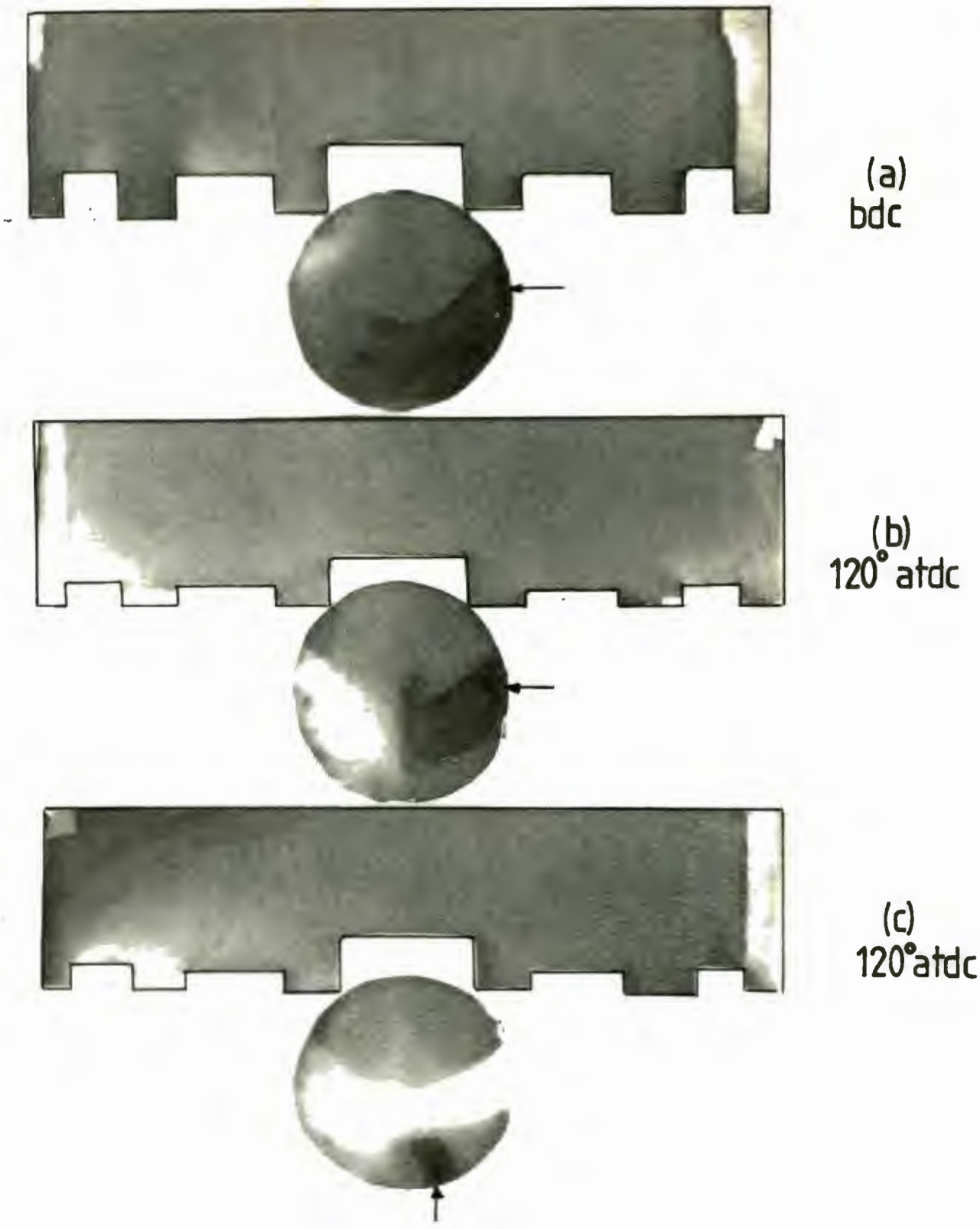

Figure 5.13 Ammonia Method: Tested engine.

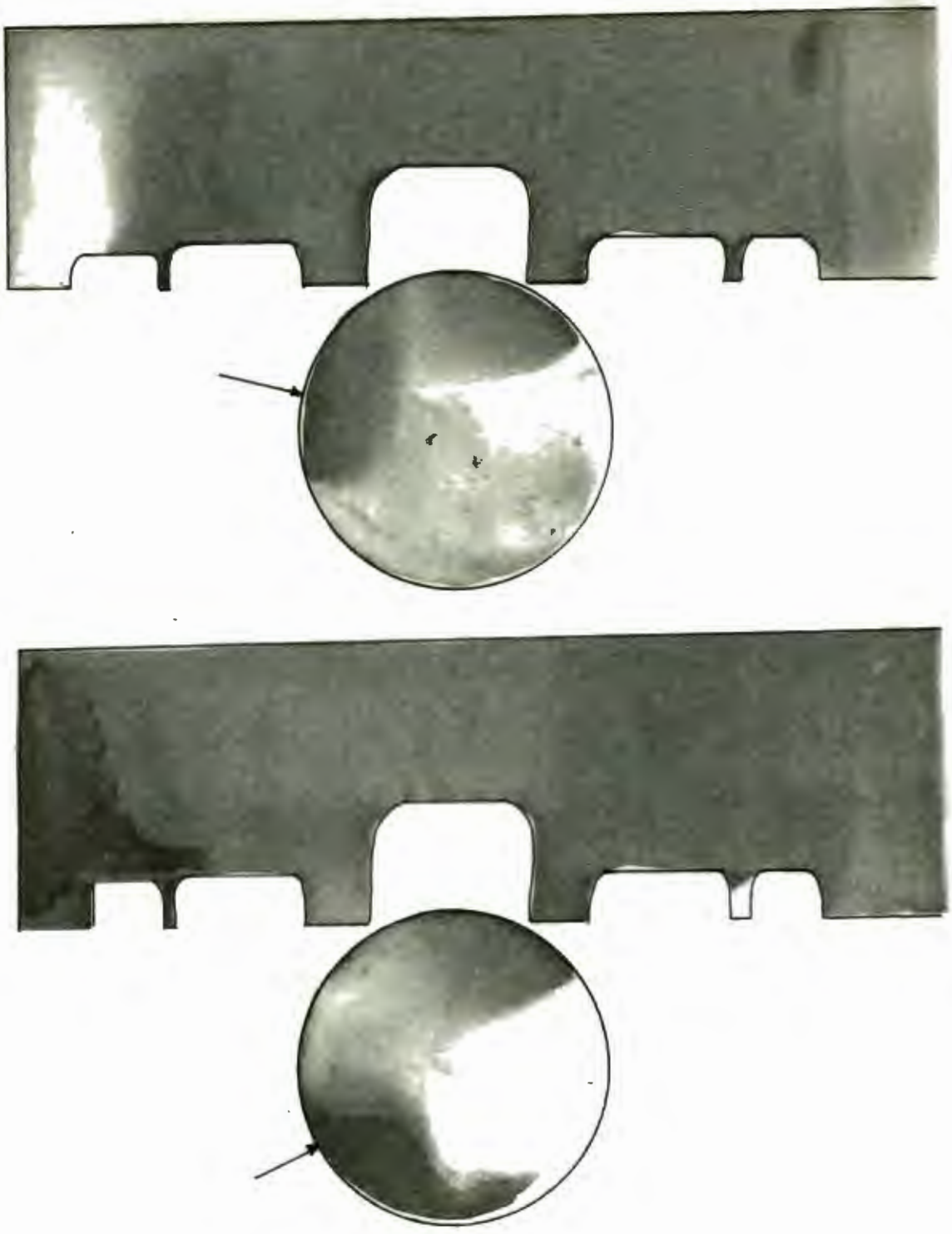

→ position of injector

Figure 5.14 Ammonia Method: Model (bdc)

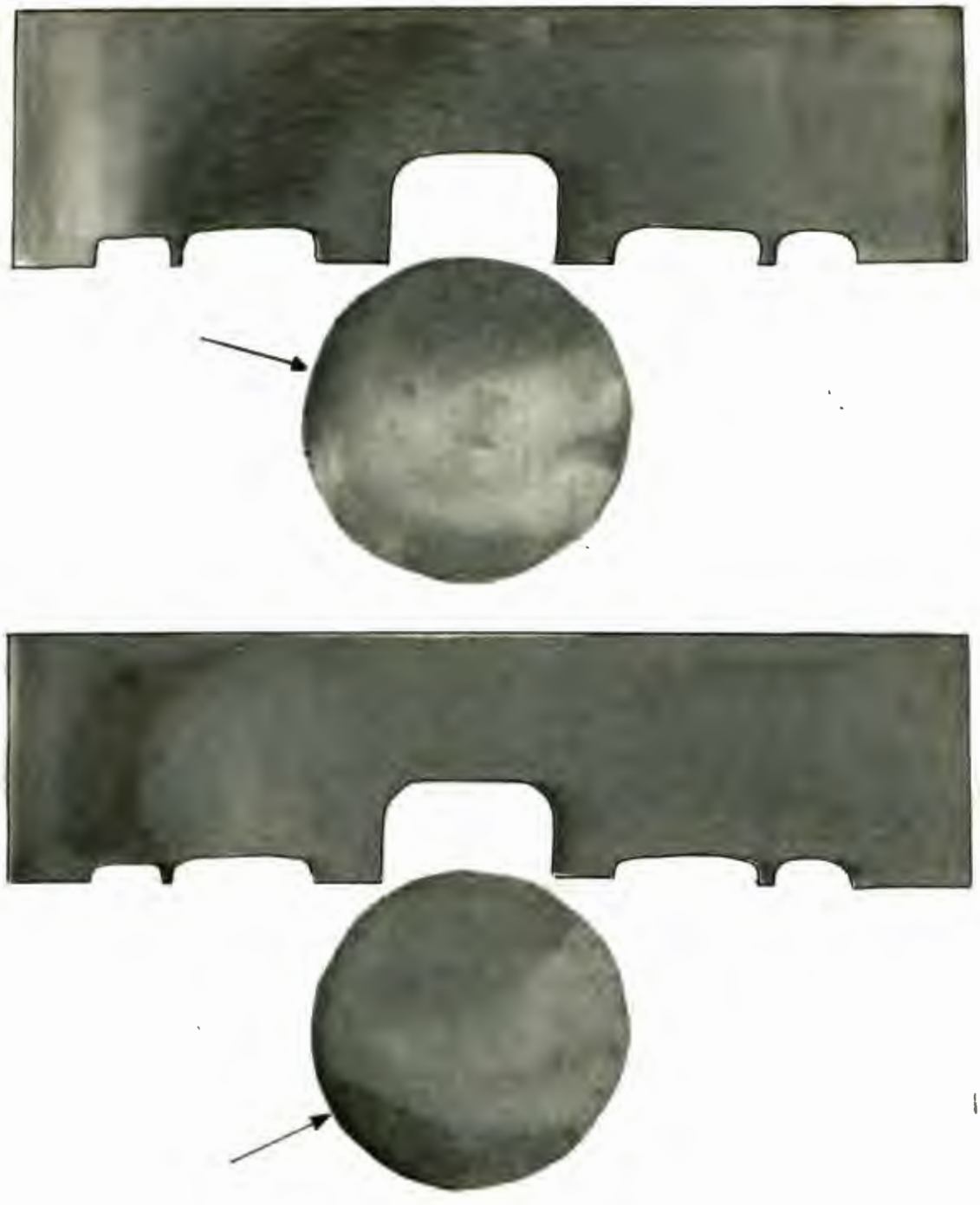

⟶ position of injector

Figure 5.15 Ammonia Method: Model (ports half open)